AD NUMBER

ADB015331

LIMITATION CHANGES

TO:

Approved for public release; distribution is unlimited.

FROM:

Distribution authorized to U.S. Gov't. agencies only; Test and Evaluation; OCT 1976. Other requests shall be referred to Army Materials and Mechanics Research Center, Attn: AMXMR-PL, Watertown, MA 02172.

AUTHORITY

ammrc, d/a ltr, 8 jun 1978

DISCLAIMER NOTICE

THIS DOCUMENT IS THE BEST QUALITY AVAILABLE.

COPY FURNISHED CONTAINED A SIGNIFICANT NUMBER OF PAGES WHICH DO NOT REPRODUCE LEGIBLY.

AMMRC CTR 76-31

BRITTLE MATERIALS DESIGN, HIGH TEMPERATURE GAS TURBINE

Technical Report By:

Arthur F. McLean, Ford Motor Company, Dearborn, Michigan 48121
Robert R. Baker, Ford Motor Company, Dearborn, Michigan 48121

October, 1976

Interim Report Number 10, January, 1976 to June 30, 1976

Contract Number DAAG 46-71-C-0162

Sponsored by the Advanced Research Projects Agency

ARPA Order Number 1849

Project Code Number 1D10

Agency Accession Number DA 0D4733

Prepared for

ARMY MATERIALS AND MECHANICS RESEARCH CENTER
Watertown, Massachusetts 02172

The findings in this report are not to be construed as an official Advanced Research Projects Agency, Department of the Army, or U. S. Government position, either expressed or implied, unless so designated by other authorized documents.

Mention of any trade names or manufacturers in this report shall not be construed as advertising nor as an official indorsement or approval of such products or companies by the United States Government.

DISPOSITION INSTRUCTIONS

Destroy this report when it is no longer needed. Do not return it to the originator.

AMMRC CTR 76-31

BRITTLE MATERIALS DESIGN, HIGH TEMPERATURE GAS TURBINE

Technical Report By:

Arthur F. McLean, Ford Motor Company, Dearborn, Michigan 48121
Robert R. Baker, Ford Motor Company, Dearborn, Michigan 48121

October, 1976

Interim Report Number 10, January 1, 1976 to June 30, 1976

Contract Number DAAG 46-71-C-0162

Sponsored by the Advanced Research Projects Agency

ARPA Order Number 1849

Project Code Number 1D10

Agency Accession Number DA OD 4733

Prepared for:

ARMY MATERIALS AND MECHANICS RESEARCH CENTER
Watertown, Massachusetts 02172

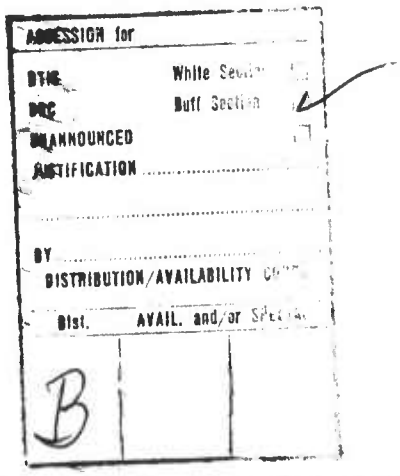

ABSTRACT

The demonstration of uncooled brittle materials in structural applications at 2500°F is the objective of the "Brittle Materials Design, High Temperature Gas Turbine" program. Ford Motor Company, the contractor, will utilize a small vehicular gas turbine comprising an entire ceramic hot flow path including the highly stressed turbine rotors. Westinghouse, the subcontractor, originally planned to evaluate ceramic first stage stator vanes in an actual 30 MW test turbine engine; however, this objective was revised to demonstrate ceramic stator vanes in a static test rig. Both companies had in-house research programs in this area prior to this contract.

In the stationary gas turbine project, the test of ceramic stator vanes in a static rig for 100 cycles up to temperatures of 2500°F has been completed. This accomplishment meets the revised objectives for the stationary turbine project and therefore, this project is completed as of the end of this reporting period. The report of the last six months progress will be included in the final report for the project and published separately.

A significant achievement, in the vehicular turbine project, was the test of a partially bladed duo-density silicon nitride turbine rotor in an experimental high temperature gas turbine engine up to a speed of 52,800 rpm and turbine inlet temperature of 2650°F before failure on a subsequent run. A modification of the ceramic hot gas flow path of the 820 turbine engine to accomplish this test is described in detail. Two rotors, with blades of 10% length, were successfully tested for 45 minutes at 32,000 rpm and 2000°F turbine inlet temperature. Rotor testing capability at elevated temperatures was initiated in two hot spin rigs which were checked out with six available ceramic rotors. Cold spin test results of nine hot pressed silicon nitride rotor hubs correlated well with analytical predictions based on Weibull MOR data from 140 test bars cut from five additional hubs. Testing of the stationary components continued with a "Refel" silicon carbide combustor tube successfully accumulating over 200 hours in the steady-state test rig, equivalent to the prescribed 200 hour engine duty cycle goal. Twenty-six hours and 40 minutes of this testing was at a turbine inlet temperature of 2500°F. Three additional thin wall combustor tubes have been successfully qualified for further engine or rig testing. Seven monolithic silicon nitride stators of 2.55 g/cc density and a rotor tip shroud successfully passed an improved qualification light-off test. A reaction bonded silicon carbide stator accumulated 147 hours of operation at 1930°F and remains crack free. Testing of stationary components at turbine inlet temperatures up to 2500°F continued with over nine hours of test time accumulated without failures.

An important fabrication development to make duo-density turbine rotors in three pieces was conceived and demonstrated a significant reduction of applied loads during hot press bonding generally eliminating blade and rim cracking. Alignment of the hot press rams and furnace was completed in addition to eliminating base plate creep by utilizing hot pressed silicon carbide base plates. During the course of process development approximately 500 design D' blade rings of 2.7 g/cc density were injection molded, twelve were flaw free after nitriding. A number of additional desired mechanical and process changes were identified to improve the yield of flaw free blade rings. The development of the blade fill operation was completed with the optimization of the slip casting fixtures and processes coupled with a laser removal technique.

Modulus of Rupture tests were conducted on 274 specimens of hot pressed silicon nitride to investigate the effects of surface finish, post machining heat treatments and process variations. MOR tests on 155 bars of 2.7 g/cc density injection molded reaction sintered silicon nitride were completed to determine room and elevated temperature strengths. Bending stress rupture tests on 15 specimens resulted in no time dependent failures for this material up to 2200°F. Twelve of the tests were suspended, without failure, after 200 plus hours at stresses of 20-30 ksi and temperatures of 1900-2200°F. The nitridation of silicon compacts of various densities was investigated for the effects of temperature schedule, atmosphere and furnace load. The key to uniform microstructure, fine porosity and associated high strengths is the control of localized nitriding exotherms so that no silicon melt out occurs.

FOREWORD

This report is the tenth semi-annual technical report of the "Brittle Materials Design, High Temperature Gas Turbine" program initiated by the Advanced Research Projects Agency, ARPA Order Number 1849, and Contract Number DAAG-46-71-C-0162. This is an incrementally-funded six year program.

Since this is an iterative design and materials development program, design concepts and materials selection and/or properties presented in this report will probably not be those finally utilized. Thus all design and property data contained in the semi-annual reports must be considered tentative, and the reports should be considered to be illustrative of the design, materials, processing, and NDT techniques being developed for brittle materials.

The principal investigator of this program is Mr. A. F. McLean, Ford Motor Company, and the technical monitor is Dr. E. S. Wright, AMMRC. The authors would like to acknowledge the valuable contributions in the performance of this work by the following people:

Ford Motor Company

N. Arnon, P. Beardmore, J. H. Buechel, D. J. Cassidy, J. C. Caverly, D. A. Davis, G. C. DeBell, E. F. Dore, A. Ezis, W. A. Fate, E. A. Fisher, M. U. Goodyear, J. W. Grant, D. L. Hartsock, P. H. Havstad, J. A. Herman, R. A. Jeryan, C. F. Johnson, K. H. Kinsman, C. A. Knapp, J. G. LaFond, J. A. Mangels, W. E. Meyer, M. E. Milberg, W. M. Miller, T. G. Mohr, P. F. Nicholls, A. Paluszny, C. Peitsch, J. R. Secord, L. R. Swank, W. Trela, J. Uy, T. J. Whalen, R. M. Williams, W. Wu

Army Material and Mechanics Research Center

G. F. Gazza, E. M. Lenoe, R. N. Katz, H. Priest

TABLE OF CONTENTS

LIST OF ILLUSTRATIONS

LIST OF ILLUSTRATIONS

LIST OF ILLUSTRATIONS

LIST OF TABLES

LIST OF TABLES

LIST OF TABLES

1. INTRODUCTION

As stipulated by the Advanced Research Projects Agency of the Department of Defense at the outset of this program, the major purpose is to demonstrate that brittle materials can be successfully utilized in demanding high temperature structural applications. ARPA's major program goal is to prove by a practical demonstration that efforts in ceramic design, materials, fabrication, testing and evaluation can by drawn together and developed to establish the usefulness of brittle materials for engineering applications.

The gas turbine engine, utilizing uncooled ceramic components in the hot flow path, was chosen as the vehicle for this demonstration. The progress of the gas turbine engine has been and continues to be closely related to the development of materials capable of withstanding the engine's environment at high operating temperature. Since the early days of the jet engine, new metals have been developed which have allowed a gradual increase in operating temperatures. Today's nickel-chrome superalloys are in use, without cooling, at turbine inlet gas temperatures of 1800° to 1900°F. However, there is considerable incentive to further increase turbine inlet temperature in order to improve specific air and fuel consumptions. The use of ceramics in the gas turbine engine promises to make a major step in increasing turbine inlet temperature to 2500°F. Such an engine offers significant advances in efficiency, power per unit weight, cost, exhaust emissions, materials utilization and fuel utilization. Successful application of ceramics to the gas turbine would therefore not only have military significance, but would also greatly influence our national concerns of air pollution, utilization of material resources, and the energy crisis.

At the program beginning, the application of ceramics was planned for two gas turbine engines of greatly different size. One was a small vehicular turbine of about 200 HP (contractor Ford) and the other was a large stationary turbine of about 30 MW (subcontractor Westinghouse). In the vehicular turbine project, the plan was to develop an entire ceramic hot flow path including the highly stressed turbine rotors. In the stationary turbine project, the engine being so large, plans were confined to the development of ceramic first stage stator vanes, and design studies of ceramic rotors. One difference in philosophy between the projects is worth noting. Because the ceramic materials, fabrication processes, and designs were not developed, the vehicular turbine engine was designed as an experimental unit and featured ease of replacement of ceramic components. Iterative developments in a component's ceramic material, process, or design can therefore be engine-evaluated fairly rapidly. This work can then parallel and augment the time-consuming efforts on material and component characterization, stress analysis, heat transfer analysis, etc. Some risk of damage to other components is present when following this approach, but this is considered out-weighed by the more rapid acquisition of actual test information. On the other hand, the stationary turbine engine is so large, so expensive to test, and contains such costly and long lead-time components which could be damaged or lost by premature failure, that very careful material and design work must be performed to minimize the possibility of expensive, time-consuming failures during rig testing and, even more critically, during engine testing. These anticipated difficulties in applying ceramics to a large stationary turbine engine have been substantiated to the extent that the scope of work for the stationary turbine project was revised to demonstrate ceramic stator vanes in a static test rig rather than the formidable task of testing in an actual 30 MW test turbine engine [8].

It should be noted that both the contractor and sub-contractor had in-house research programs in this area prior to initiation of this program. Silicon nitride and silicon carbide had been selected as the primary material candidates. Preliminary design concepts were in existence and, in the case of the vehicular engine, hardware had been built and testing had been initiated.

At the outset, the program was considered to be both highly innovative and risky. However, it showed promise of large scale financial and technological payoff as well as stimulation of the pertinent technical communities. This reporting period is in the fifth year of the program and major accomplishments have been achieved. In the vehicular turbine project, the first 100 hour durability demonstration of stationary ceramic hot flow path components (a nose cone and stator, two shrouds and a spacer) was carried out in an engine completely coupled with a control system and producing power. In addition, a partially bladed ceramic turbine rotor has been tested in an experimental high temperature gas turbine engine up to a speed of 52,800 rpm and turbine inlet temperature of 2650°F before subsequent failure. In the stationary turbine project ceramic stator vanes have been tested in a static test rig for 100 cycles up to temperatures of 2500°F. This latter accomplishment meets the revised objectives for the stationary turbine project and therefore this project is completed as of the end of this reporting period.

This is the 10th semi-annual report of progress. The format is different than previous reports in that the stationary turbine project has been completed while the vehicular turbine project is continuing. The report of the last six months progress on the stationary turbine project will be included in the final report for that project and published separately [17]. This and future interim reports will cover the progress and accomplishments on the vehicular turbine project.

Note: Numbers in parantheses refer to references listed in Section 5.0.

2. INTRODUCTION AND SUMMARY

The principal objective of the Vehicular Turbine Project is to develop ceramic components and demonstrate them in a 200-HP size high temperature vehicular gas turbine engine. The entire hot flow path will comprise uncooled parts. The attainment of this objective will be demonstrated by 200 hours of operation over a representative duty cycle at turbine inlet temperatures of up to 2500°F. Successful completion of this program objective demonstrates that ceramics are viable structural engineering materials, but will also represent a significant breakthrough by removing the temperature barrier which has for so long held back more widespread use of the small gas turbine engine.

Development of the small vehicular regenerative gas turbine engine using superalloy materials has been motivated by its potentially superior characteristics when compared with the piston engine. These include:

- Continuous combustion with inherently low exhaust emissions
- Multi-fuel capability
- Simple machine - fewer moving parts
- Potentially very reliable and durable
- Low maintenance
- Smooth, vibration-free production of power
- Low oil consumption
- Good cold starting capabilities
- Rapid warm-up time

With such impressive potential, the small gas turbine engine using superalloys has been under investigation by every major on-highway and off-highway vehicle manufacturer in the world.

In addition, the small gas turbine engine without exhaust heat recovery (i.e., non-regenerative) is an existing, proven type of power plant widely used for auxiliary power generation, emergency standby and continuous power for generator sets, pump and compressor drives, air supply units, industrial power plants, aircraft turboprops, helicopter engines, aircraft jet engines, marine engines, small portable power plants, total energy systems, and hydrofoil craft engines. While this variety of applications of the small gas turbine using superalloys is impressive, more widespread use of this type engine has been hampered by two major barriers, efficiency and cost. This is particularly so in the case of high volume automotive applications.

Since the gas turbine is a heat engine, efficiency is directly related to cycle temperature. In current small gas turbines, maximum temperature is limited not by combustion, which at stoichiometric fuel/air ratios could produce temperatures well in excess of 3500°F, but by the capabilities of the hot component materials. Today, nickel-chrome superalloys are used in small gas turbines where blade cooling is impractical, and this limits maximum turbine inlet gas temperature to about 1800°F. At this temperature limit, and considering state-of-the-art component efficiencies, the potential overall efficiency of the small regenerative gas turbine

is not significantly better than that of the gasoline engine and not as good as the Diesel. On the other hand a ceramic gas turbine engine operating at 2500°F will have fuel economies superior to the Diesel at significant weight savings.

The other major barrier is cost and this too is strongly related to the hot component materials. Nickel-chrome superalloys, and more significantly cobalt based superalloys which meet typical turbine engine specifications, contain strategic materials not found in this country and cost well over $5/lb.; this is an excessive cost with respect to high volume applications such as trucks or automobiles. High temperature ceramics such as silicon nitride or silicon carbide, on the other hand, are made from readily available and vastly abundant raw materials and show promise of significantly reduced cost compared to superalloys, probably by at least an order of magnitude.

Thus, successful application of ceramics to the small gas turbine engine, with an associated quantum jump to 2500°F would not only offer all of the attributes listed earlier, but in addition offer superior fuel economy and less weight at competitive cost with the piston engine.

2.1 VEHICULAR TURBINE PROJECT PLAN

The vehicular turbine project is organized to design and develop an entire ceramic hot flow path for a high temperature, vehicular gas turbine engine. Figure 2.1 shows a schematic of this regenerative engine. Air is induced through an intake silencer and filter into a radial compressor, and then is compressed and ducted through one side of each of two rotary regenerators. The hot compressed air is then supplied to a combustion chamber where fuel is added and combustion takes place.

The hot gas discharging from the combustor is then directed into the turbine stages by a turbine inlet nose cone. The gas then passes through the turbine stages which comprise two turbine stators, each having stationary airfoil blades which direct the gas onto each corresponding turbine rotor. In passing through the turbine, the gas expands and generates work to drive the compressor and supply useful power. The expanded turbine exhaust gas is then ducted through the hot side of each of the two regenerators which, to conserve fuel, transfer much of the exhaust heat back into the compressed air. The hot flow path components, subject to peak cycle temperature and made out of superalloys in today's gas turbine, are the combustor, the turbine inlet nose cone, the turbine stators, the turbine tip shrouds, and the turbine rotors. These are areas where the use of ceramics could result in the greatest benefits, therefore these components have been selected for application in the vehicular turbine project.

Successful development of the entire ceramic flow path, as demonstrated in a high temperature vehicular gas turbine engine, will involve a complex iterative

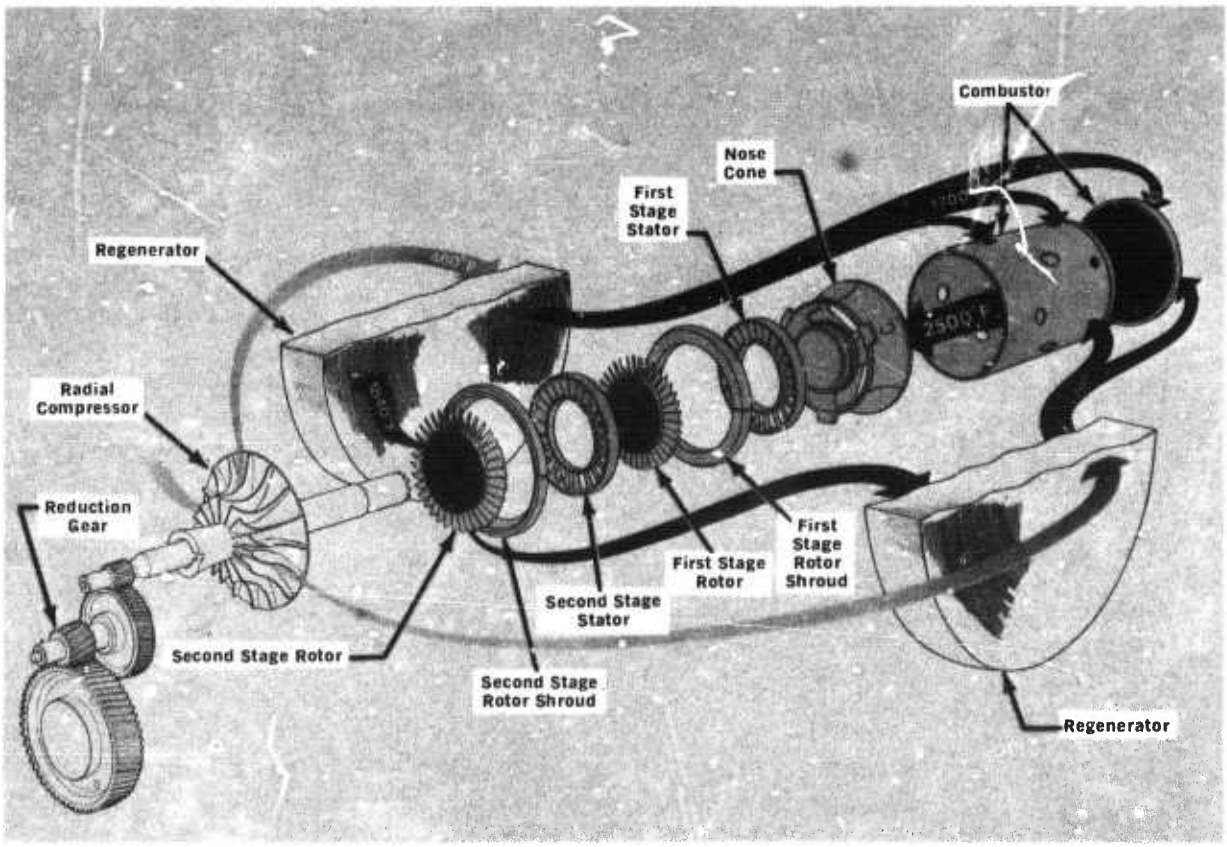

Figure 2.1 Schematic View of the Vehicular Gas Turbine Engine Flowpath

development. Figure 2.2 shows a block diagram flow chart, including the feedback loops, of the major factors involved, and serves to illustrate the magnitude of this complex and comprehensive iterative development program. Of particular importance is the inter-relationship of design, materials development, ceramic processes, component rig testing, engine testing, non-destructive evaluation and failure analysis. One cannot divorce the development of ceramic materials from processes for making parts; no more so can one isolate the design of those parts from how they are made or from what they are made. Likewise, the design of mountings and attachments between metal and ceramic parts within the engine are equally important. Innovation in the control of the environment of critical engine components is another link in the chain. Each of these factors has a relationship with the others, and to obtain success in any one may involve compromises in the others. Testing plays an important role during the iterative development since it provides a positive, objective way of evaluating the various combinations of factors involved. If successful, the test yields the credibility to move on to the next link in the development chain. If unsuccessful the test flags a warning and prompts feedback to earlier developments to seek out and solve the problem which has resulted in failure. Finally, all of the links in the chain are evaluated by a complete engine test, by which means the ultimate objective of the program will be demonstrated. It is important then to recognize that this is a systems development program — no single area is independent, but each one feeds into the total iterative system.

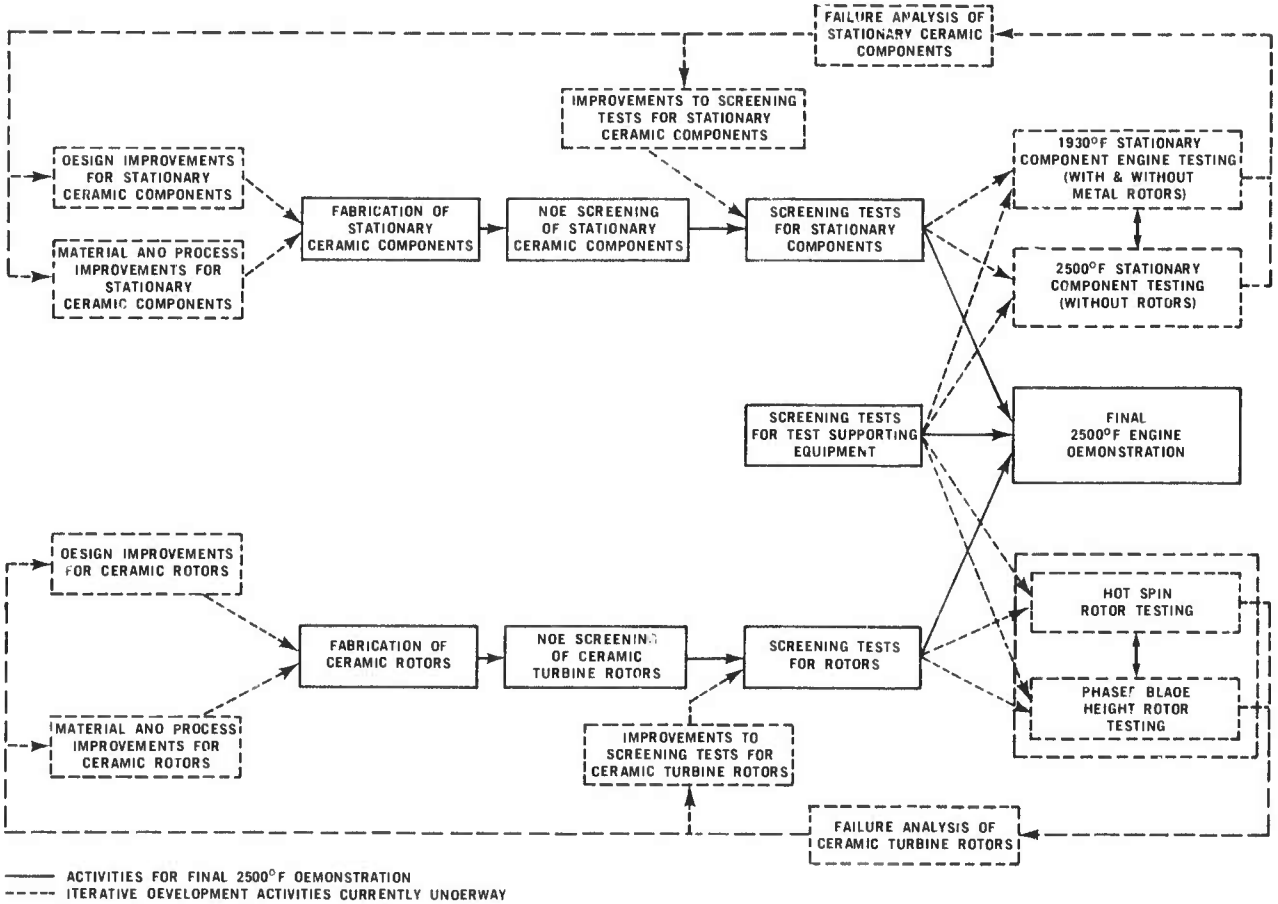

Figure 2.2 ARPA/Ford Ceramic Turbine [illegible]-Major Project and Development Loops

2.2 PROGRESS AND CUMULATIVE STATUS SUMMARY

To meet the program objectives, the work has been divided into two major tasks.

1. Ceramic Component Development

2. Materials Technology

The progress and present status in each of these is summarized in Section 2.2.1 and 2.2.2.

2.2.1 CERAMIC COMPONENT DEVELOPMENT

Two categories of ceramic components are under development: rotating parts (i.e. ceramic rotors), and stationary parts (i.e. ceramic stators, rotor shrouds, nose cones, and combustors). In this iterative development, each component will pass through various phases comprising design and analysis, materials and fabrication, and testing.

Ceramic Rotors

The development of the ceramic turbine rotors is by far the most difficult task in the ARPA program. This is because of:

- the very complex shape of the turbine rotor forcing the development of new and unique fabrication capabilities.
- the high centrifugal stresses associated with maximum rotor speeds of 64,240 rpm.
- the high thermal stresses and associated thermal fatigue resulting from both steady state and transient high temperature gradients from the rotor rim to the rotor hub.
- the hostile environment associated with the products of combustion from the combustor.
- the high temperature of the uncooled blades resulting from turbine inlet gas temperatures of 2500^{o}F.

During the last reporting period, a Turbine Rotor Fabrication Task Force was established to maximize the effort on duo-density silicon nitride turbine rotor fabrication by deferring all work on stationary ceramic component fabrication and material problems. During this reporting period, the Task Force was continued and met its goals of establishing the major process parameters for fabricating duo-density silicon nitride turbine rotors. While process refinements, particularly with respect to hot pressed silicon nitride starting powders, are still required to produce flaw-free rotors, the decision was made to wind-down the Task Force so that fabrication of stationary ceramic components could be resumed during this reporting period.

Progress and Status

- Fully dense Si_3N_4 first and second stage integral rotors were designed and analyzed [1,2,3,4].
- A method of attaching rotors was conceived and designed [1,2].
- The following approaches for making integral rotors were investigated but discontinued:
  - Direct hot pressing of an integral Si_3N_4 rotor [1].
  - Ultrasonic machining of a rotor from a hot pressed Si_3N_4 billet [1,2,3].
  - Hot pressing an assembly of individually hot pressed Si_3N_4 blades [1,2].
  - Pseudo-isostatic hot pressing of an injection molded Si_3N_4 preform [1,2,3].
  - Hot pressing using comformable tooling of preformed Si N blades and hub [2,3,4].
  - Fabrication of a dense SiC blade ring by chemical vapor desposition [1,2,3,4].
  - Electric discharge machining of a rotor from a hot pressed SiC billet [2,3,4].
- A "duo-density" Si_3N_4 ceramic rotor was conceived and designed [3].
- Tooling to injection mold Si_3N_4 blade rings was designed and procured [3].
- Over 375 hot press bonding of duo-density rotors were carried out [10]. These have progressed from rotors with flat-sided hubs to current fully-countoured hubs made simultaneously with the hot press bonding operation. Prior severe blade ring distortion problems have been solved by using a double blade fill to support the blade ring during bonding. In addition, the diffusion bond has been improved to its current excellent quality as evidenced by microstructural examination. New experiments were conducted using magnesium nitrate instead of magnesium oxide as a densification aid. Excellent bonding and density were achieved but strength was deficient. Successful modifications were made to the graphite wedge system to reduce blade ring cracking and tearing problems. Problems which remain are occasional blade ring and rim cracking [4,5,6,7,8].
- Over 110 cold spin tests resulted in blade failures over a range of speeds, some of which exceeded full speed requirements of the new Design D' blading. However, an improvement in consistency is required if a reasonable yield from the blade ring fabrication process is to be achieved. This emphasizes the need for three-dimensional blade stress analysis as well as development of a higher strength, better quality blade material. Cold spin testing of rotor hubs of hot pressed Si N showed a characteristic failure speed of 115,965 rpm with a Weibull rpm slope of 17.66 [7]. Several hot pressed hubs, made by the hot press bonding process, were cold spun to destruction, and showed results consistent with the hot pressed hubs [8]. A high speed motion picture study (3000 frames/sec) was conducted of a turbine rotor failure in the cold spin pit [8].
- A three dimensional model of the rotor blade along with heat transfer coefficients has been generated for three dimensional thermal and stress analysis [5,6,8].

- Development of a better quality blade rings continues. X-ray radiography of green parts has proved effective in detecting major flaws. Slip cast Si_3N_4 test bars having a density of 2.7 gm/cm^3 show four point MOR of 40,000 psi therefore, processes to slip cast a rotor blade ring are under investigation as are methods of achieving 2.7 gm/cm^3 density with injection molded material [6,7,8].

- Thermal shock testing simulating the engine light-off condition was conducted on rotor blade rings for approximately 2,500 cycles without damage [5,6].

- A technique to evaluate probability of failure using Weibull's theories was developed, and applied to ceramic rotors [5].

- A test rig was designed and built to simulate the engine for hot spin testing of ceramic rotors [3,4,5]. A set of low quality duo-density rotors was spin tested to 20% speed and 1950°F for a short time before failure, believed due to an axial rub [7].

- A revised rotor design (Design D) was conceived, using common rotors at first and second stage locations [7].

- A lower stress version of the Design D rotor, designated Design D', has been designed using radially stacked blade sections. Blade centrifugal stresses were reduced from 21,000 psi in Design D to 12,180 psi in Design D' [8].

- The rotor test rig was rebuilt and testing initiated to evaluate the rotor attachment mechanism and the curvic coupling mounting design. Hot-pressed Si_3N_4 rotor hubs were subjected to 10 operating cycles from 900 to 1950°F, during a 3-3/4 hour test, without damage [8].

- Design codes for ceramics were refined to include nonlinear thermal properties of materials and to allow for the specification of the MOR-strength and Weibull "m" requirements for a given failure at a specified loading and reliability level [9,10].

- Rotor hubs were successfully densified and press bonded at both 2% and 3-1/2% MgO levels, resulting in elimination of MgO migration into the blade ring and improved high temperature strength over previous pressings with 5% MgO [9].

- A design C duo-density rotor with a few obvious flawed blades removed was cold spin tested after static oxidation at 1900°F for 200 hours. A single half-blade failure occurred at 53,710 rpm, which corrects to 68,000 rpm or 105% speed for the present shorter bladed Design D configuration. The results of a number of spin tests of slip cast Si_3N_4 blade segments were combined to yield a median failure speed of 64,000 rpm [9].

- Over five hundred blade rings, previous to Design D', were injection molded for press bonding experiments, cold spin tests, and hot tests [9].

- New tooling to injection mold lower stressed Design D' rotor blade rings was received and trial moldings to establish molding parameters were initiated [9].

- Progress has been made in several aspects of the press-bonding step of duo-density rotor fabrication. A problem of excessive deflection of the graphite support structure beneath the rotor assembly, permitting bending and subsequent blade fracture, was solved by the substitution of high modulus hot pressed SiC for the low modulus graphite. Increasing the rate of pressure application also improved the quality of the hub sections [9].

- A new hot spin test rig, designed to improve the turn-around-time in testing turbine rotors, has been constructed, and is currently in the shakedown testing phase. Using gas burners instead of a gas turbine combustion system, this rig simulates the engine environment and was designed to be quickly rebuilt following rotor failures [9].

- In the program to engine evaluate ceramic rotors having reduced blade length (and less risk of catastrophic failure), two duo-density Si_3N_4 rotors with the blades shortened to 10% of the design length have been selected and cold spun to 64,000 rpm [9]. These rotors were then hot tested in an engine for 45 minutes at 32,000 rpm and 2000°F turbine inlet temperature without failure [10].

- The aerodynamic design of the increased efficiency Design E turbine was initiated. Flowpath optimization, a one dimensional stress analysis, and preliminary detailed blade section definition were completed for both the first and second stage turbine strators and rotors [9].

- A process has been developed to slip cast turbine rotor blade rings [9].

- 3-D stress and reliability analyses were performed on preliminary blade configurations for the increased efficiency Design E turbine rotors [10].

- 500 Design D' blade rings have been injection molded which will nitride to 2.7 g/cc density [10].

- A new fabrication approach to make duo-density silicon nitride turbine rotors in three pieces was conceived and demonstrated a significant reduction of applied loads during hot press bonding generally eliminating blade and rim cracking [10].

- Good correlation was demonstrated between predicted cold burst speed and actual spin test results on nine rotor hubs spun to destruction [10].

- Six available duo-density turbine rotors of imperfect quality were used to check out the hot spin rigs by hot spin testing to failure speeds ranging from 12,000 rpm to 35,300 rpm at rotor rim temperatures of 1780° to 2250°F, (corresponding to equivalent blade tip temperatures in an engine estimated to be 1930°F to 2400°F) [10].

- Duo-density rotor #709 with flawed blades removed achieved 52,800 rpm in the modified design engine with ceramic stationary flowpath prior to an unscheduled dynamometer shutdown. A maximum turbine inlet temperature of 2650°F was observed during this run. Post inspection showed all ceramic parts to be crack free. A rotor failure occurred on a subsequent run at 50,000 rpm and 2300°F T.I.T. [10].

Ceramic Stators, Rotor Shrouds, Nose Cones, and Combustors

While development of the ceramic turbine rotor is the most difficult task, development of the stationary ceramic flow path components is also necessary to meet the objective of running an uncooled 2500°F vehicular turbine engine. In addition, success in designing, making, and testing these ceramic components will have an important impact on the many current applications of the small gas turbine where stationary ceramics alone can be extremely beneficial. The progress and status of these developments is summarized below, taking each component in turn.

Progress and Status

CERAMIC STATORS

- Early Design A first stage stators incorporating the turbine tip shrouds had been designed, made by assembling individual injection molded Si_3N_4 vanes, and tested, revealing short time thermal stress vane failures at the vane root [1].

- Investigations of a number of modified designs led to Design B where the rotor shroud was separated from the stator. Short time thermal stress vane failures at the vane root were eliminated [1].

- In the fabrication of stators, the starting silicon powder, the molding mixture and the nitriding cycle were optimized for 2.2 gm/cm^3 density (18 ksi-MOR) material [2,3].

- Engine and thermal shock testing of first stage Design B stators revealed a longer term vane cracking problem at the vane mid-span. This led to modification of the vane cord, designated the Design C configuration, which solved the vane mid-span cracking problem [3].

- A remaining problem in first and second stage Design B stators was cracking of outer shrouds, believed due to the notch effect between adjacent vanes. To solve this, tooling for a one-piece first stage Design C stator was procured [4,5].

- The Design B second stage stator could not be made in one piece due to vane overlap, so an "inverted channel" design was investigated to eliminate notches at the outside diameter. However, engine testing showed that axial cracking of the outer shroud remained a problem [3,4,5,6].

- A 50 hour duty-cycle engine test of the hot flow path components to 1930°F was completed. The assembled first stage Design C stator was in excellent condition; 8 out of 33 vanes in the second stage inverted channel stator had developed fine cracks [6].

- A 100 hour duty-cycle engine test of the hot flow path components (without a second stage stator) to 1930°F was completed. The reaction bonded silicon nitride (2.55 g/cc density) one piece first stage Design C stator successfully survived this test [7].

- Improvements in materials and processing resulted in the fabrication of flaw free one piece stators of 2.55 gm/cm^3 density [8].

- A test was devised for mechanically loading stator vanes to failure which provided useful information for material and process development [8].

- Thermal shock testing of 2.7 gm/cm^3 density stator vanes revealed no detectable cracking and negligible strength degradation after 9000 cycles of heating to 2700°F and cooling in the thermal shock rig [8].

- Processing of 2.55 gm/cm^3 density injection molded stators continued. Consistently high weight gains (61-62%) have been obtained using the Brew all-metal furnace employing a slow, gradual rate-of-rise cycle, 4% H_2- 96% N_2 gas under static pressure, and Si_3N_4 setters and muffles [9].

- An injection molded stator of 2.55 gm/cm^3 density Si_3N_4 survived static testing (no rotors) for 175 hours at 1930°F steady state. Weight gain of the stator was less

than 1%, which stabilized after 10 hours of testing. The stator is in excellent condition [9].

- Testing of stators up to 2500°F in the Flow Path Qualification Test Rig was initiated with over eight hours of testing accumulated at 2500°F [9].

- A reaction bonded silicon carbide stator successfully accumulated 147 hours of testing at 1930°F and remains crack free [10].

- Over nine hours of testing a silicon nitride stator were accumulated without incident in themodified engine configuration to a maximum turbine inlet temperature of 2650°F [10].

CERAMIC ROTOR SHROUDS

- Separate first and second stage ceramic rotor shrouds, which are essentially split rings, evolved in the stator change from Design A to Design B [1].

- As a result of rig and engine testing, rotor shrouds made of cold pressed, reaction sintered Si_3N_4 were modified to have flat rather than conical side faces [2].

- Because of occasional cracking, cold pressing was replaced with slip casting for making higher density rotor shrouds, resulting in 2-3 times increase in strength [3].

- Slip casting of rotor shrouds solved the cracking problem but revealed a dimensional change problem as a function of operating time. This was solved by incorporation of nitriding aids and heat treatment cycles and other changes in the fabrication process which reduced instability to acceptable levels [4,5,6].

- A 50 hour duty cycle engine test of the hot flow path components to 1930°F was completed, after which both first and second stage rotor shrouds were in excellent condition [6].

- A 100 hour duty-cycle engine test of the hot flow path components to 1930°F was completed, after which both first and second stage rotor shrouds were in excellent condition [7].

- Further testing of rotor shrouds to 245 hours and over 100 lights showed them to remain crack free and in excellent condition [7].

CERAMIC COMBUSTOR

- Combustor tubes made of slip cast Si_3N_4 and various grades of recrystallized SiC (Crystar) cracked during light off tests in the combustor rig [4].

- A thick-walled, reaction bonded silicon carbide (REFEL) combustor successfully completed the 200 hour duty cycle. A total of 26 hours and 40 minutes was accumulated at 2500°F turbine inlet temperature [10]. This combustor was also successfully tested in an engine [8].

- Three thin-walled, reaction bonded silicon carbide (REFEL) combustors were successfully qualified over a 10 hour portion of the ARPA duty cycle [10].

- Over nine hours of testing a first and second stage rotor tip shroud were accumulated without incident in the modified engine configuration to a maximum turbine inlet temperature of 2650°F [10].

CERAMIC NOSE CONES (with integral transition duct)

- Early Design A nose cones had been designed, made from injection molded reaction sintered Si_3N_4, and tested [1].

- The nose cone was modified to Design B to accommodate the Design B first stage stator. Several Design B nose cones were made and tested in rigs and engines [2].

- Voids in molding nose cones were minimized by preferentially heating the tooling during molding [5].

- Circumferential cracking and axial cracking problems led to preslotted, scalloped nose cones designated Design C [3, 4, 5, 6].

- A 50 hour duty-cycle engine test of the hot flow patch components to 1930°F was completed, after which the Design C nose cone was in excellent condition [7].

- A 100 hour duty-cycle engine test of the hot flow path components to 1930°F was completed, after which the Design C nose cone was in excellent condition [7].

- Further such testing of the 2.2 g/cc density nose cone to 221 hours showed it to remain crack free and in excellent condition [7].

- Improvements in materials and processing resulted in the fabrication of flaw free nose cones of 2.55 gm/cm^3 density [8].

- Processing of 2.55 gm/cm^3 density injection molded nose cones continued. Consistently high weight gains (61-62%) have been obtained using the Brew all-metal furnace employing a slow, gradual rate-of-rise cycle, 4% H- 96% N gas under static pressure and Si_3N_4 setters and muffles [9].

- Testing of nose cones up to 2500°F in the Flow Path Qualification Test Rig was initiated with over eight hours of testing accumulated at 2500°F [9].

- Over nine hours of testing a silicon nitride nose cone were accumulated without incident in the modified engine configuration to a maximum turbine inlet temperature of 2650°F [10].

2.2.2 MATERIALS TECHNOLOGY

Materials technology forms the basis for component development including component design, component fabrication, material quality in the component as-made, and evaluation by testing. There are three major categories under materials technology — materials engineering data, materials science, and non-destructive evaluation. Progress and present status in each of these areas is summarized below:

Materials Engineering Data

- Techniques were developed and applied for correlating the strength of simple ceramic spin disks with bend test specimens using Weibull probability theories [5].
- Elastic property data as a function of temperature was determined for various grades of silicon nitride and silicon carbide [2, 3, 4, 5, 6, 7, 9].
- The flexural strength vs. temperature of several grades of SiC and Si_3N_4 was determined [3, 4, 5, 6, 9, 10].
- The compressive strength vs. temperature of hot pressed SiC and hot pressed Si_3N_4 was determined [4].
- Creep in bending at several conditions of stress and temperature was determined for various grades of reaction sintered silicon nitride [4, 5, 6, 9].
- The specific heat vs. temperature of 2.23 gm/cm^3 reaction sintered Si_3N_4 was measured, as were thermal conductivity and thermal diffusivity vs. temperature for both 2.23 gm/cm^3 and 2.68 gm/cm^3 reaction sintered Si_3N_4 [4].
- Stress-rupture data was obtained for reaction sintered silicon nitride under several conditions of load and temperature [6, 9, 10].
- A group of 31.2.7 gm/cm^3 density injection molded Si_3N_4 test bars, made using the best current nitriding cycle and an atmosphere of 4% H_2, 96% N_2, resulted in a Weibull characteristic strength of 44.3 ksi and an m value of 6.8. Additional material development work is aimed at obtaining a higher m value [9].
- The effects of surface finish and post machining heat treatment on the room temperature strength of hot pressed silicon nitride were determined [10].
- The variation in MOR of hot pressed silicon nitride was determined from rotor-to-rotor, within one rotor and as a function of initial material preparation [10].
- Room and elevated temperature flexure strengths of injection molded reaction sintered silicon nitride of 2.7g/cc were determined [10].
- No time dependent failures were observed for 2.7g/cc injection molded reaction sintered silicon nitride up to 200 hours at stresses of 20-30 ksi and temperatures of 1900-2200°F [10].

Materials Science

- A technique was developed and applied to perform quantitative x-ray diffraction analyses of the phases in silicon nitride [2].

- An etching technique was developed and used for the study of the microstructure of several types of reaction sintered silicon nitride [2].

- The relationship of some processing parameters upon the properties of reaction sintered Si_3N_4 were evaluated [3,4,5,6,10].

- The oxidation behavior of 2.2 gm/cm^3 density Si_3N_4 was determined at several different temperatures. The effect of oxidation was found to be reduced when the density of reaction sintered Si_3N_4 increased [3,7].

- The relationship of impurities to strength and creep of reaction sintered silicon nitride was studied, and material was developed having considerably improved creep resistance [4,5,6,9].

- Fractography and slow crack growth studies were performed on reaction sintered SiC [5] and hot pressed Si_3N_4. [6,7].

- The development of sintered Sialon-type materials was initiated [7]. The effects of Yttria additives are being studied expecially as it relates to the formation of glassy phases [8,10].

- A higher density (2.72 gm/cm^3) molded Si_3N_4 has been developed which will be used for component fabrication. Four point bend strengths of 43 ksi at room temperature were measured [8].

- An experimental study showed that high pressures did not facilitate nitriding of relatively dense silicon compacts. A parallel theoretical study showed that to store sufficient nitrogen within the pores and avoid diffusion an impractically high pressure would be needed [8].

- Three techniques to improve the oxidation resistance of 2.7 gm/cm^3 injection molded Si_3N_4 were evaluated [9].

- Nitriding exotherms resulting in localized silicon temperatures in excess of 1420°C produced silicon "melt out" with resulting large porosity and lower strength. Eliminating these exotherms by controlling furnace temperature appears to be the key to uniform microstructure, fine porosity and higher strengths [10].

Non-Destructive Evaluation

- Ultrasonic C-scan techniques were developed and applied for the measurement of internal flaws in turbine ceramics [1,2,3,4].

- Sonic velocity measurements were utilized as a means of quality determination of hot pressed Si_3N_4 [2,3,5,9].

- A computer-aided-ultrasonic system was used to enhance the sensitivity of defect analysis in hot pressed Si_3N_4 [3,4,6].

- Acoustic emission was applied for the detection of crack propagation and the onset of catastrophic failure in ceramic materials [1,2,5,6].

- A method was developed and applied for the detection of small surface cracks in hot pressed Si_3N_4 combining laser scanning with acoustic emission [4].

- X-ray radiography was applied for the detection of internal defects in turbine ceramics [2,3,4,5].

- Hidden flaws in as-molded stators and rotor blade rings were located by x-ray radiography [5,6,7]. Such NDE of as-molded parts has been used to develop processes to make flaw-free components [8].

- A dye penetrant has been used to detect surface cracks in components made of the 2.55 gm/cm^3 Si_3N_4 [8].

- A state-of-the-art summary of NDE methods as applied to the ceramic turbine programs was compiled [6].

- 500 injection molded blade rings were examined, most of them in detail using 30X magnification and X-ray radiography NDE techniques[10].

2.3 FUTURE PLANS

Section 2.2 of this report summarizes the progress made in ceramic component development and materials technology over the contract period. Significant accomplishments have been realized, though there are still problems to be solved before achieving the target demonstration of stationary flow path components and ceramic turbine rotors.

Ceramic Component Development

A major effort during the next reporting period will concentrate on the three-piece duo-density silicon nitride turbine rotor. Although flaw-free rotor blade rings have been fabricated, improvements to the injection molding process are planned to increase yield. A new gating configuration is planned together with closer quality control over material preparation which should reduce subsurface voids. In addition, a solid state control system to control time and temperature of all phases of the injection molding process is expected to improve the repeatability of fabrication.

The design change to a three piece rotor greatly reduced the incidence of blade breakage and gross rim distortions occurring during hot press bonding, but additional process refinements are required to eliminate minor blade cracking and maximize the strength and Weibull modulus of the hot pressed materials.

Evaluation of the improved hot press bonded rotor hub material will be carried out in order to update the reliability analysis of the rotors utilizing the latest 3-D probabilistic design codes. The analytical investigation of time dependent failure modes of rotors due to subcritical crack growth is planned. Correlation analysis of predicted versus actual burst speeds will continue in an effort to refine the analytical tools utilized to design ceramic components.

Further refinements will be incorporated into the two hot spin test rigs to insure greater consistency of test conditions and to improve the quality of monitoring data used in the failure analysis of turbine rotors. In terms of 2500°F engine testing, further work is required on the modified engine configuration to check out its durability at high speeds and temperatures. A second engine will be converted to the modified engine design to increase the capability of engine testing ceramic turbine rotors up to 2500°F.

The fabrication and testing of improved stationary hot flow path components will be resumed. The injection molding of one-piece monolithic stators of 2.7 g/cc density will begin. The improved oxidation resistance of this material should significantly increase the stator's outer shroud life. Stator testing in the 2500°F flow path qualification rig, the ceramic structures rigs and in regular and modified engines will be conducted to confirm the life improvement. The redesigned nose cone tooling and improvements made to the injection molding control system should reduce the incidence of molded flaws in nose cones. Nose cones of 2.7 g/cc density will be evaluated in rigs and engines to determine if further improvements are necessary to meet the 200 hour goal. Slip cast turbine rotor tip shrouds will also be evaluated in rigs and engines.

Materials Technology

Work is continuing to improve room temperature strength, high temperature strength and Weibull, 'm', value of hot pressed silicon nitride used in duo-density turbine rotor fabrication. Principal approaches include the use of high purity silicon nitride starting powders, refined powder processing and closer control

over critical hot pressing parameters. These improvements will be confirmed by the continuing effort to characterize the material with a statistically significant number of test specimens.

Further work is planned on improving the nitridation processing of reaction sintered silicon nitride components. Closer temperature control to reduce local nitriding exotherms will be investigated with respect to finer porosity, more uniform microstructure and associated higher strengths. The effect of furnace load on component strength will continue to be investigated in an effort to increase the production capability of fully nitrided, high strength parts.

The slip casting process will be further investigated in order to develop a slip with less sensitive parameters that will produce components which can be fully nitrided. Other process modifications are aimed at increasing the strength on a consistent basis thereby improving the yield of useable components.

Improvements in injection molding will be realized through further refinement and control of the molding parameters used to fabricate components in addition to tighter quality control over material preparation. Further characterization of room and high temperature strengths combined with additional stress rupture/creep testing will provide the material data required for reliability and failure analyses of ceramic turbine rotors.

Statistical techniques will continue to be developed in the areas of parameter estimation and confidence interval estimates and will be included in the next report. In addition development of significance testing and goodness of fit tests will be undertaken and published in a later report.

3. PROGRESS ON CERAMIC COMPONENT DEVELOPMENT

3.1 DUO-DENSITY CERAMIC ROTOR DEVELOPMENT

SUMMARY

To provide for testing ceramic turbine rotors over the full speed range at turbine inlet temperatures of up to 2500°F, the hot gas flow path of an 820 turbine engine was modified to allow a portion of the compressor delivery and combustor entry air to re-enter the main hot gas flow path upstream of the regenerators to protect them from over-temperatures.

An approach to make duo-density rotors in three pieces has been conceived; these three pieces consist of the blade ring, the inner hub, and an intermediate bonding ring between the hub and blade ring. The purpose was to minimize the press bonding forces contributing to damage of the blade ring, and to achieve better control of material strength in the hub region. A strength analysis of the three piece, first stage rotor was conducted on the basis of desired reliability or known material properties. Strength requirements for 95% + reliability of the three piece concept appear achievable with known physical properties of silicon nitride.

Analysis of the improved efficiency Design E turbine rotors continued. Blade sections for first and second stage stators were designed and a two-dimensional gas flow analysis indicates the diffusion parameters to be acceptable. A three dimensional finite element stress analysis and a probability of failure analysis were conducted for the first stage rotor and several designs of the second stage rotor.

The new D' rotor tooling was utilized to injection mold approximately 500 blade rings of 2.7 gm/cm^3 silicon nitride material most of which were examined in detail by 30X visual magnification and by X-ray radiography. After nitriding, a total of 12 visual and X-rayed flaw free parts were obtained. A number of additional desired mechanical and process changes have been identified and are being incorporated to improve the yield of flaw-free blade rings.

Development of a system of blade filling of rotor blade rings prior to press bonding has been completed. The system produces repeatable results and consists of centrifugally casting a low density silicon slip between and around the blades utilizing a special fixture developed for this purpose. A graphite and plaster block fixture is used to form the cavity for casting of the low density silicon slip and a BN coating is used to prevent bonding between the blade fill and rotor blades. After casting, the assembly is dried, nitrided, and machined preparatory to press bonding. After press bonding, a CO_2 laser is used to cut through the blade fill for easy removal of the blade inserts.

In the graphite wedge hot press bonding system used to fabricate duo-density turbine rotors, the graphite base plates have been removed and replaced with high density SiC, which has eliminated the base plate permanent deformation problem. Alignment of the press rams and the furnace in the press was improved to alleviate out-of-parallelism of the graphite piston faces. An important development during this reporting period was that of a new approach to make duo-density silicon nitride turbine rotors in three pieces to effect a significant reduction of loads during the hot press bonding process. In this concept, a pre-formed hot pressed silicon nitride hub is hot press bonded to a reaction sintered silicon nitride blade ring by means of a separate bonding ring of hot pressed silicon nitride. The advantages of this system are reduced damage to the blade ring because of lowered hot pressing forces, and greater flexibility in the fabrication of the center hub since it is formed

in a separate operation. Problems of inconsistent density in the bonding ring were overcome by a slight change to the hot pressing piston dimensions at the expense of additional final contour machining. Several three piece duo-density rotors were made for preliminary hot spin testing.

The blade bend test fixture was modified to improve both load application, and indexing of the blade ring to reduce set-up time. Several blade rings were tested on the new fixture to evaluate fabrication methods and material processing.

A correlation analysis was carried out to compare the calculated rotor hub failure distribution, utilizing Weibull theory as applied to brittle materials, versus the actual failure distribution of nine hubs tested to destruction in the cold spin pit. A further five hubs of identical material were used to obtain Weibull MOR bar data for the analysis. Hub burst speeds ranged from 94,570 rpm to 115,810 rpm, with a Weibull slope of 14.8, and characteristic failure speed of 108,500 rpm. The calculated failure distribution is within the 90% confidence bands superimposed on the experimental failure distribution.

Check out of the two hot spin rigs continued; cooling air quantity for metallic components was determined to be satisfactory, and the natural gas burner system is functional. Burst of a rotor hub at 41,000 rpm showed minimal damage to rig parts with the exception of flaring of a pilot diameter on the high speed turbine mounting shaft which led to corrective design modifications. A viewing port for optical measurement of rotor temperatures was added to the rig, and a failure detector was incorporated to shut down the test rig and provide a strip chart failure record. Six available duo-density turbine rotors of imperfect quality were used to check out the rigs by hot spin testing to failure speeds ranging from 12,000 rpm to 35,300 rpm at rotor rim temperatures of 1780°F to 2250°F (corresponding to equivalent blade tip temperatures in an engine estimated to be 1930°F to 2400°F). Preliminary test plans were formulated for validation of analytical predictions of reliability versus speed, temperature and time.

Face splines (Curvic Couplings) are used to mount and pilot the ceramic turbine rotors to the high speed shaft in the engine. Two new lubricants for the curvic coupling teeth were evaluated over an improved test cycle and one of these was successful during one-half hour of engine operation at 2500°F Turbine Inlet Temperature (T.I.T.).

To gain early running experience with ceramic rotors in an engine, two rotors with blades of 10% length were tested for 45 minutes at 32,000 rpm and 2000°F T.I.T. After test, the rotors were undamaged except for evidence of slight abrasion of ceramic surfaces in contact with metal surfaces.

A ceramic rotor was tested at high temperatures in the engine with modified hot flow path ceramic parts to protect the regenerators from over-temperature. The modified ceramic parts were checked out successfully in test rigs and used to build a modified engine. A set of bladeless turbine rotor hubs was used to check out the modified engine. Following this, a poor quality duo-density turbine rotor with ten 90% length aerodynamically functional blades was tested in the engine to 52,800 rpm and 2650°F T.I.T. A rotor failure occurred on a subsequent run at 50,000 rpm and 2300°F T.I.T.

3.1.1 DESIGN AND ANALYSIS

Introduction

An 820 ceramic turbine engine was modified to facilitate testing of ceramic rotors over the full speed range at turbine inlet temperatures of up to 2500°F (1370°C). The modification involved by-passing of cold compressor and preheated combustor inlet air to the downstream side of the turbine stages where it was mixed with hot exhaust gas thereby reducing the turbine exit temperature to a level that was acceptable for safe operation of the regenerators (2000°F).

Strength requirements for the new three piece concept duo-density ceramic rotor were analyzed and plotted using previously derived and reported [9] equations as function of Weibull slope m and reliability requirements.

Increased efficiency design E turbine blading was analyzed for stresses and reliability under centrifugal loading using three dimensional finite element computer codes. Calculated blade ring reliabilities were 98% and 92% for the first and second stages respectively based on a characteristic strength (MOR) of 40 ksi and a Weibull slope of 12. Further analysis is required to assess rotor hub reliabilities and complete rotor reliabilities. Design refinements may be required to maintain high reliabilities under conditions of both centrifugal and thermal stresses.

Modified Engine Design

The Turbine Inlet Temperature (T.I.T.) schedule planned for the 820 ceramic turbine engine is 1930°F over the 55-90% speed range and 1930°F to 2500°F over the 90-100% speed range. The two stage axial turbine extracts work from the hot gases reducing the turbine exit temperature (regenerator inlet) to an acceptable level (about 1840°F at 100% speed and 2500°F T.I.T.). However, during the development phase, ceramic rotors with reduced height blades and/or non-fully bladed rotors[9] need to be engine tested at 2500°F T.I.T. at lower speeds (55-90%) using only one rotor.

To accommodate these developmental testing requirements, the engine design was modified to facilitate 2500°F T.I.T. over the entire speed range without exceeding regenerator inlet temperature limits. The modified engine was used to supplement ceramic rotor testing in the hot spin rigs which is described in section 3.1.3 of this report.

Mechanical Design Modifications

The standard engine configuration, previously shown in Figure 2.1, directs all the compressor delivery air through the regenerators, into the combustor, through the ceramic flowpath and exits through the regenerators. The Design D' flowpath, shown in Figure 3.1, was modified to allow a portion of the compressor delivery air to re-enter the main stream just aft of the turbines and before the regenerator (Figure 3.2). Additional air from the combustor inlet area was routed past the combustor, the nose cone, 1st stator and 1st shroud and re-entered the main stream in the 2nd stage stator location. The amount of air through these two routes can be independently controlled.

The hardware was procurred and tested as reported in sections 3.1.3 and 3.2 of this report.

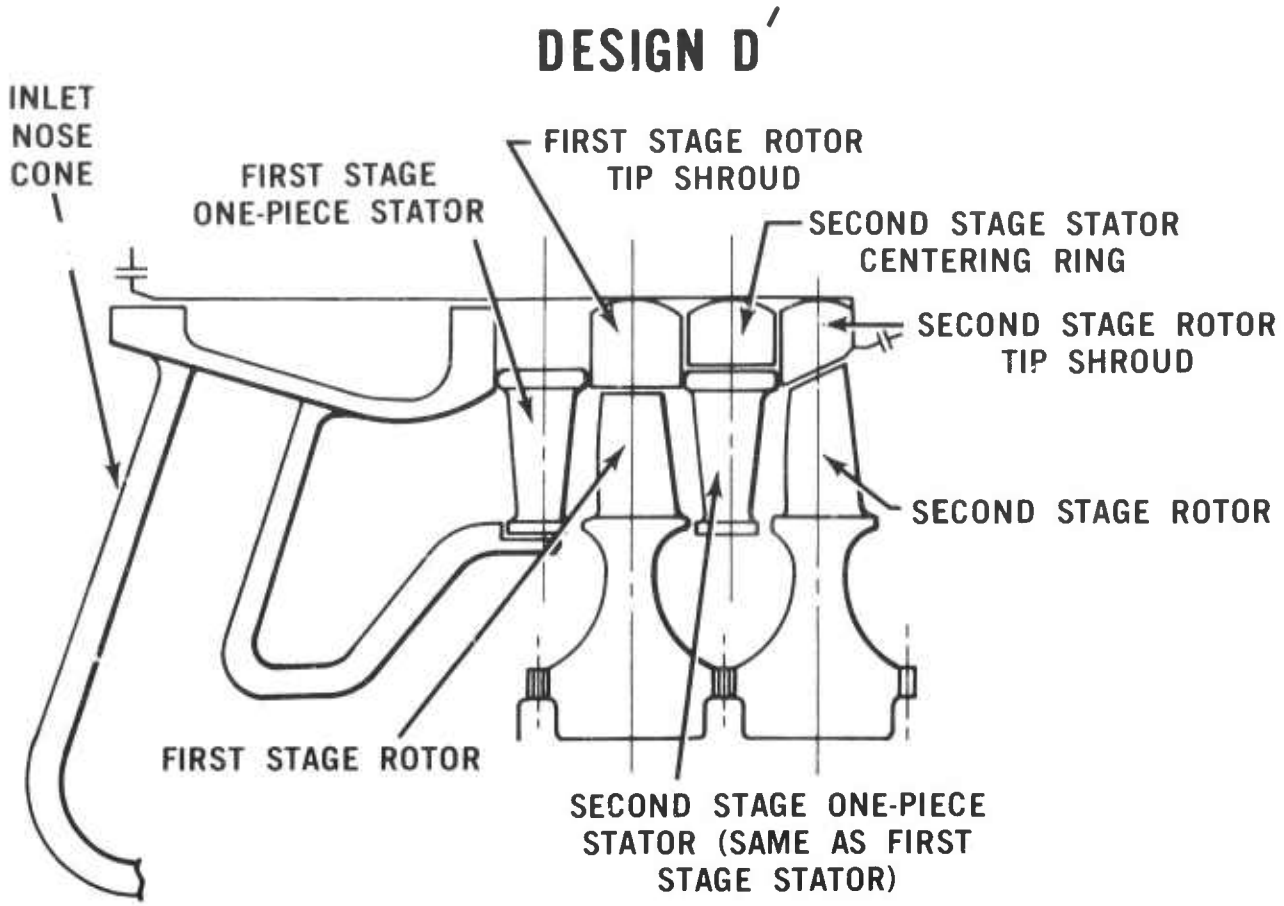

Figure 3.1 Schematic Cross-Section of Design D' Hot Flowpath Configuration.

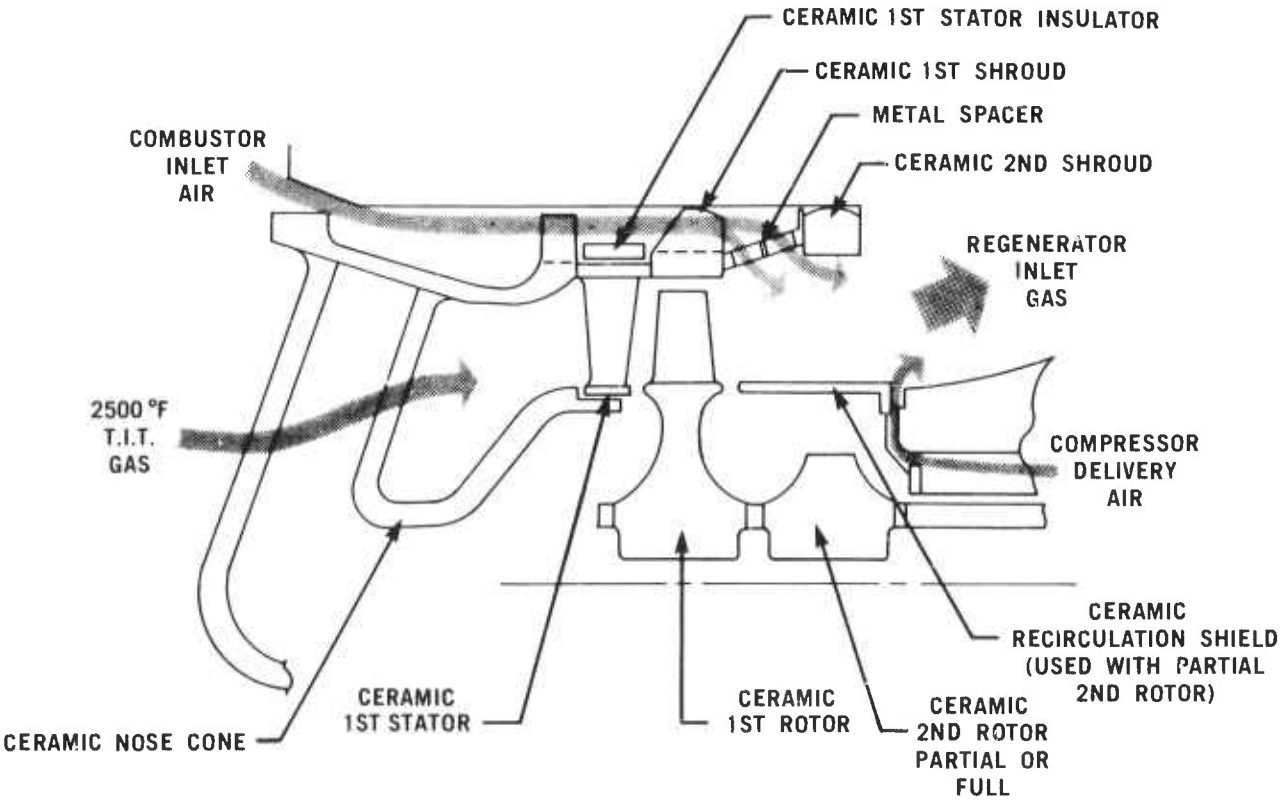

Figure 3.2 Schematic Cross-Section of Modified Engine Flowpath Configuration.

Mechanical Analysis of the Three-Piece Design

An approach to make duo-density Si_3N_4 turbine rotors in three-pieces has been conceived and is shown in Figure 3.3; the purpose is to minimize the risk of blade damage in the press bonding operation and to allow for better control of material strength in the hub region. In this concept, the rotor is fabricated from three Si_3N_4 compositions which differ in their elastic and thermal properties. As a consequence, the stress distributions in both 1st and 2nd stage rotors are improved relative to those reported previously[8,9].

A two-dimensional analysis was performed on a first stage turbine rotor and temperature and stress distributions at full power operation (2500°F and 100% speed) were obtained using boundary conditions derived earlier for the two-piece concept and reported in the eighth interim report[8]. The new temperature map is shown in Figure 3.4. Figure 3.5 shows corresponding maximum principal tensile stresses which are somewhat lower throughout the disk than those for a duo-density, two-piece concept reported previously[8].

Utilizing three-dimensional finite element computer codes and the boundary conditions previously derived, the blade centrifugal and thermal stresses were computed at full power loading. Temperature distributions for Design D', shown in Figure 3.6, were determined using a 3-D finite element heat transfer program TAP [9]. For boundary input data to this program, film coefficients and adiabatic wall temperatures from TSONIC[8] and BLAYER [8] were defined at the pressure and suction surfaces of the blade, while additional convection data and heat fluxes were supplied at the disk surfaces and at the disk throat of the three-dimensional rotor model as shown in Figure 3.7.

With these temperatures and the blade material mechanical properties, SAPIII[8] was used to calculate the blade stresses which are shown in Figures 3.8 and 3.9. Figures 3.8 and 3.9 show the maximum principal tensile stresses on the camberline plane, and on the pressure and suction surfaces respectively at the full power condition. The blade stresses in these two figures also include the effects of aerodynamic gas loads.

Strength and Reliability Considerations

In a previous report[9] equations for MOR strength requirement were derived as function of a specified reliability. These have now been applied to the three-piece rotor concept with results shown in Figures 3.10 through 3.14.

Figure 3.10 is a contour map of characteristic MOR strength requirements for the first stage rotor corresponding to 90% overall reliability at full power operation, i.e., 2500°F T.I.T. and 100% shaft speed. In this plot the reliability and the Weibull parameter, "m", are assumed to be uniform throughout the structure. The strengths quoted are in terms of a standard "A" size (0.125 x 0.25 x 1.00 inches) MOR specimens tested in 4 point bending. By crossplotting strength requirements with the temperature map of Figure 3.4 an envelope of strength requirement as a function of temperature, shown in Figure 3.11, was obtained. Figure 3.12 is a similar plot to Figure 3.11 but with rotor reliability as a parameter at a fixed value of the Weibull Slope "m" of 10. Figures 3.13 and 3.14 give similar plots of strength requirements for the blade, again at full power operation.

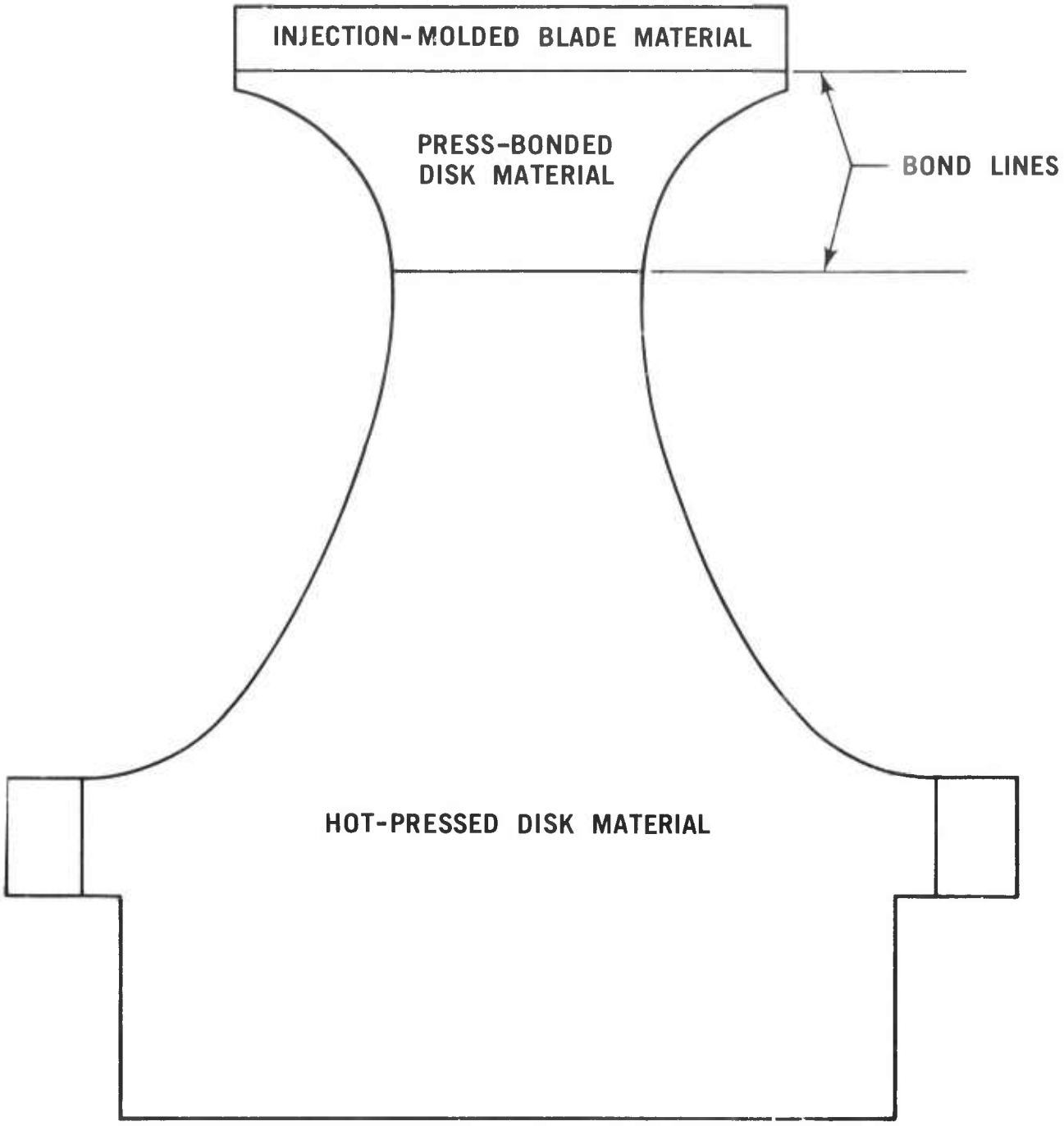

Figure 3.3 Duo-Density Three-Piece D' Rotor Design.

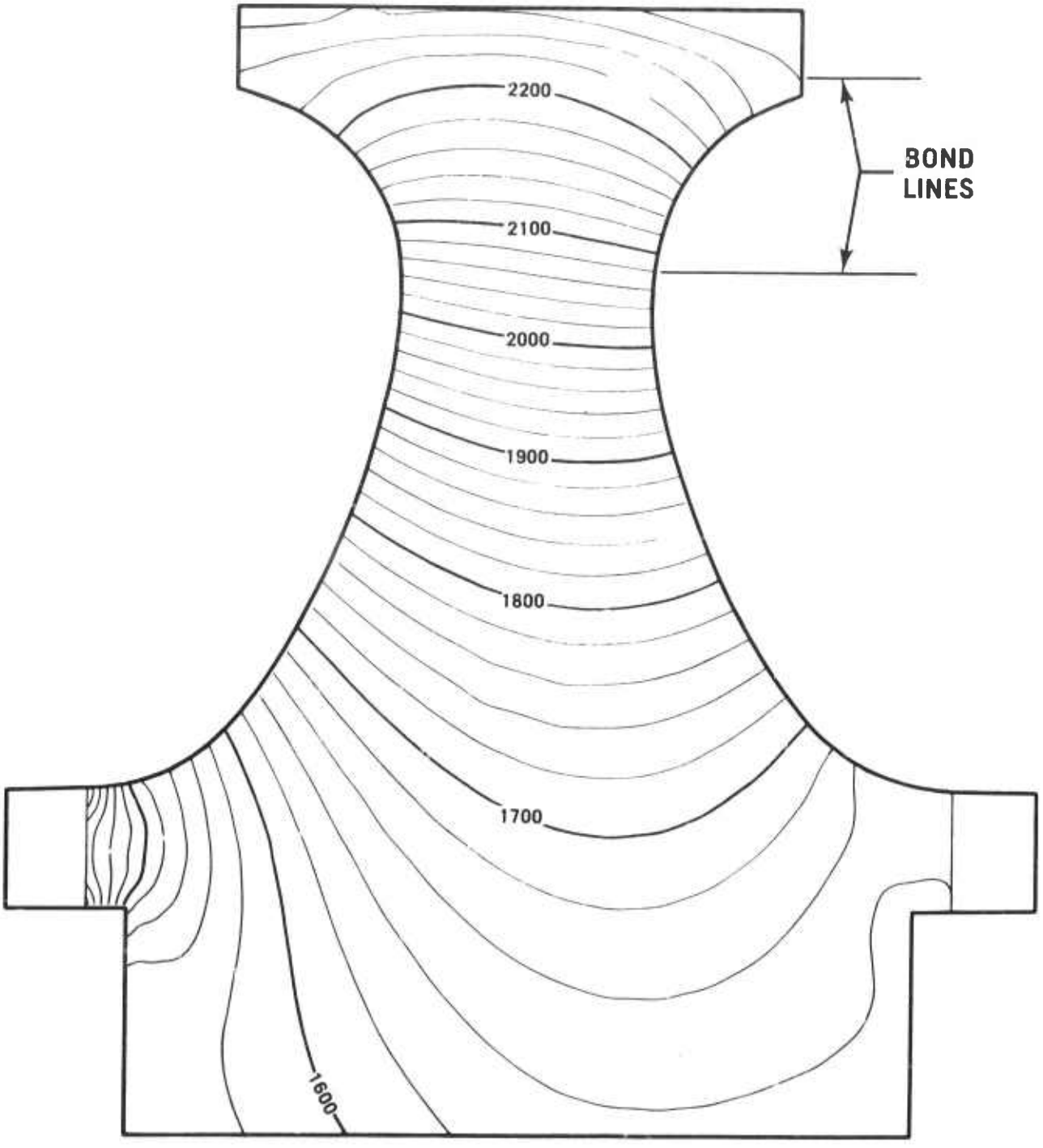

Figure 3.4 Temperature Contour Map at 2500°F T.I.T. and 100% Speed - First Stage Turbine Disk.

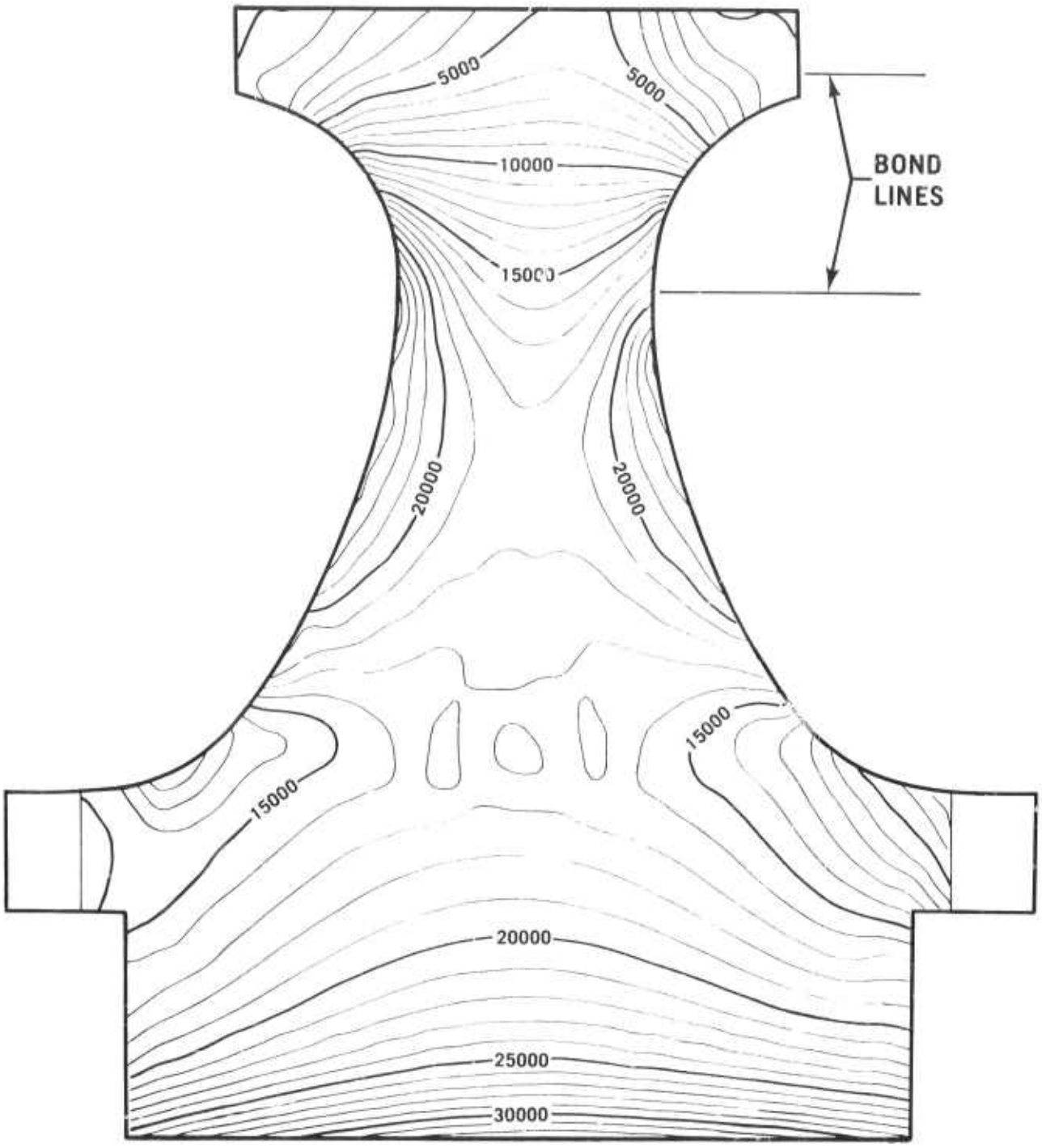

Figure 3.5 Contour Map of Maximum Principal Tensile Stresses at 2500°F T.I.T. and 100% Speed - First Stage Turbine Disk.

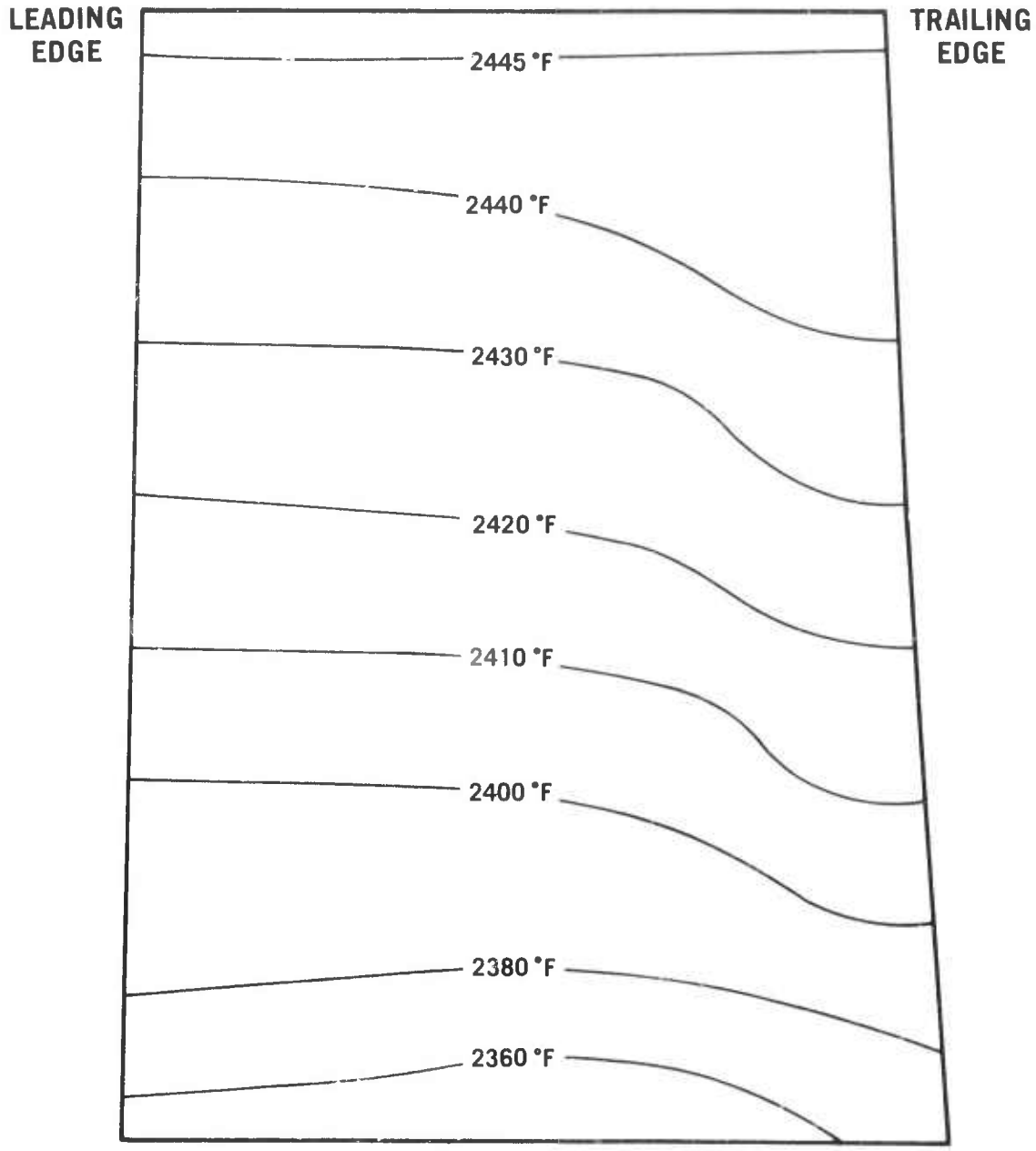

Figure 3.6 Temperature Contour Map at 2500°F T.I.T. and 100% Speed - First Stage Turbine Rotor Blade Design D'.

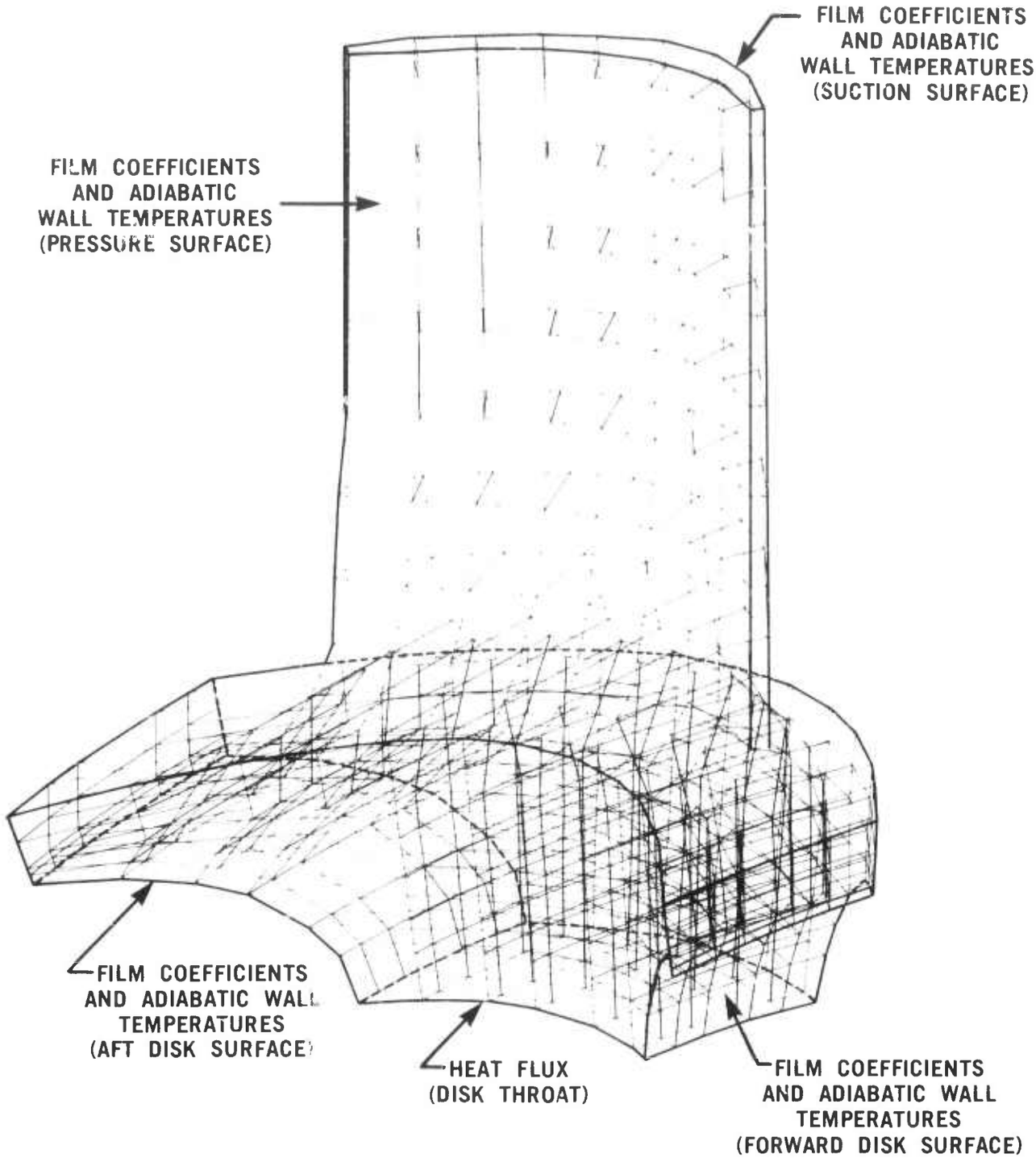

Figure 3.7 Thermal Boundaries for Three-Dimensional Heat Transfer Analysis - First Stage Turbine Rotor Blade.

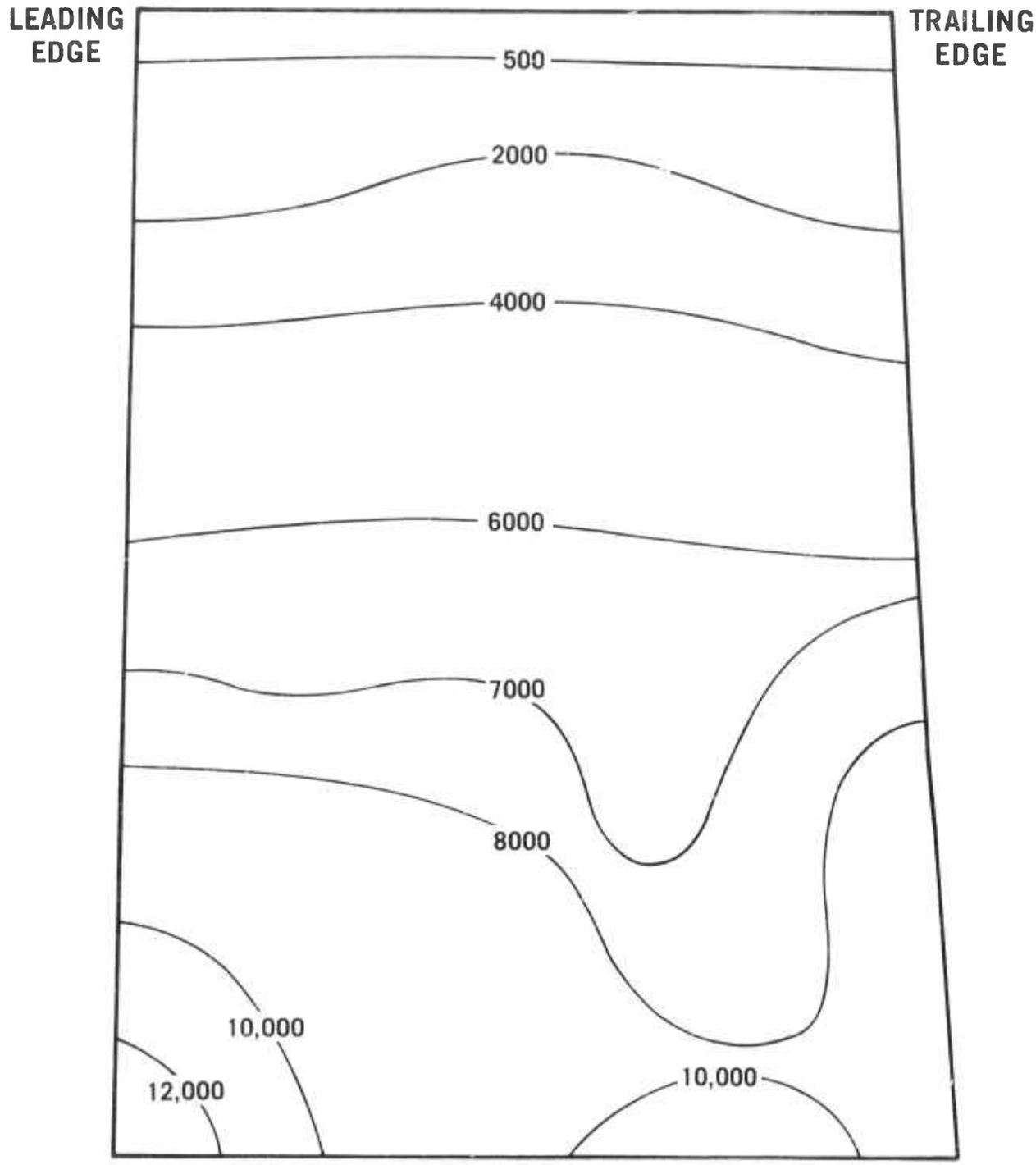

Figure 3.8 Contour Map of Maximum Principal Tensile Stresses at Camberline of First Stage Turbine Rotor Blade at 2500°F T.I.T. and 100% Speed.

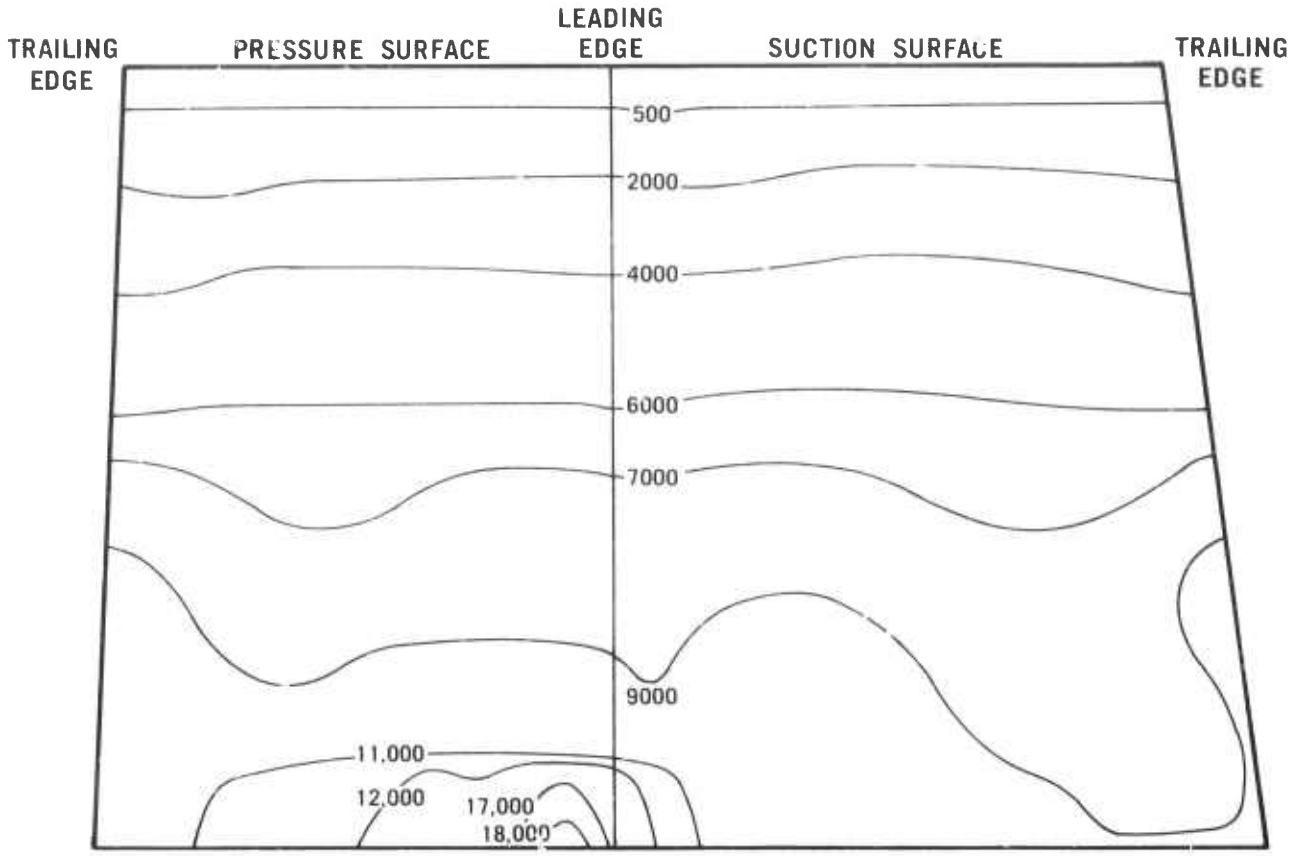

Figure 3.9 Contour Map of Maximum Principal Tensile Surface Stresses of First Stage Turbine Rotor Blade at 2500°F T.I.T. and 100% Speed.

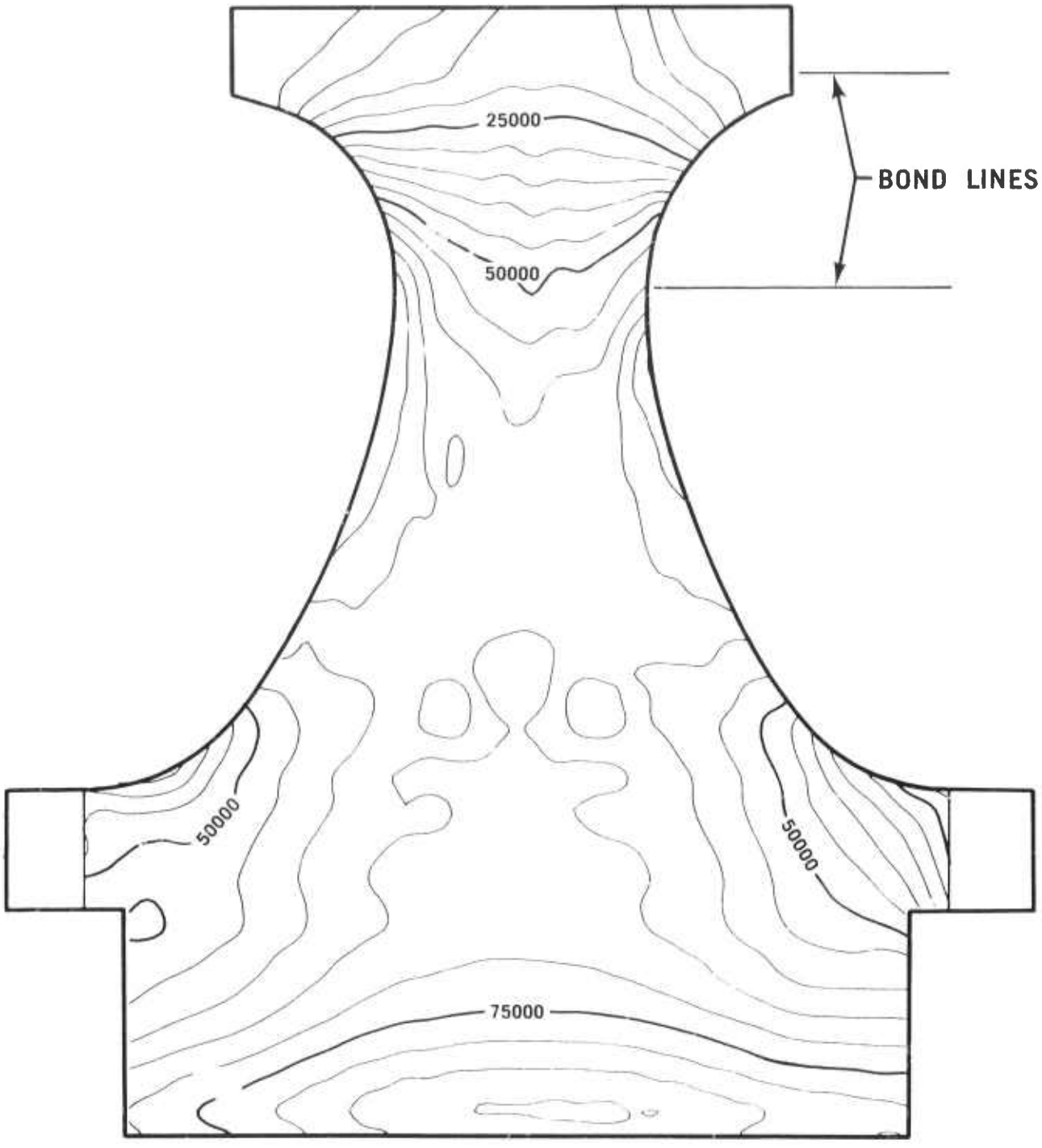

Figure 3.10 Contour Map of Characteristic MOR Strength Requirements of First Stage Turbine Rotor Disk at 2500°F T.I.T. and 100% Speed for m = 10 and R = 90%.

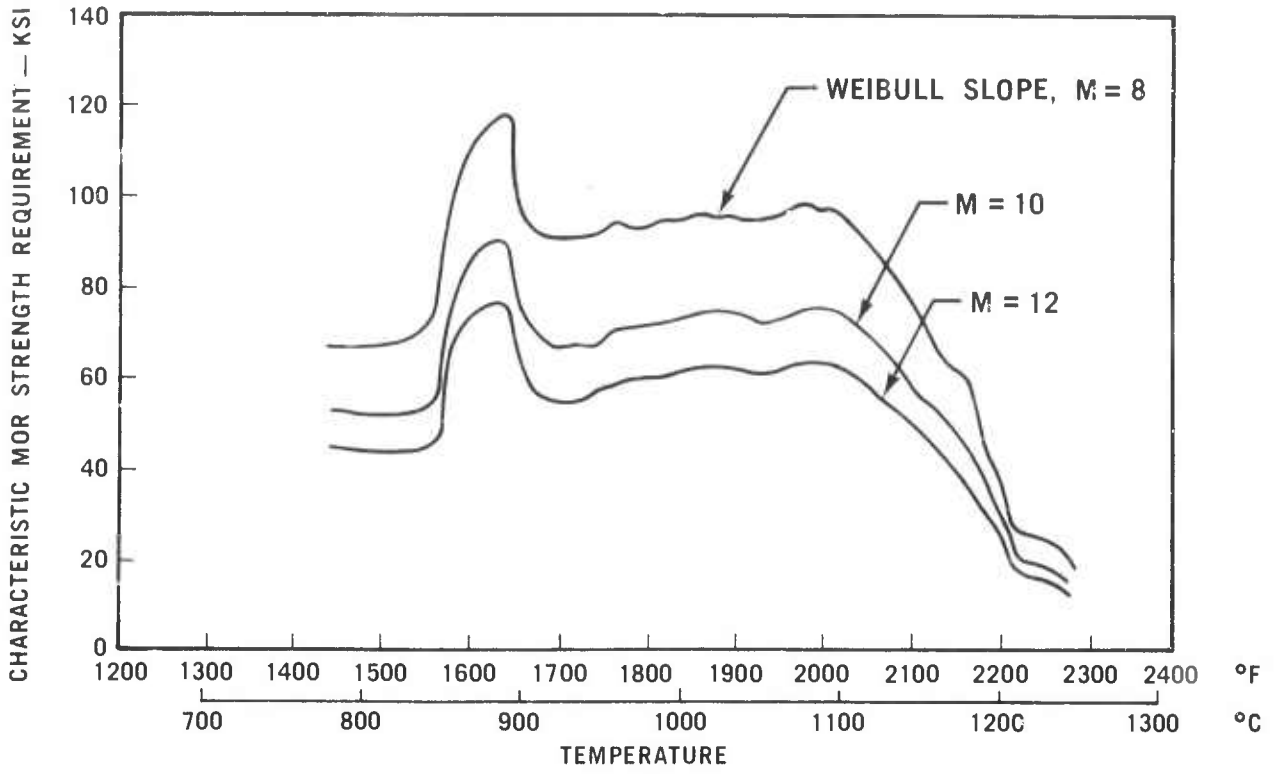

Figure 3.11 Envelope of Characteristic MOR Strength Requirements Versus Temperature for the First Stage Turbine Rotor Disk at 2500°F T.I.T. and 100% Speed for 90% Reliability.

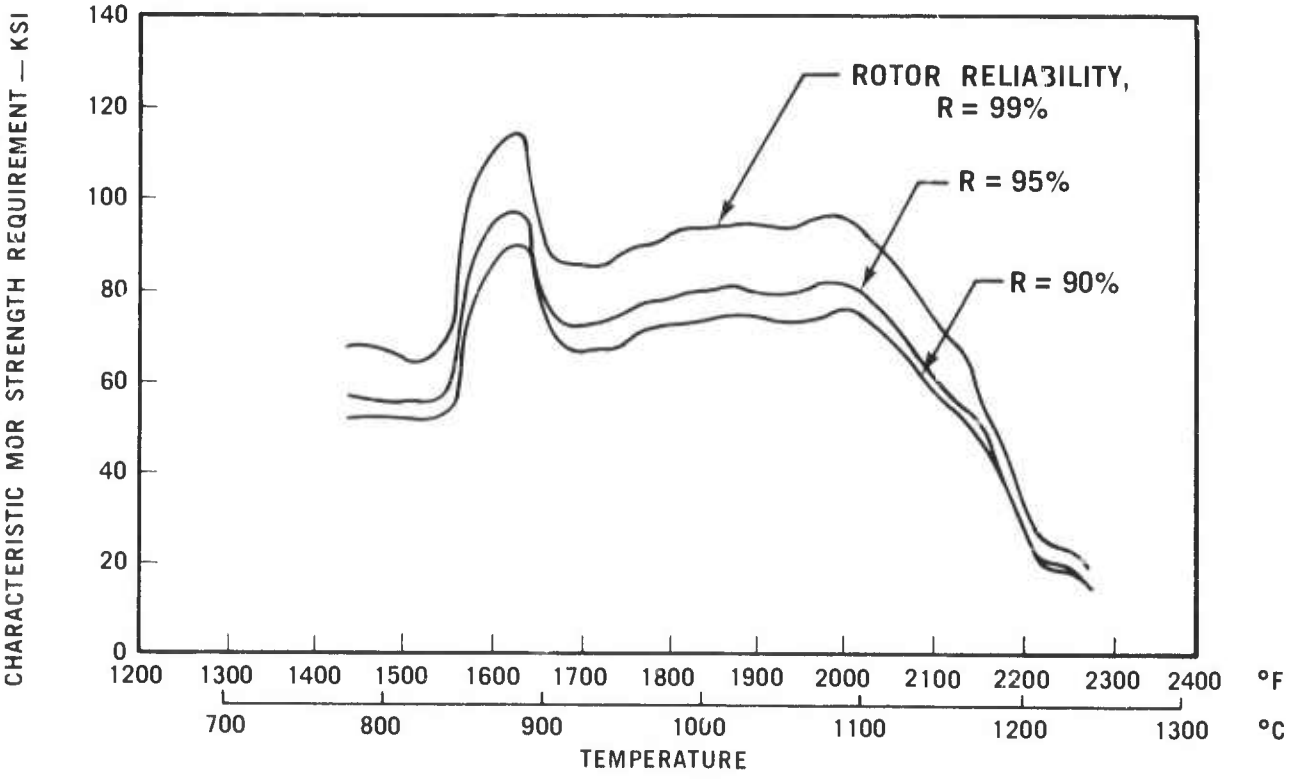

Figure 3.12 Envelope of Characteristic MOR Strength Requirements Versus Temperature for the First Stage Turbine Rotor Disk at 2500°F F.I.T. and 100% Speed for Weibull Slope = 10.

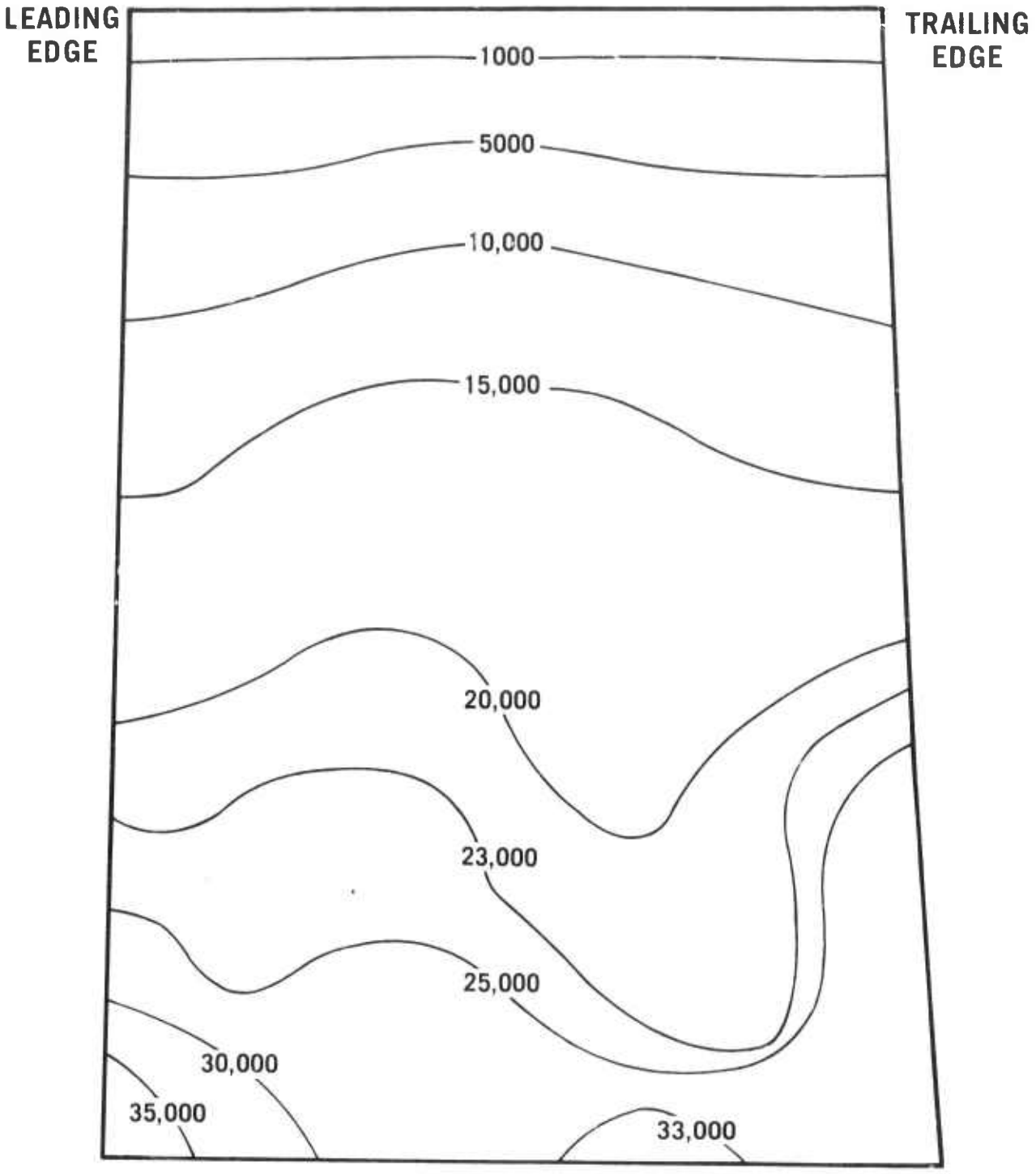

Figure 3.13 Contour Map of Characteristic MOR Strength Requirements for the First Stage Turbine Rotor Blade at 2500°F T.I.T. and 100% Speed for m = 10 and R = 90%.

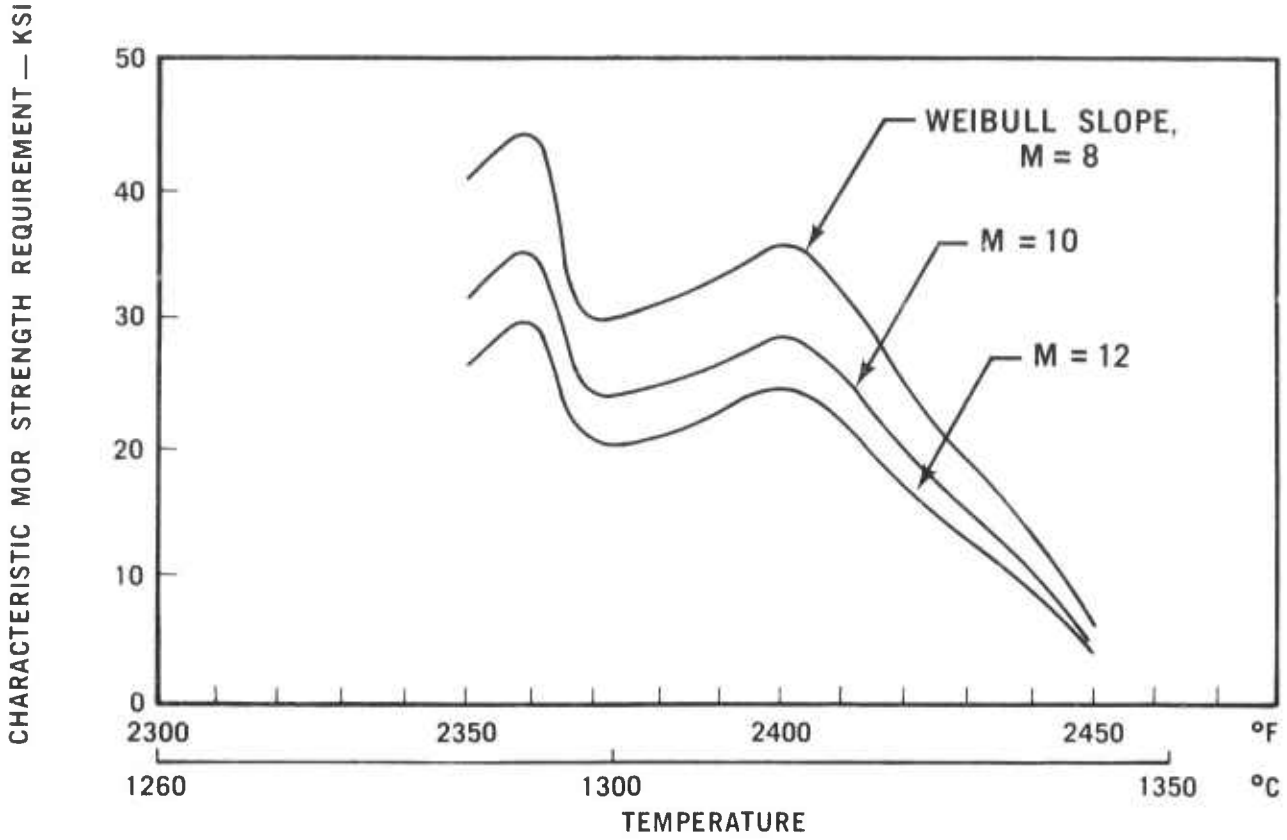

Figure 3.14 Envelope of Characteristic MOR Strength Requirements Versus Temperature for the First Stage Turbine Rotor Blade at 2500°F T.I.T. and 100% Speed for 90% Reliability.

Design E Turbine

Introduction

During this reporting period, analysis of the improved efficiency ceramic turbine rotors, designated Design E, was continued. The objective of this design is to evaluate the efficiency potential of a turbine designed with the experience and constraints of ceramics that have been learned on the program. In this first phase, a preliminary design of blading for a two stage axial turbine was completed. The rotor designs incorporated the low stress helical stacking concept discussed in previous reports[8,9]. Aerodynamic analysis was continued to define the stator sections and to establish basic surface gas velocities of both rotors and stators. Three dimensional stress and reliability analysis was initiated to evaluate the acceptability of the rotor blade designs. This E design turbine is estimated to be 7 1/2 percentage points higher in total-to-total efficiency than the current D' turbine.

Aerodynamic Analysis

Blade sections for both the first and second stage stators were designed assuming fabrication by axial draw injection molding techniques. This implies (a) no channel divergence within the blade; (b) circumferential clearance between blades (.050" minimum); and (c) low blade inlet angles (5° or less). Stator exit angles were selected to maximize overall turbine performance when coupled with the low stress rotors. The overall aerodynamic flow path is shown in Figure 3.15. As would be expected for best efficiency, the stators and rotors are not common for both stages as they were in design D' to expedite ceramics development.

A basic two-dimensional analysis of the gas flow fields of both the rotors and stators was accomplished using the NASA computer program TSONIC[11]. Gas and rotor speed conditions corresponded to those in the engine at 100% speed. The principal objective of this flow analysis at this point in the design process was to establish that excessive suction side adverse pressure gradients were not present in the blading. Suction surface aerodynamic diffusion parameters were evaluated at the hub, mean and tip sections of both rotors and stators. For all

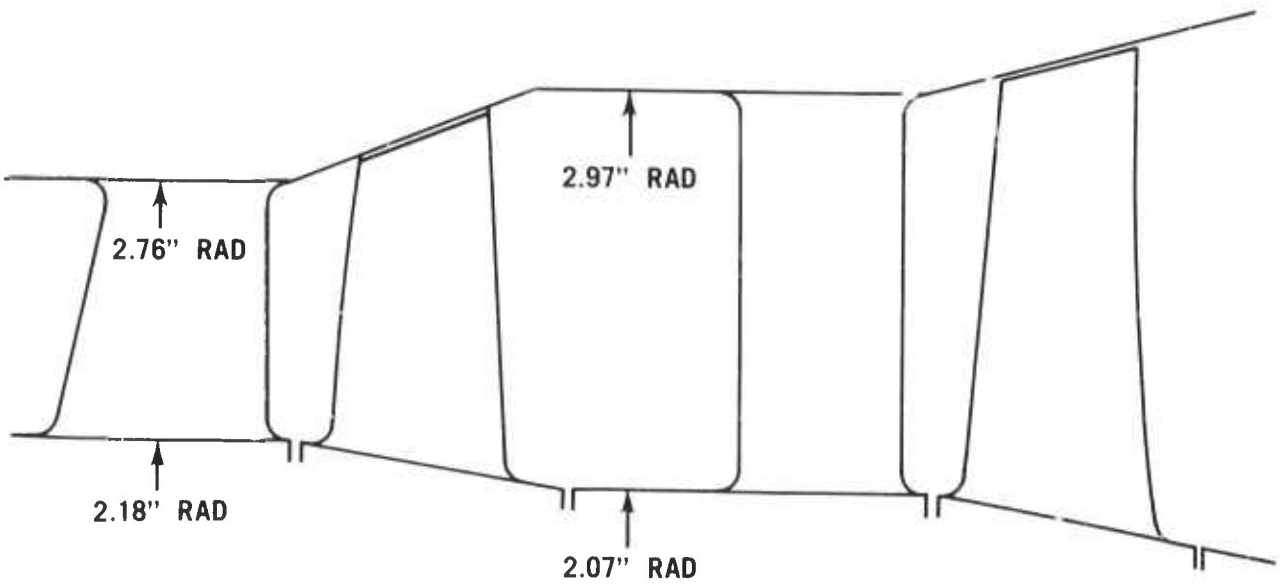

Figure 3.15 Proposed Design E Aerodynamic Flowpath.

sections, the diffusion parameters were below the maximum value of 2.0 as recommend d by Stewart and Glassman[12].

Stress Analysis

In order to evaluate the acceptability of the preliminary design E turbine, three-dimensional stress and reliability analyses were performed on both the first and second stage rotor blades. Three-dimensional finite element models of the first and second stage rotor blades were developed, with the blades modeled as being fixed at the platform. Previous analysis has indicated that this assumption is adequate for preliminary blade analysis[8]. Gas loading was calculated and applied to the pressure side of the airfoil models. Stresses in the blades were predicted using an in-house version of the SAPIII[8] computer program for the 110% speed condition. For the second stage rotor, the basic aerodynamic design and two alternative designs (A) and (B), were studied. The motivation for looking at these two alternatives was to determine the effect of straightening the rotor trailing edge for the purpose of easier tooling construction. In configuration (A), the mean section trailing edge was extended, while in configuration (B), the tip section trailing edge was shortened shown schematically in Figure 3.16. Maximum principal stress results for all configurations studied are shown in Table 3.1.

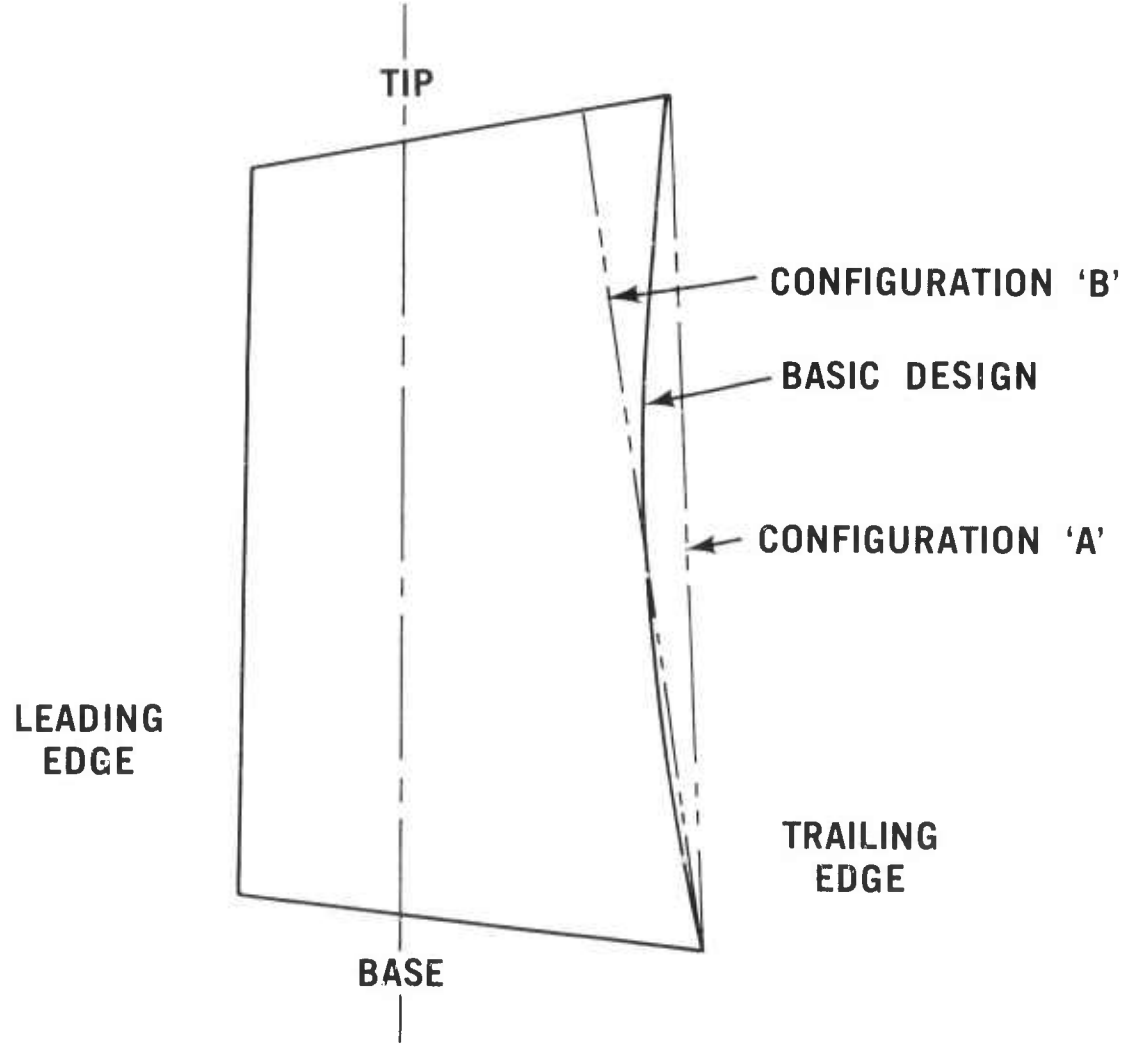

Figure 3.16 Design E Second Stage Rotor Blade Trailing Edge Configurations

A probability of failure analysis described in previous reports[8,9], and accounting for volumetric effects only, was performed on the above rotor blade configurations using the SAPIII[8] stress results. The resultant reliabilities are shown in Table 3.1. Reliabilities are shown for both individual blades and for the total blade ring of thirty-one blades. The first stage rotor has an overall reliability of 98.7% while the second stage rotor configurations are slightly less reliable. Configuration 2A has a reduced reliability compared to 2 and 2B, despite a relatively low stress level, apparently because of a greater volume of stressed material. Although rotor 2B has a higher reliability than (2) and (2A), approximately four degrees of tip turning were sacrificed which is undesirable from an aerodynamic performance standpoint.

Before further refinement is performed on this two stage design, an examination will be made of the potential efficiency and reliability of a three stage ceramic turbine. The objective will be to determine any increase in reliability of the turbine rotors for given ceramic materials without compromising turbine efficiency.

TABLE 3.1

PREDICTED STRESSES AND RELIABILITIES OF PRELIMINARY DESIGN E TURBINE BLADES AT 110% DESIGN SPEED

Rotor Configuration	First Stage 1	Second Stage 2	2A	2B
Maximum Principal Stress				
Centroid ksi	19.0	19.5	19.1	18.0
Surface ksi	20.2	20.1	19.1	19.1
Reliability				
Blade	.9996	.9981	.9975	.9987
Blade Ring (31 blades)	.987	.943	.925	.960

Material: Silicon Nitride 2.7 gm/cm^3

Assumed Material Properties:*

Characteristic MOR: 40 ksi at all temperatures

Weibull Slope (m): 12.0 at all temperatures

* Within the capability of developed 2.7 gm/cm^3 density reaction sintered silicon nitride. MOR of 44.2 ksi and m of 7.5 achieved on test bars, see Table 4.13.

3.1.2 MATERIALS AND FABRICATION

Introduction

In the duo-density silicon nitride turbine rotor program, design D' rotor blade rings of reaction sintered Si_3N_4 were fabricated to 2.7 gm/cm^3 density using the injection molding process. Development of the blade fill technique has been completed with refinements to the casting process and blade fill removal process using a laser. The press-bonding operation was improved by press alignment and increasing the stiffness of the foundation. A significant modification to improve the press-bonding process was the introduction of the three-piece duo-density rotor concept.

Injection Molded Blade Ring Fabrication

The new D' blade ring tooling[9] was received and installed and molding trials made. In initial molding runs, blades were torn from the rim when the tooling was opened. The blade damage problem was traced to insert surface finish, insert timing, and clamp force application. Finishing the die inserts to a high polish aided in blade release from the die. Insert withdrawal was altered from simultaneous to staggered with a 0.010 inch delay between adjacent inserts. Mold clamping was adjusted to give nil preload on inserts when the die is fully clamped while allowing no insert movement during injection.

Molding trials using the reworked D' tool were successful and a parametric study to optimize molding parameters was initiated. All process times, material composition and die clamping loads were maintained constant at the levels used for design D rotor fabrication. Die and material temperature were varied from 70°F to 85°F and 180°F to 220°F respectively. Seven rotors were molded at each temperature combination selected and the resulting rotors were visually and X-ray inspected. Evaluation of the NDT results indicated a die temperature of 80°F and a material temperature of 190°F to be optimum for molding 2.7 gm/cm^3 design D' rotors.

As previously reported[9], preliminary molding studies indicated that the material flow in the D' tooling was more conducive to formation of molded components free of fold and flow lines. Two gating configurations, shown in the last report[9], and repeated here as Figure 3.17, were evaluated for their effect on component quality. A center gate configuration in which material was gated at the component centerline over 360° proved superior to an end gate. The end gate distributed material over 360° at the trailing edge of the rotor platform. It was initially believed that an end gate would force the material to form a uniform front of advancement into the cavity as it was forced through the cylindrical rim area. Although a unified material front was formed, the longer path length caused chilling of the front. Further investigation proved that the change in blade shape from design D to design D' was sufficient to eliminate fold and flow lines.

Quality control inspections of molded rotor blade rings revealed three major flaws present in D' rotor blade rings. Blade base cracks at the trailing edge, unmelted inclusions, and small voids in the platform and blades which were located by visual and X-ray techniques. Several process changes were made to eliminate these flaws. Cracking was eliminated through realignment of the tooling. To eliminate unmelted inclusions in the rotor blades, an improved mixing technique has been employed. Following initial blending of the silicon powder with the polymers, an extrusion operation has been added to break up agglomerates of unmixed silicon - polymer. Evacuation of the extrusion cylinder prior to extrusion eliminates most large gas bubbles from the mix, and the shearing

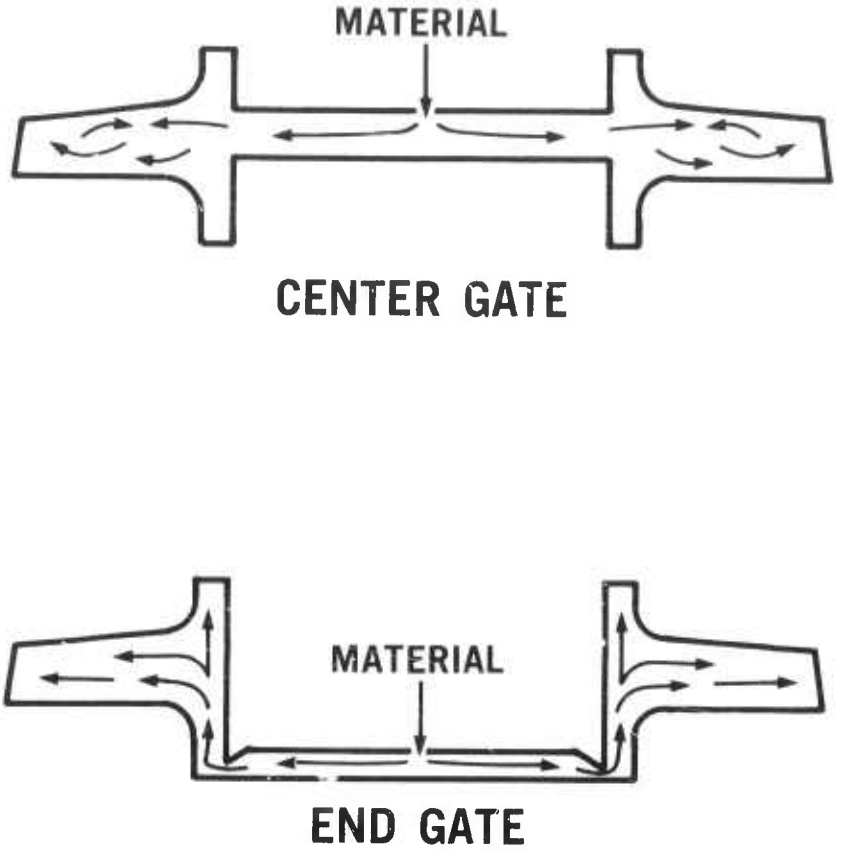

Figure 3.17 Gating Configurations of Rotor Tooling.

action of the extrusion die further eliminates trapped gas. However, some voids still appear in the molded rotors and in an effort to eliminate all detectable voids, a new material gating eonfiguration has been designed and fabricated, Figure 3.18. The new gate utilizes an overflow reservoir similar to that used in the stator mold to trap the initial front of material which flows into the die. Molding experience with the stator indieates that most voids enter the die in the initial material front. Providing a 60% overflow reservoir will trap the initial material front and should eliminate voids.

Vacuum level control has been added to the rotor tooling in order to eliminate possible molding of components at inadequate vacuum levels. The injection cyele is sequenced eontingent upon attainment of a maximum of 6 inches of mercury absolute pressure in the die eavity. Failure to attain the required vacuum will lock out the injection cyele until the eondition is eorrected.

During this reporting period significant progress has been made in the fabrication of 2.7 gm/cm^3 silicon nitride blade rings. The new D' rotor tooling was utilized to mold approximately 500 blade rings during the eourse of proeess development; other than those with obvious flaws, each of these blade rings were inspeeted in detail by 30X visual magnification and X-ray radiography; 330 werc aeeeptable having no visible flaws, and 150 were aecepted for proeessing following X-ray evaluation. While only 12 flaw-free blade rings, having no visible or X-ray defects, remained after nitriding, a number of additional desired meehanieal and process changes have been identified and are eurrently being incorporated as a means of improving the yield of flaw-free rotor blade rings.

Figure 3.18 Overflow Reservoir on D' Rotor Tooling.

Blade Fill Development

During this reporting period, development of a eonsistent blade fill process has been eompleted.

The silieon nitride blade rings, after maehining and inspeetion, were dipped in a boron nitride/methylethyl ketone slurry. The viseosity of the slurry was eontrolled so that reproduetible BN thieknesses were aehieved. The BN served as a lubricant for subsequent blade fill removal and also served as a barrier material which prevented blade ring to blade fill bonding during the nitriding step.

The first blade fill operation consisted of manufaeturing the extraetable inserts between the rotor blades. The BN eoated rotor blade ring, with its

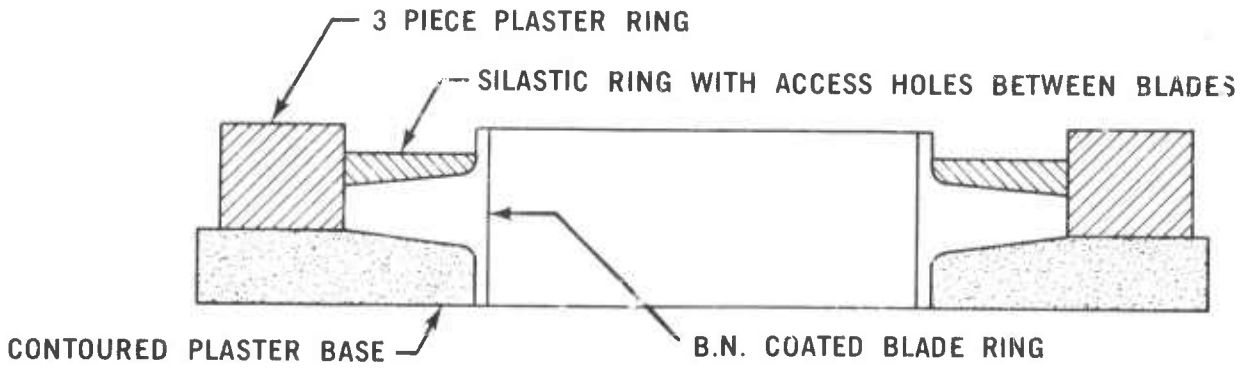

Figure 3.19 Schematic of First Blade Fill Operation.

trailing edge down, was placed into a countoured plaster block, Figure 3.19. A concentric silastic rubber ring with access holes to each blade cavity was press fitted over the leading edge contour of the blade ring. Having masked the leading and trailing edges of the blades, the independent casting cavities were formed by placing a plaster ring over the outside of the rotor blade ring. Once the above assembly was completed, a low density silicon metal slip was introduced centrifugally into the cavities through the access holes in the silastic rubber. When casting was complete, the fixturing was removed and the rotor blade ring with its cast inserts was dried.

The second blade fill operation was initiated by applying another coating of BN to the blade ring/first blade fill assembly. Once the coating had dried, the assembly was centered in a graphite retaining ring on a plaster block. A low density silicon metal slip was introduced into the cavity which encases the first blade fill assembly. After casting, the total blade filled unit was dried, nitrided and diamond ground to final dimension prior to press-bonding.

Subsequent to the press-bonding operation, described later in this section, the blade fills must be removed without damaging the encapsulated blade ring. A 300 Watt CO_2 laser was used to make a 0.100" deep circumferential cut around the second or outer blade fill as shown in Figure 3.20. Next a series of four to six radial cuts, 0.250" deep, were made along the top and bottom surfaces as shown in Figure 3.21. The pie shaped segments of the outer blade fill were easily removed from the rotor assembly which in turn allowed removal of the individual inserts between the blades.

Duo-Density Rotor Fabrication

The majority of work during this reporting period was on the three-piece duo-density rotor concept discussed previously. However, prior to this, work on developing two-piece duo-density rotors was directed toward further refinement of the graphite wedge hot-press bonding system[7,8,9] for bonding a theoretically dense Si_3N_4 hub to a reaction sintered Si_3N_4 blade ring. It was reported earlier [9] that a hot-pressed silicon carbide foundation was substituted for the graphite base supporting the blade ring and lower piston to prevent relaxation of the blade ring support. Since it became apparent that the available one inch thick hot-pressed SiC (Norton NC-203) material was inadequate to support the loads without excessive internal stresses and permanent deformation, a three inch thick hot-pressed SiC foundation was tried and proven successful. The combination of increased thickness and reduced loading, discussed later, has resulted in a reduction in stress level to a point where permanent deformations are no longer a problem.

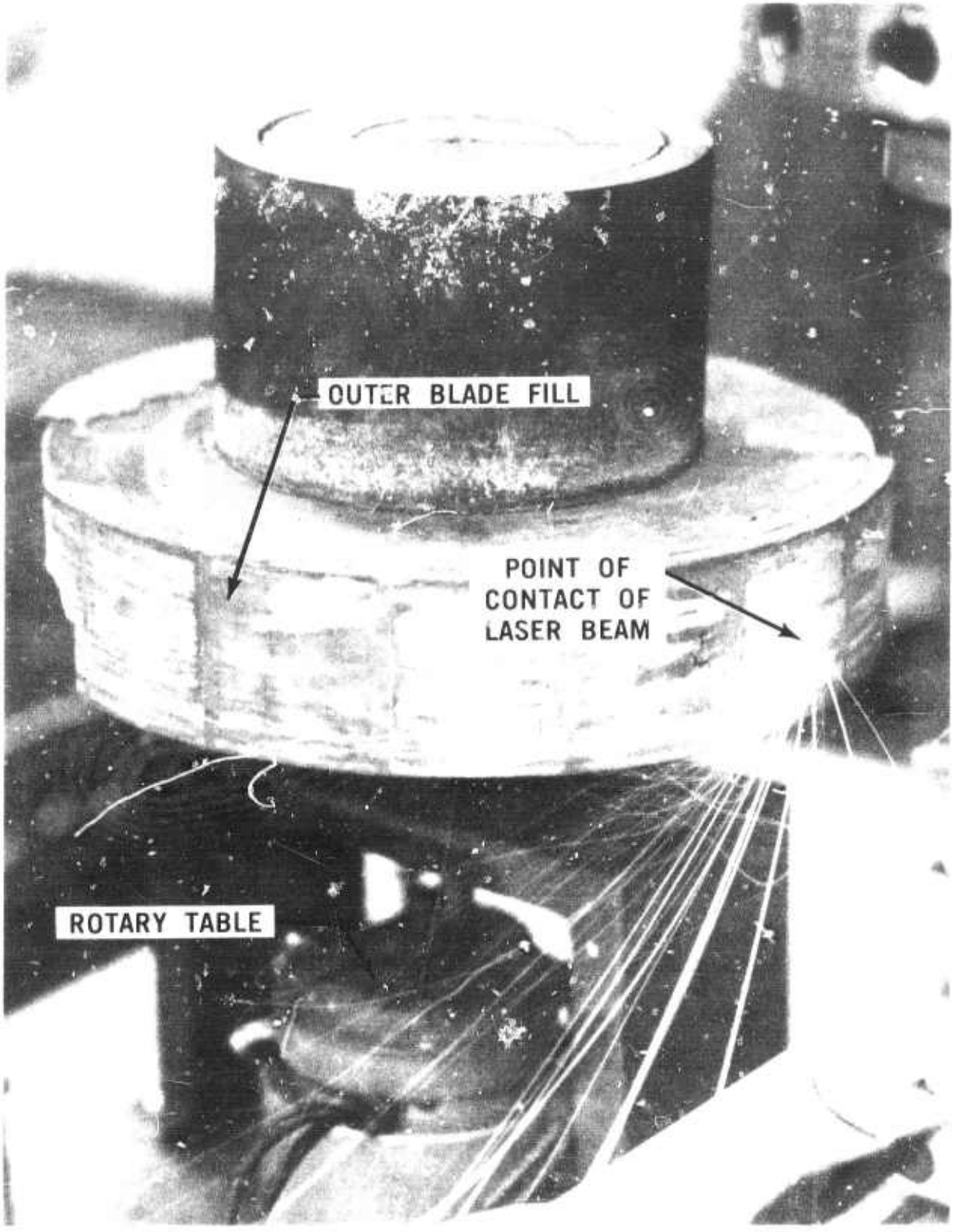

Figure 3.20 Circumferential Cutting of Outer Blade Fill With CO_2 Laser.

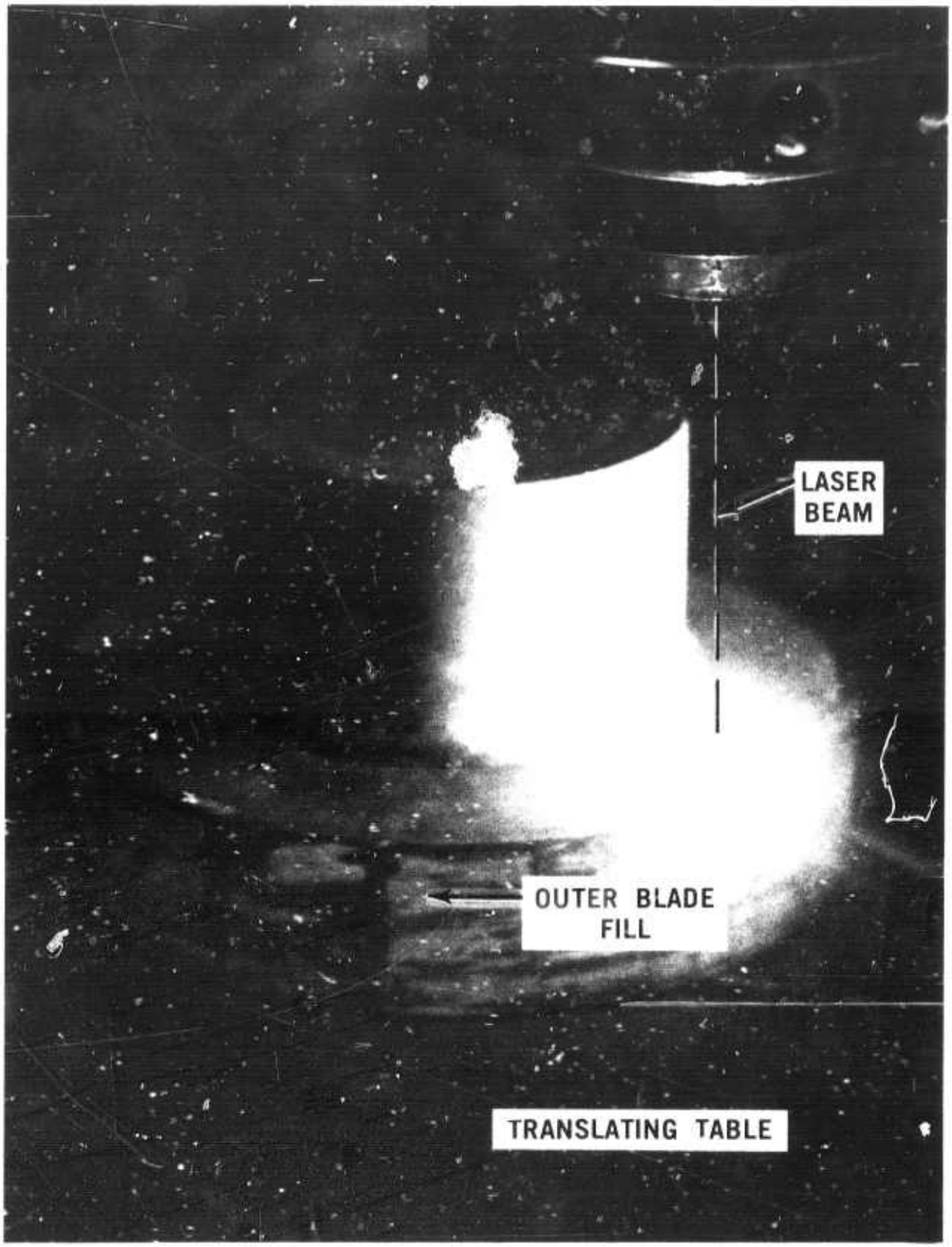

Figure 3.21 Radial Cutting of Outer Blade Fill With CO_2 Laser.

When the SiC foundation was initially incorporated the blade ring remained supported on a thin (0.26 in.) graphite ring (above the foundation), used to center the lower piston. This ring has since been eliminated and the blade ring is now supported directly on a boron nitride-coated SiC foundation. The lower piston, which also rests on the SiC foundation, is now centered by the blade ring. This change was made to eliminate the last vestige of low modulus material supporting the blade ring.

Measurements of parallelism of the faces of the upper and lower pistons, shown in Figure 3.9 of Reference 9, after removal from the press indicated that the faces of the pressed hubs were out of parallel in varying amounts up to 0.035 inches over a three inch diameter. This prompted a review of both the alignment of the press rams to each other and alignment of the graphite furnace components with the press rams. Press alignment was checked and the rams were found to be out of concentricity by a small amount. The press was re-aligned and checked under maximum load.

A review of the furnace configuration revealed this to be the primary cause of the misalignment. The furnace was redesigned to provide spherical seats at each press ram and direct centering of the susceptor to the rams rather than through the furnace box. Measurements of parallelism of the faces of the pistons showed considerable improvement (0.007" max.) after the alignment modifications were incorporated.

While these modifications improved the situation, they did not eliminate all problems, indicating that lower fabrication pressures may be required to solve the blade and rim cracking problem.

An important development during this reporting period was that of a new approach to make duo-density silicon nitride turbine rotors in three-pieces to achieve a significant reduction of loads during the hot press bonding process. This is known as the three-piece duo-density turbine rotor previously introduced in Section 3.1.1. A schematic of this concept is shown in Figure 3.22. A pre-formed Si_3N_4 hub is hot-pressed to theoretical density and placed in the graphite wedge assembly with the contoured graphite pistons attached. This fabrication technique then involves hot-pressing a circular ring of Si_3N_4 powder to theoretical density and simultaneously bonding it to both the reaction-sintered blade ring and pre-formed hub.

The main advantage of this approach is a lower applied load during hot-press bonding, resulting in less damage to the blades and the rim. Due to the small area of the circular segment, the applied load required to densify and bond the Si_3N_4 powder was reduced by approximately two-thirds while maintaining the same pressure. This has reduced the magnitude of the non-uniform loading across the foundation of the assembly thereby diminishing the deflection of the SiC base and corresponding deflection of the blade ring. In addition, since the pre-formed Si_3N_4 hub is hot-pressed in a separate operation, fabrication pressure of up to 5000 psi can be used in forming the hub.

Many Si_3N_4 turbine rotors have been fabricated by this technique. These rotors were hot-press bonded at 1775°C for three hours at pressures ranging from 1500 to 2500 psi. A coating of boron nitride was used to minimize the formation of silicon carbide on the surfaces of the silicon nitride hub and blade ring.

The results indicate that the lower pressure of 1500 psi produced, on a more consistent basis, a rotor with minor rim and/or blade root eracks. However, the lower hot-pressing pressure did not consistently achieve a high uniform density in the bond region. One potential problem is the inability to evenly distribute the Si_3N_4 powder in the bond eavity. Cold pressing techniques are being evaluated to solve this problem. Experienee has shown that densities greater than 95% of theoretical are neeessary to produee diffusion bonding.

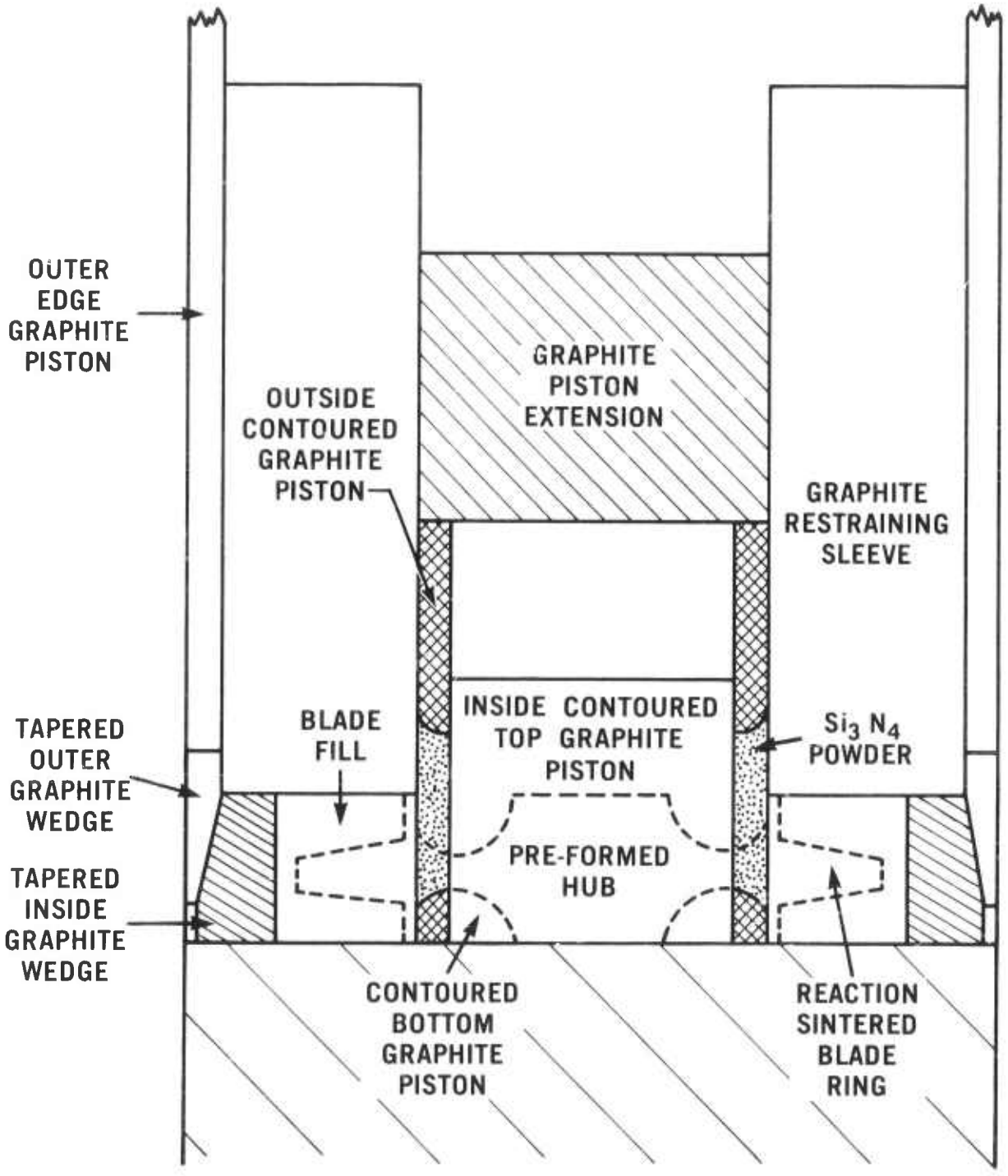

Figure 3.22 Hot Press Bonding Assembly - Three-Pieee Duo-Density Rotor Coneept.

Full density also becomes a problem in the lower platform region as shown in Figure 3.23. The low density area is indicated by the light color. This problem is aggravated by the shape of the bottom contoured graphite piston and the lower piston remaining stationary during hot-press bonding. Pressure is applied uniaxially from the top side only. Complete diffusion bonding at the upper portion of the platform has occured as indicated by the darkening of the blade ring. A scanning electron micrograph showing the microstructure typical of the bond between the blade ring and bond material is shown in Figure 3.24.

To overcome the lower side densification problem, and achieve better pressure distribution, the bottom contoured graphite piston was modified as shown in Figure 3.25. This modification greatly improved both densification and bonding at the expense of additional final contour machining of the Si_3N_4 hub.

The three-piece duo-density fabrication technique has been used to make several duo-density turbine rotors for preliminary testing. The main fabrication effort in the future will be to refine the hot-press bonding procedures and establish the Si_3N_4 powder processing parameters to optimize material properties.

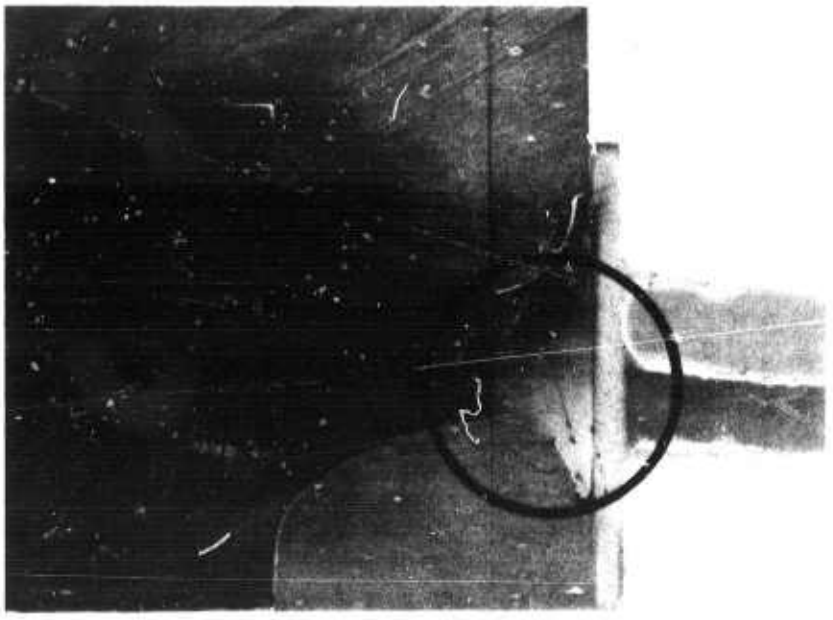

Figure 3.23 Light Area Indicative of Lower Density in the Lower Platform Region.

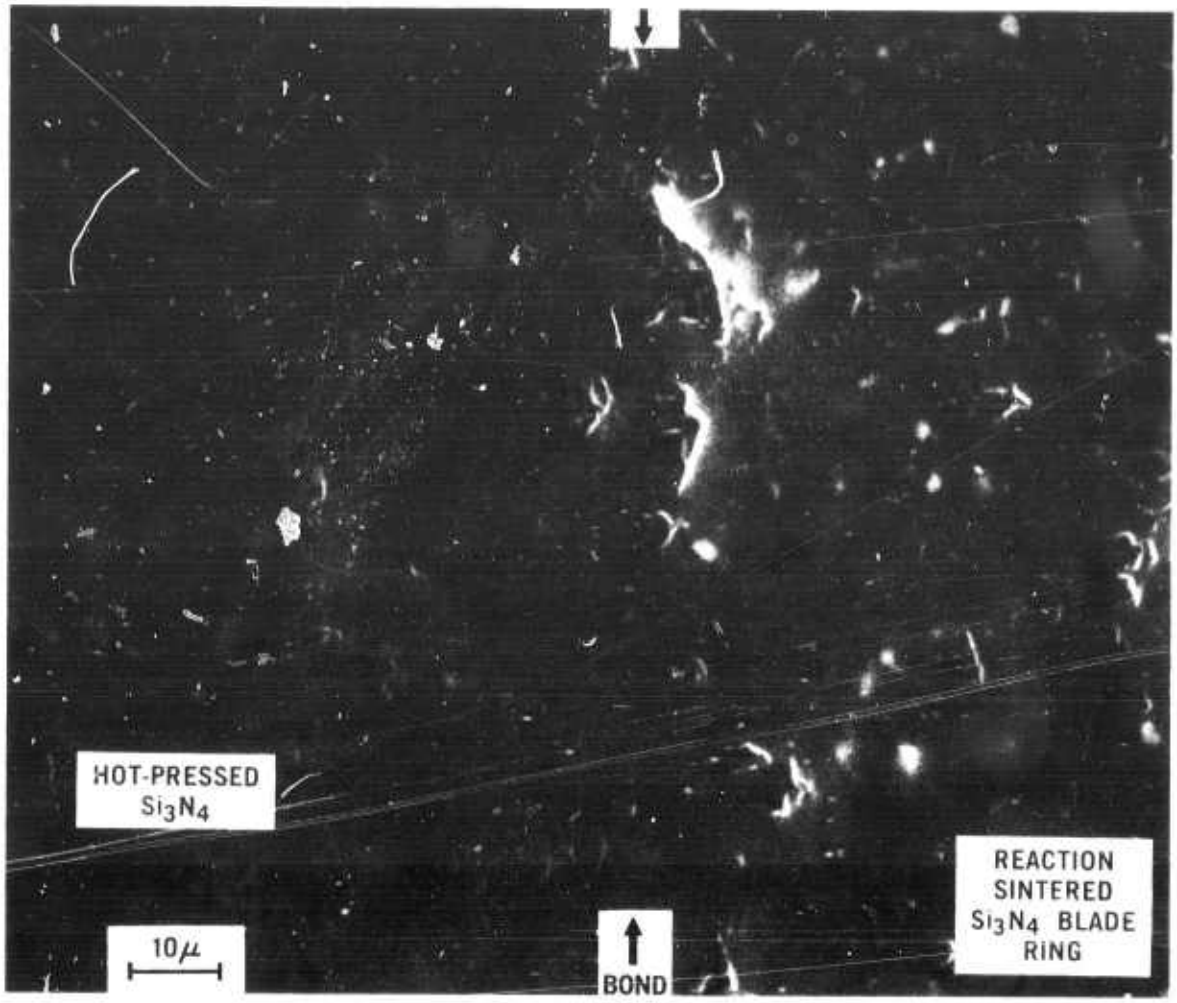

Figure 3.24 S.E.M. of Typical Bond Joint.

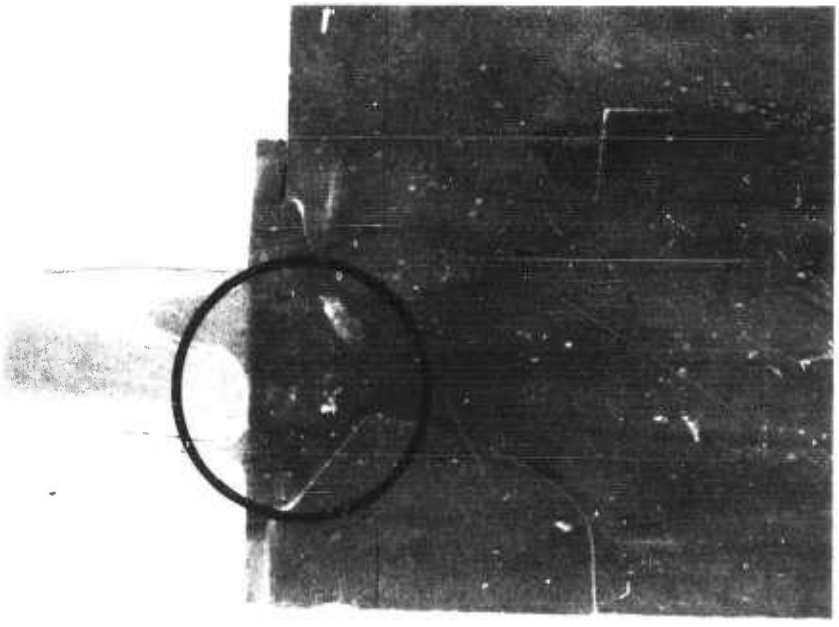

Figure 3.25 Modification of Bottom Contoured Piston.

3.1.3. ROTOR TESTING

Introduction

Emphasis during this reporting period was placed on the development and check out of two hot spin rigs for evaluation of ceramic rotors under simulated engine operating conditions and several rotors were tested in these rigs. Testing of the Design D' rotor blades was started both on a revised bend test fixture and in the hot spin rigs. Spin pit testing of a new series of silicon nitride rotor hubs, with 2% MgO, was completed and the analysis showed the test results correlated well with predicted analytical results. Two new lubricants, used at the ceramic rotor/metal part interface, have been evaluated and the lubricant evaluation test cycle revised. Two duo-density turbine rotors with 10% blade lengths were tested in an engine at 50% speed and 2000°F inlet temperature. A modified version of the engine has been used to demonstrate rotor testing capability. A duo-density rotor with 90% length blades was run in the modified engine to 52,800 rpm and 2650°F turbine inlet temperature.

Blade Bend Test

Work continued during this reporting period on bend testing of rotor blades. The design D blade bend test fixture, described previously [9] was modified to accommodate the design D' rotor blade. The revised fixture shown in Figure 3.26 incorporated several new features such as: the minimization of the frictional component of the load, the addition of an indexing head and revised mounting plate to reduce set-up time, and a revised load stylus which can apply either a tensile or compressive load to the leading and trailing edges of the blade root section. With the revised fixture, the point of load application was 0.480 inches from the blade root section.

Design D' blade bend tests were conducted in a similar manner to the design D blade bend tests[9]. The rotor blade ring was keyed into position and epoxy bonded onto the mounting plate. The mounting plate was accurately attached to a 36 slot index plate which was rigidly mounted to the crosshead of an Instron Model TT-D Universal Test Rig. The test blade could then be properly oriented with the load stylus and the load applied at a constant displacement rate of 0.02 inches/minute until blade failure. A strip chart recorder was used to plot the applied load versus stylus displacement up to the failure load. As a means of assessing material potential at this stage of testing, test data was accepted only if, upon visual examination of the fracture surface, no gross fabrication flaws, such as voids, white areas of alpha silicon nitride whiskers (which indicated presence of a crack prior to nitridation) or large inclusions, were discernible. Prior to testing, all blades were subjected to a 30X microscopic examination to determine the presence of surface flaws and any blades found to be defective were excluded.

A summary of the bend test failure data accumulated since the last report period is presented in Tables 3.2 and 3.3. In all cases reported, the leading and trailing edges were tested in compression. Table 3.2 shows the D' rotor blade test results for both slip cast and injection molded materials. Three high density (2.9 g/cc) slip cast blade rings (475, 476, 479) were evaluated after an experimental double nitriding firing cycle was unsuccessfully used to achieve complete nitridation. A second series (497-504) of experimental slip cast blade rings of 2.7g/cc density was also evaluated during this reporting period.

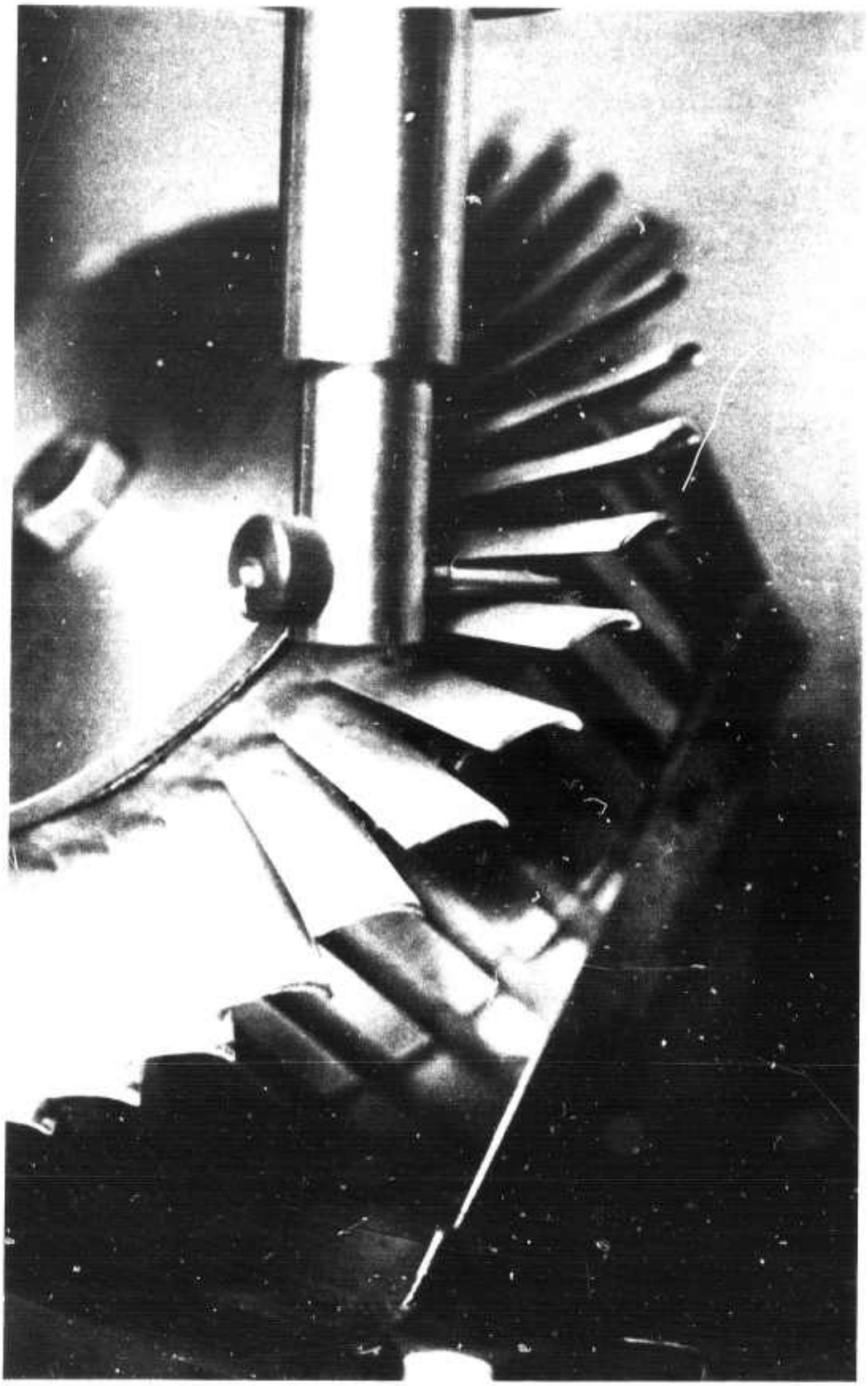

Figure 3.26 Revised Design D' Blade Bend Test Fixture.

TABLE 3.2

SILICON NITRIDE DESIGN D' BLADE BEND TEST RESULTS

Blade Ring Number	Process: Slip Cast	Process: Inj. Molded	Nominal Density g/cc	Number of Data Points	Weibull Slope	Characteristic Load-Lbs	Comment
475	x		2.9	10	20.1	46	Double nitride experiment
476	x		2.9	8	6.8	37	Double nitride experiment
479	x		2.9	5	2.5	43	Double nitride experiment
497	x		2.7	10	4.8	60	Second phase silicon nitride grog inclusions
502	x		2.7	9	16.8	58	Second phase silicon nitride grog inclusions
503	x		2.7	10	11.1	52	Second phase silicon nitride grog inclusions
504	x		2.7	14	12.5	50	Second phase silicon nitride grog inclusions
1346		x	2.7	12	7.1	86	
1356		x	2.7	15	12.8	90	
1377		x	2.7	18	6.6	82	
1386		x	2.7	15	13.0	89	
1410		x	2.7	19	14.1	95	
1474		x	2.7	15	5.3	74	
1534		x	2.7	13	12.1	82	
1554		x	2.7	17	11.9	84	
1568		x	2.7	18	13.9	96	
1606		x	2.7	11	8.5	96	

One of the primary funetions of the blade bend test was to evaluate changes as they are incorporated in the fabrication process and provide timely feedback. Most of the D' blade bend test data aeeumulated to date was on injeetion molded blade rings and resulted in eonsiderable variability of Weibull slopes from 5.3 to 14.1 (Table 3.2). Based on 90% eonfidence, this difference in Weibull slope is statistically significant. This feedbaek has prompted a eurrent program to refine the nitriding step in the rotor fabrication process to produce blade rings of more homogeneous mierostructure.

A summary of injeetion molded design D bend test data is given in Table 3.3 to allow comparison with the baseline slip cast material results previously reported[9] and summarized in Table 3.4. Charaeteristie failure loads ranged from 69 to 123 lbs for injection molded material and from 69 to 130 for the slip cast material. Based on this limited amount of data, it appears that there is no significant differenee in the room temperature strength of these two fabrieation proeesses.

TABLE 3.3

INJECTION MOLDED SILICON NITRIDE DESIGN D BLADE BEND TEST RESULTS

Blade Ring Number	Nominal Density g/cc	Number of Data Points	Weibull Slope m	Characteristic Failure Load Lbs	Comment
1109	2.7	15	5.3	93	Baseline
1109	2.7	10	7.7	109	200 hour thermal soak at 1900°F
1145	2.7	8	10.5	93	Baseline
1145	2.7	19	8.6	113	200 hour thermal soak at 1900°F
1117	2.7	28	16.1	123	Baseline
1186	2.7	8	5.7	69	Baseline

Two injection molded blade rings were tested before and after a 200 hour furnaee soak in air at 1900°F. In this limited sample, failure loads of the thermal treated blades were slightly higher than the untreated blades (Table 3.3). This is eontrary to the results obtained wi th the slip east 2.8 g/ce material presented in the last report[9] where a strength degradation oecurred. The difference in behavior between the 2.8 g/ee slip cast and the 2.7 g/ce injeetion molded materials is attributed to the effeet of unreacted silieon present because of incomplete nitridation of the higher density slip cast material[9].

TABLE 3.4

BASELINE SLIP CAST SILICON NITRIDE DESIGN D BLADE BEND

TEST RESULTS

Blade Ring Number	Nominal Density g/cc	Number of Data Points	Weibull Slope m	Characteristic Failure Load Lbs
92	2.84	14	8.7	96
129	2.8	28	15.6	69
190	2.82	12	13.2	130
204	2.82	19	16.8	116
222	2.8	9	11.6	82
273	2.8	8	16.1	103

Cold Spin Testing of Hot Pressed Silicon Nitride Rotor Hubs

Fourteen hot pressed Si_3N_4 rotor hubs were made from 2% MgO Si_3N_4 powder for correlation analysis testing. The purpose of the correlation analysis was to compare the calculated rotor hub failure distribution with the experimentally determined failure distribution. Care was taken to fabricate these parts under as identical conditions as possible. Nine of the fourteen test hubs were selected for destructive cold spin pit testing. The remaining five hubs were sectioned for determination of Weibull data for correlation analysis.

A minimum amount of machining was done on the hubs prior to testing in order to minimize machining damage. The blade platform width was machined to 0.87 inches, the center line width to 1.23 inches, and the center bore to 0.50 $\pm$ 0.005 inches. A formed grinding tool was used to radius each end of the center bore. Surface finish of the machined surfaces, measured perpendicular to the grinding direction, showed a maximum surface roughness of 10 microinches arithmetic average. All other surfaces were as hot pressed.

The test procedures adapted for this test have been described in detail previously[7,8,9]. All hubs were tested to destruction, and photographed at burst speed with failures typical of previously published hub bursts[7,9]. Burst speeds ranged from 94,570 rpm to 115,810 rpm. The Weibull slope for the hub burst speed was 14.8 with a characteristic speed of 108,500 rpm, as shown in Figure 3.27. The failure distribution was determined using the maximum likelihood estimator technique.

A correlation study was made utilizing the Weibull data from test bars cut from the five sectioned hubs and presented in Table 3.5. The purpose of the correlation study was to check the validity of the use of Weibull theory[4] as applied to brittle materials by calculating a failure distribution versus speed and comparing it to the experimentally determined failure distribution. As shown in

Figure 3.27, the calculated Weibull slope was 16.8 and characteristic speed was 103,800 rpm. The calculated failure distribution falls within the 90 percent confidence band of the experimental failure distribution. This indicates acceptable correlation between calculated and experimental results and confirms the use of Weibull theory in the prediction of rotor hub failure distributions in the cold spin pit.

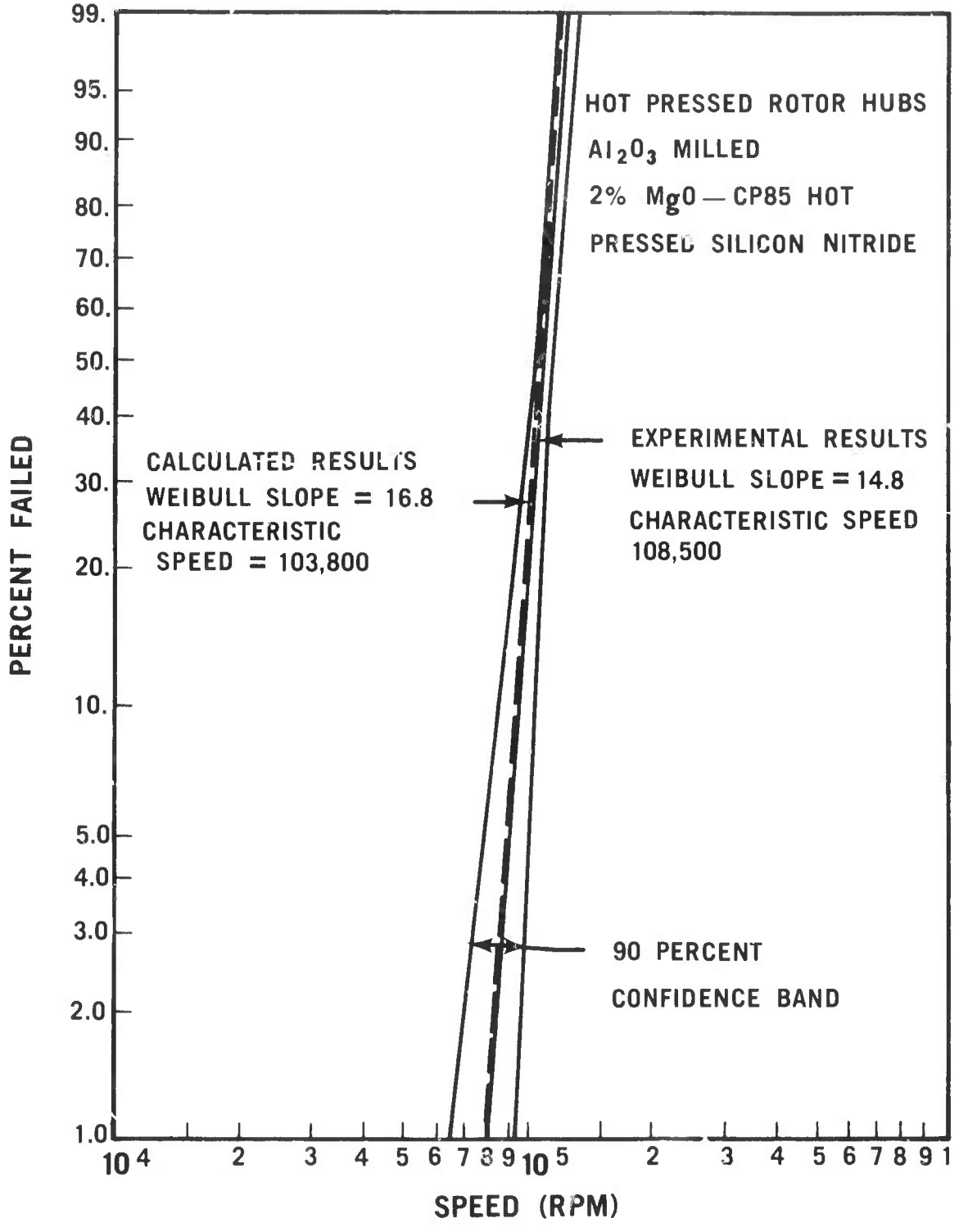

Figure 3.27 Predicted and Actual Weibull Distributions of Burst Rotor Hubs.

TABLE 3.5

WEIBULL TEST BAR DATA USED IN THE CORRELATION STUDY

	Characteristic Modulus of Rupture	Weibull Modulus	Number of Test Bars
Curvic Region	98,300	10.3	60
Web — Region	94,600	8.4	77

Test bar geometry: 0.125 x 0.250 x 1.0 inch

Test spans: 0.375 inch top span, 0.750 inch bottom span

Crosshead speed: 0.020 inches per minute

Detailed test bar data is presented in Tables 4.6 and 4.7 in Section 4.1 of this report.

The calculated maximum principal tensile stress contours of the rotor hub at 116,000 rpm, is shown in Figure 3.28. The 116,000 rpm speed was chosen so that the stress levels could be compared directly with stress levels of a previously tested series of rotor hubs[7]. The curvic recesses were omitted from the present series to minimize machining. Comparison of the principal stresses for this series of rotor hubs, and the previous series show the same general level of stresses throughout the rotor hub.

Hot Spin Rig Testing

Testing of the hot spin rig, shown in Figure 3.29, was primarily confined to rig development, during this reporting period, as follows:

- the rig cooling system
- quick turn around capability

Non-rotational tests of the hot spin rig were continued to determine the cooling air flow rate required to prevent overheating of rig metallic components. It was determined that for a gas temperature of 2500°F at the turbine inlet, 0.02 lb/sec cooling flow rate was sufficient to cool all metallic components to below 600°F except the rig combustor mounting cover which operated at approximately 900°F.

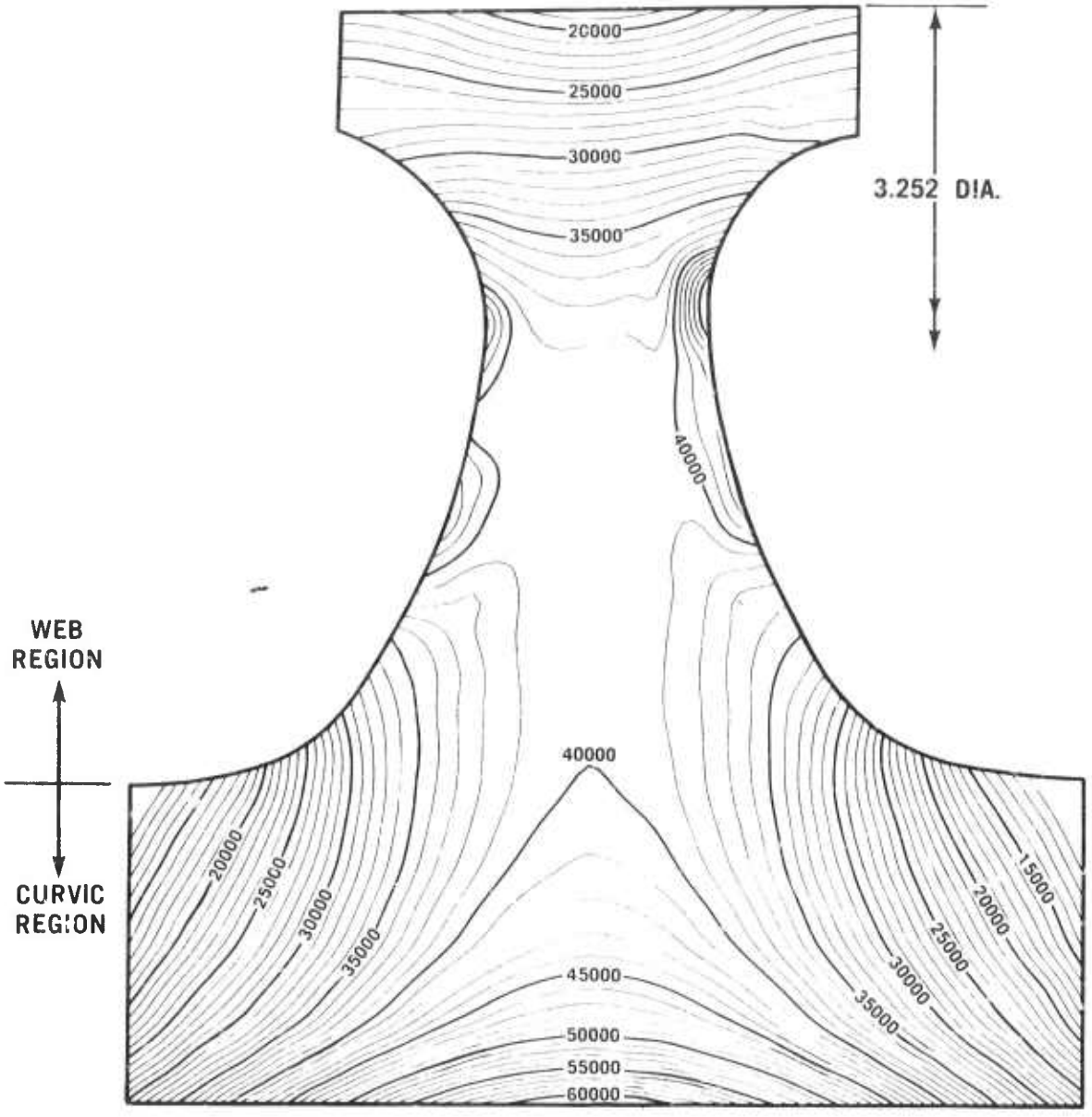

Figure 3.28 Maximum Principal Tensile Stress Contours of a Si_3N_4 Rotor Hub at 116,000 rpm and Room Temperature.

The second phase of the testing consisted of proving the relatively low cost, quick turn around of the rig after a turbine rotor burst. An early rig test was that of a rotor hub with no blades using the original design rotor mounting system shown in Figure 3.29. The hub burst at 41,000 rpm with the following results:

- The tension member of the simplified bolt fractured as provided for in its design.
- The ceramic fiber insulation at the rotor OD absorbed the energy of the burst rotor as expected.
- Some flaring occurred at the metal cone pilot on the end of the rotor shaft.

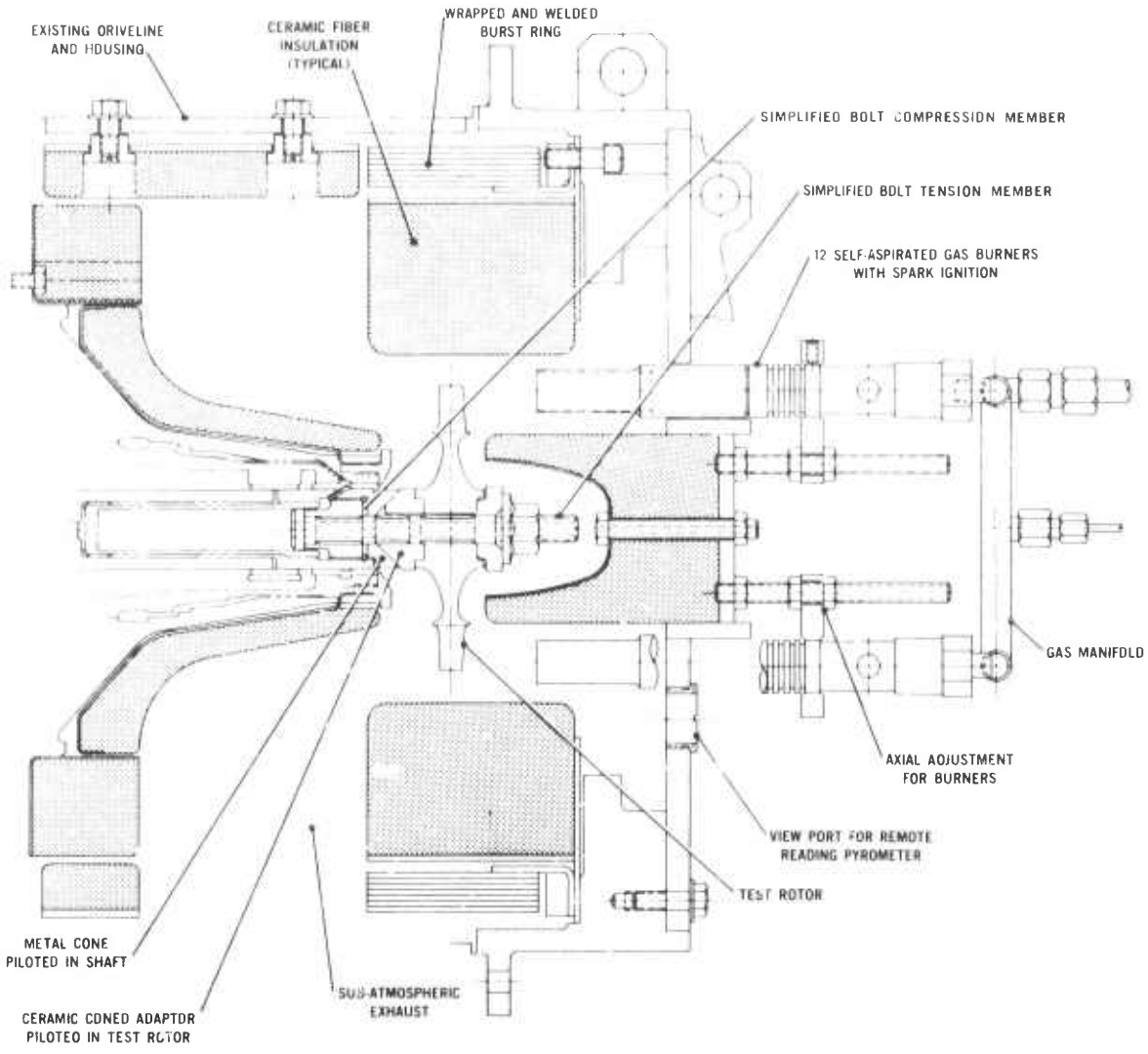

Figure 3.29 Hot Spin Rig Configuration Prior to Redesign.

Design changes were made to reduce flaring of the shaft pilot for the metal cone, to provide a viewing port for measurement of temperature of the rear surface of the rotor by optical pyrometer, and to incorporate a failure detector. These design changes are shown in Figures 3.30 and 3.31. The rotor mounting changes, Figure 3.30, incorporated an OD pilot of the metal adaptor cone and increased the contact diameters between the parts to increase the resistance to unbalance forces resulting from blade failures. Addition of the viewing port to measure rotor temperature from the discharge side by optical pyrometer, is shown in Figure 3.31.

The hot spin rig has also been modified to include automatic shutdown of the test rig after a rotor burst. A burst detector was installed around the outer diameter of the rotor and consists of a sleeve of insulating material wound with closely spaced continuous high temperature chromel wire. The fine wire is cut by a broken blade or other rotor failure debris and automatically shuts down the dynamometer, turns off the fuel, and indicates failure on a strip chart recorder. The strip chart from the recorder provides a record of pertinent operating data at time of failure.

During these developments on the hot spin rig, its capability for relatively low cost, quick turn around was demonstrated. Six available duo-density turbine

rotors of imperfect quality were used for this purpose and hot spin tested to failure speeds ranging from 12,000 to 35,300 rpm at rotor rim temperatures of 1780°F to 2250°F (corresponding to equivalent blade tip temperatures in an engine estimated to be 1930°F to 2400°F).

Preliminary plans have been established for hot spin testing ceramic turbine rotors to assess rotor reliability versus speed, time and temperature. Correlation of short time reliability versus speed with analytical predictions will be determined by testing a number of turbine rotors at temperature in the following manner:

- Establish a base speed and adjust gas burners to achieve the desired rotor hub temperature gradient (measured by an optical pyrometer).
- Accelerate the rotor to failure speed.

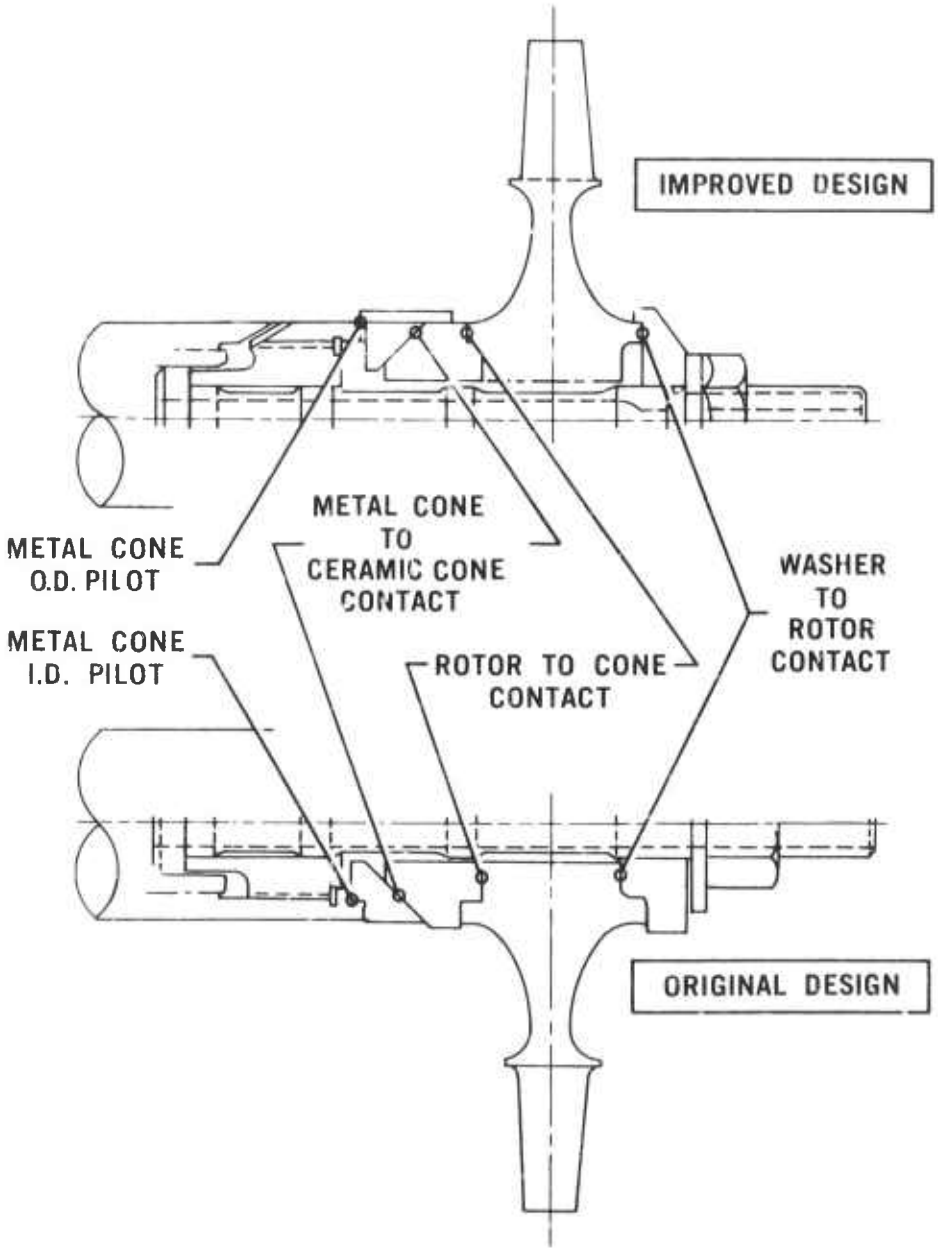

Figure 3.30 Improved Rotor Mounting Configuration in Hot Spin Rig.

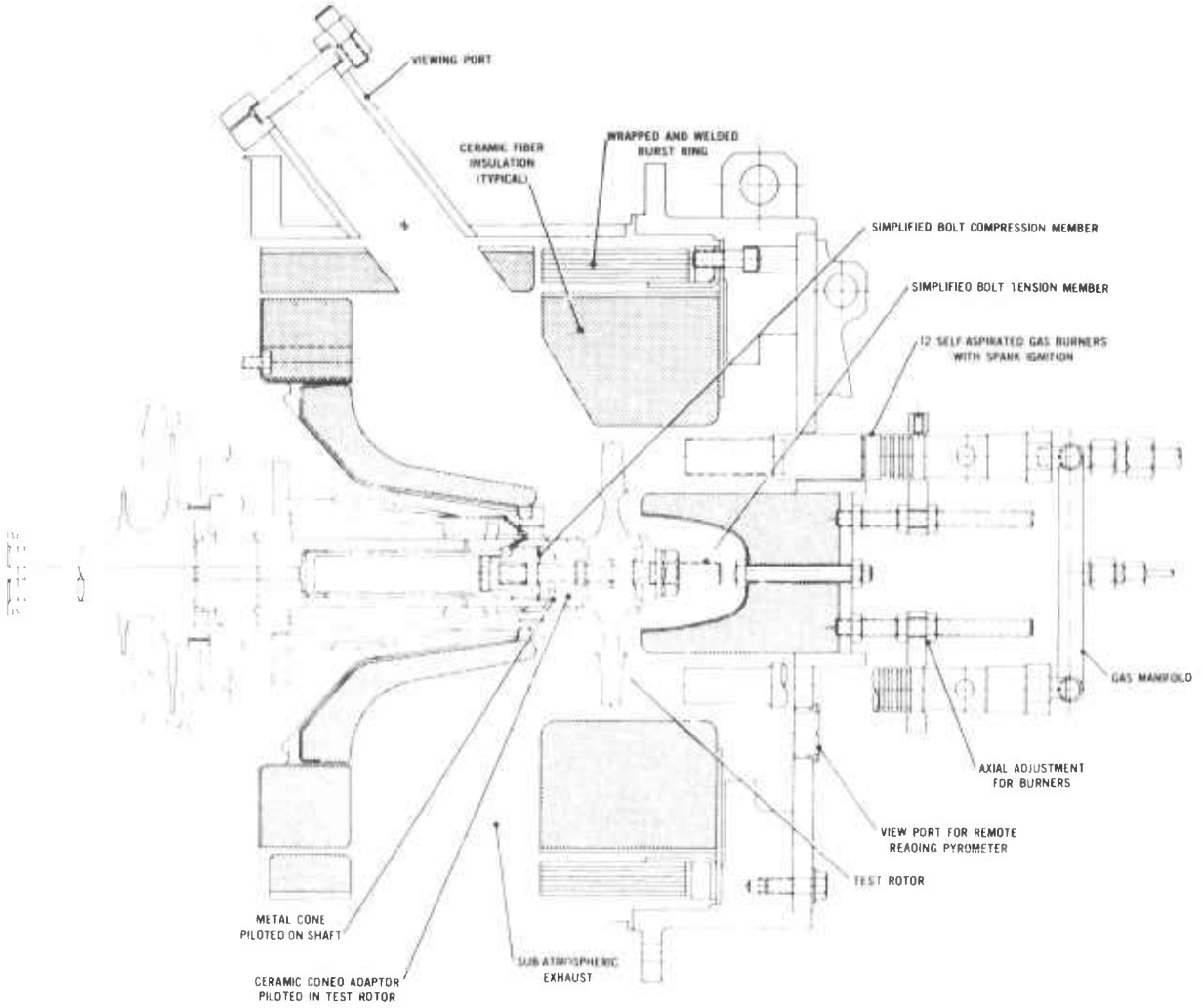

Figure 3.31 Redesigned Hot Spin Rig Configuration.

Correlation of long time ($\leq$ 200 hours) reliability with analytical predictions will be determined by testing rotors at a constant speed and temperature until failure occurs.

Engine Testing

Rotor Attachment

Unlike the simplified conical mounting system used in the hot spin rigs, as discussed earlier in this section, a face spline coupling is used to mount ceramic rotors to the high speed shaft in the engine. This face spline, called a Curvic Coupling(TM), is machined in the ceramic rotor hubs and metal shaft interfaces as previously reported[1,2]. Their function is to transmit rotor torque to the engine shaft while maintaining the concentricity of the rotors to the shaft and allowing relative motion between ceramic and metal resulting from the difference in thermal expansion of the two materials. The need for a lubricant at the metal to ceramic interface to allow this relative motion has been documented[4,5,9] and during this reporting period two new lubricants were evaluated and an improved test cycle formulated.

The new test cycle, Figure 3.32, subjected candidate lubricants to loads and temperatures which closely simulate the engine operating conditions of

the curvic coupling between the first stage rotor and the metal curvic adaptor (see Figure 3.33). The test load and temperature was produced in a mechanical press equipped with an electric oven. The temperature was monitored with a chromel-alumel thermocouple embedded in a metal curvic adaptor tooth. The test conditions selected were the most severe in terms of temperature, relative motion between parts, and destructiveness to the lubricant as found under engine operating conditions.

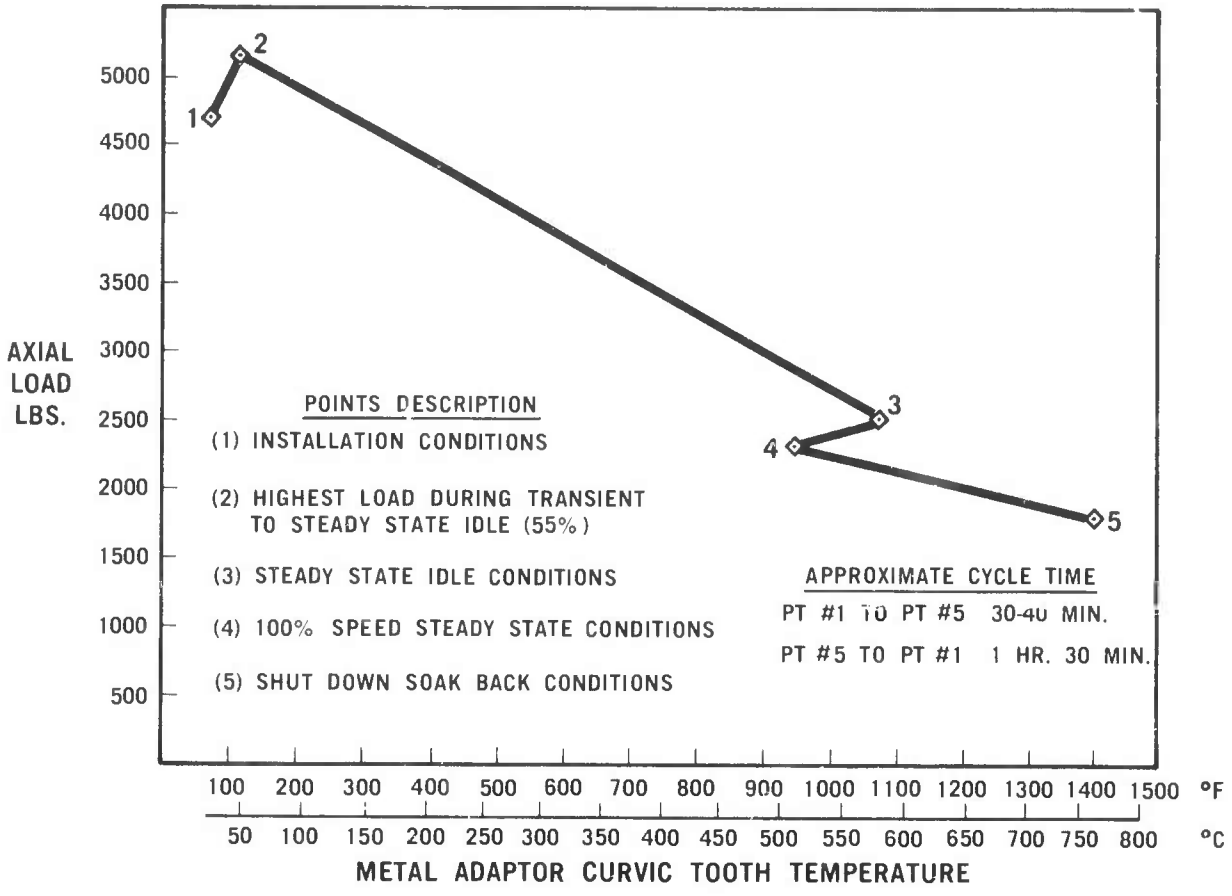

Figure 3.32 Thermal/Load Cycle Schedule for Curvic Tooth Lubrication Tests.

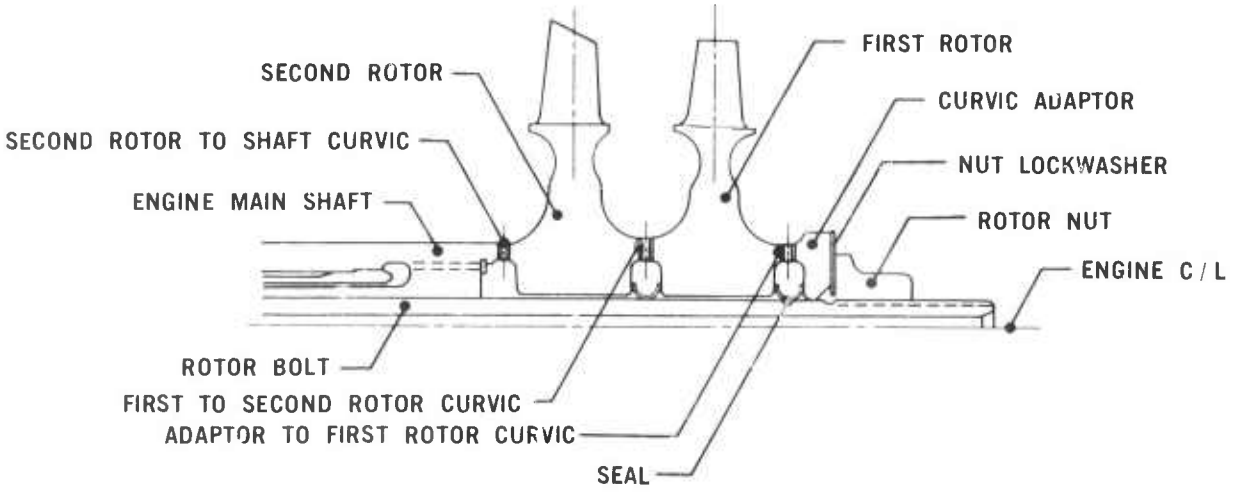

Figure 3.33 Illustration of Rotor Attachment Parts.

Previous tests[9] had shown that the lubricant initially used (Dow Corning Molykote 321) would survive two test cycles without failure of the ceramic curvic teeth. However, long term engine tests required a better lubricant, so two new lubricants, Borkote (Advanced Metals Company of Woburn, Massachusetts) and Electrofilm 1000X (Electrofilm Corporation of Los Angeles, California) were evaluated.

Borkote was applied to a metal curvic adaptor and subjected to the test cycle which it successfully completed. However, examination showed the hard top layer of the coating to be separating. The metal curvic adaptor was made of Inconel X750 and the aluminum content (0.80%) has been determined to be the cause of this problem. A new metal curvic adaptor of an aluminum free metal will be fabricated and the Borkote test repeated.

The second lubricant tested was Electro Film 1000X which has passed three test cycles. Figure 3.34 shows the test samples after the three test cycles. This lubricant was also used in an engine test of a bladeless first stage ceramic turbine rotor hub of reduced outside diameter operated at 2500°F turbine inlet temperature for one half hour during the initial checkout of the modified engine (described later in this section).

Phased Rotor Testing

In order to gain early engine running experience with ceramic rotors and the mounting system[8, 9], two duo-density rotors with blades 10% of full length were tested in an engine at 32,000 rpm and 2000°F turbine inlet temperature for 45 minutes.

The rotors (S.N.716 and S.N.717) were mounted with curvic couplings, as shown in Figure 3.35, lubricated with Molykote 321(TM). The bolt attachment scheme was modified to allow a lower initial clamping load and more elastic stretch of the bolt tensile member to reduce the clamping load drop-off caused by bolt heating.

The rotors were tested in an engine using a manual fuel control. The test consisted of combustor lite-off and rotor acceleration to 50% speed. Turbine inlet temperature was held at 2000°F. This condition was maintained for 45 minutes whereupon the engine was shutdown and disassembled.

Post inspection showed the ceramic rotors to be in good condition. However, they did show some abrasive wear of ceramic surfaces in contact with metal parts. The metal seal between the rotors had abraded a groove into the surface of the first stage rotor and the metal seal between the first stage rotor and metal curvic adaptor had worn a circular groove into the rotor surface at the outer edge of the seal where it contacted the rotor. This latter metal seal had permanently collapsed indicating a higher-than-expected operating temperature. The first rotor curvic tooth surface had also worn slightly where it contacted the metal curvic adaptor. There was very little of the Molykote 321 lubricant remaining.

The rotor bolt, metal curvic adaptor and nut had all been over-heated. The bolt was permanently elongated 0.007" inches and the adaptor, bolt and nut had softened indicating temperatures in excess of the metal heat treat temperature. It is believed that undercooling of the metal parts was caused by a leak path in the engine which affected the pressure drop across the bolt and hence the bolt cooling air flow. Also, the high temperatures occurring during soak back contributed to overheating of metal parts. These problems will be circumvented in future engine testing by using an external cooling air supply.

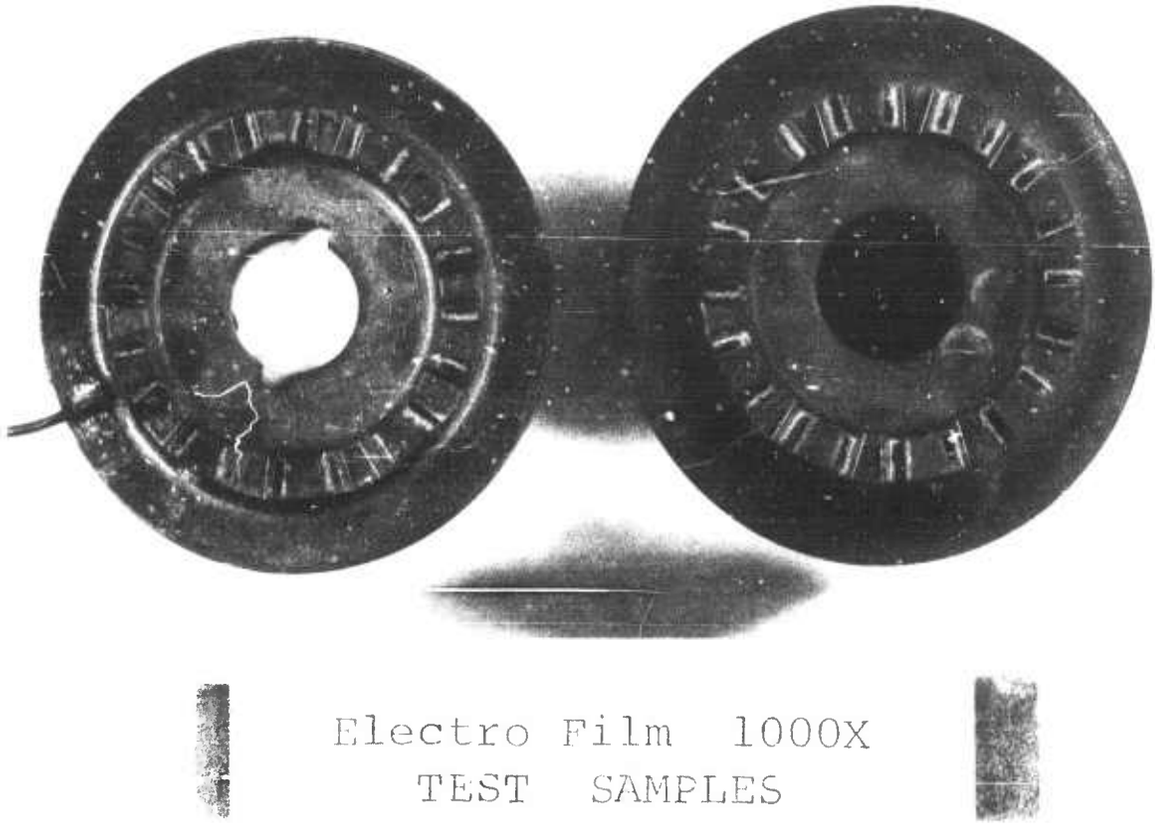

Figure 3.34 Electro Film 1000X Lubricant After Three Test Cycles.

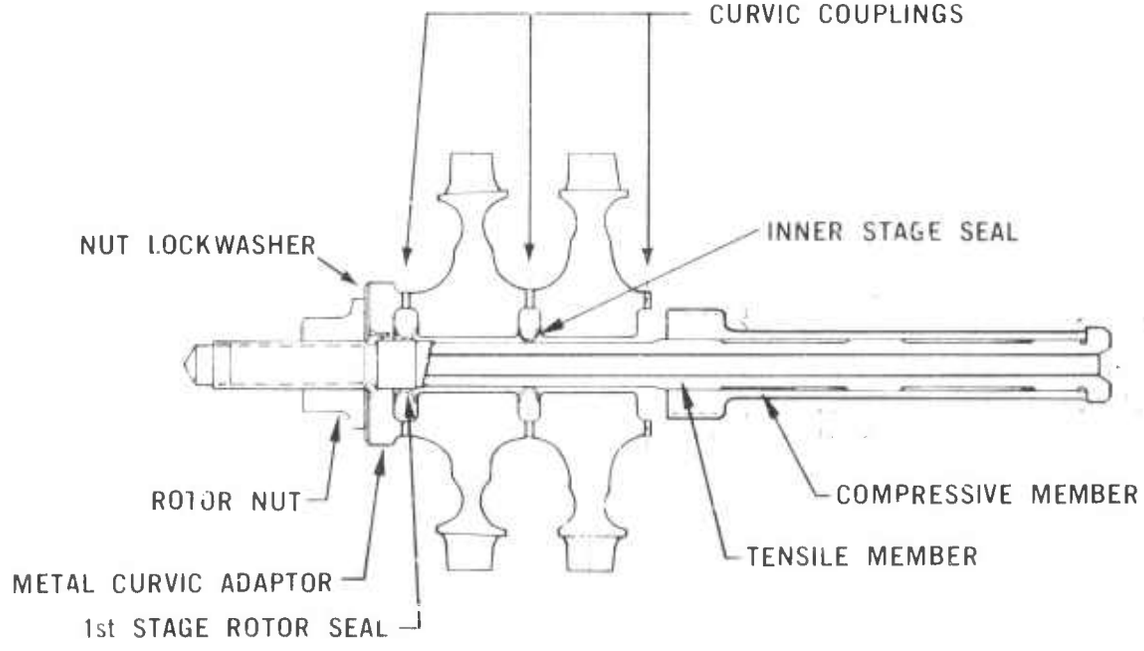

Figure 3.35 Turbine Rotor Shaft Assembly.

Rotor Testing in the Modified Engine

The need for the modified engine configuration was presented in Section 3.1.1. Before incorporating the modified hardware into an engine, preliminary testing and check out was done in available test rigs. The combustor operation was evaluated in the 2500°F Flow Path Qualification Rig (FPQR)[9] and modified flow path ceramic hardware was evaluated in the Ceramic Structures Rigs (CSR)[9].

The modified engine design configuration redistributed air flow in such a way that the combustor overall fuel/air ratio was increased by a factor of 3. A standard metal combustor and a redesigned version of it (with a leaner primary zone) were tested in the FPQR at the modified fuel/air ratios, air flow and pressure levels. The standard combustor demonstrated a significant problem with carbon formation in the primary zone which was overcome with the leaner combustion configuration.

Modified flow path ceramic hardware was first qualified by the 10 cold light test and then installed in a Ceramic Structures Rig and used to verify the effectiveness of the modified design in reducing the 2500°F gas temperature to acceptable levels before reaching the ceramic regenerator cores.

After testing, all hardware, including the regenerator cores, was in satisfactory condition and was used to build the modified engine for testing ceramic rotors.

Initial check out of the modified engine, complete with ceramic stationary hardware described in Sections 3.1.1. and 3.2., was carried out using two ceramic bladeless rotor hubs of reduced outside diameter. This check out run comprised a successful test to 50% speed and 2500°F Turbine Inlet Temperature (T.I.T.). The first stage hub was then removed in preparation for installation of a ceramic turbine rotor.

To expedite rotor testing in a modified engine, ceramic rotor #709 was selected from available hardware. Though of poor quality because of cracks in the rim and most of the blades this rotor had been previously proof spun to 53,710 rpm cold. To further enhance its quality for a run at temperature, blades with probable flaws were removed prior to its installation in the modified engine, in addition the 10 remaining blades were reduced to 90% length to increase blade tip clearances. The metal spacer (Figure 3.2) was instrumented with chromel-alumel thermocouples to prevent any inadvertant over-temperature. The externally supplied cooling air discharging from the rotor bolt was also monitored to assure adequate cooling air flow. Turbine inlet temperatures were monitored by three platinum aspirated probes and constantly displayed on digital readouts. Electrofilm 1000X lubricant was used on the metal curvic adaptor teeth and Dow Molykote 321 was used on all other curvic teeth. A 4700 lb rotor attachment bolt load was obtained by stretching the tension member of the bolting system.

Figure 3.36 shows the speed and turbine inlet temperature versus time for the first test of rotor #709. This test ended at 52,800 rpm when a safety circuit was actuated by a stray signal causing an automatic shut-down. The ceramic rotor and other ceramic stationary parts were inspected and found undamaged by the 2650°F T.I.T. and 52,800 rpm conditions experienced during this test.

The engine was reassembled and a second run was made to 50,000 rpm and 2300°F T.I.T. Figure 3.37 presents the data for this run. After 2.4 minutes rotor #709 failed and the engine was shut down. Examination showed complete destruction of the rotor and ceramic hot gas flow path parts.

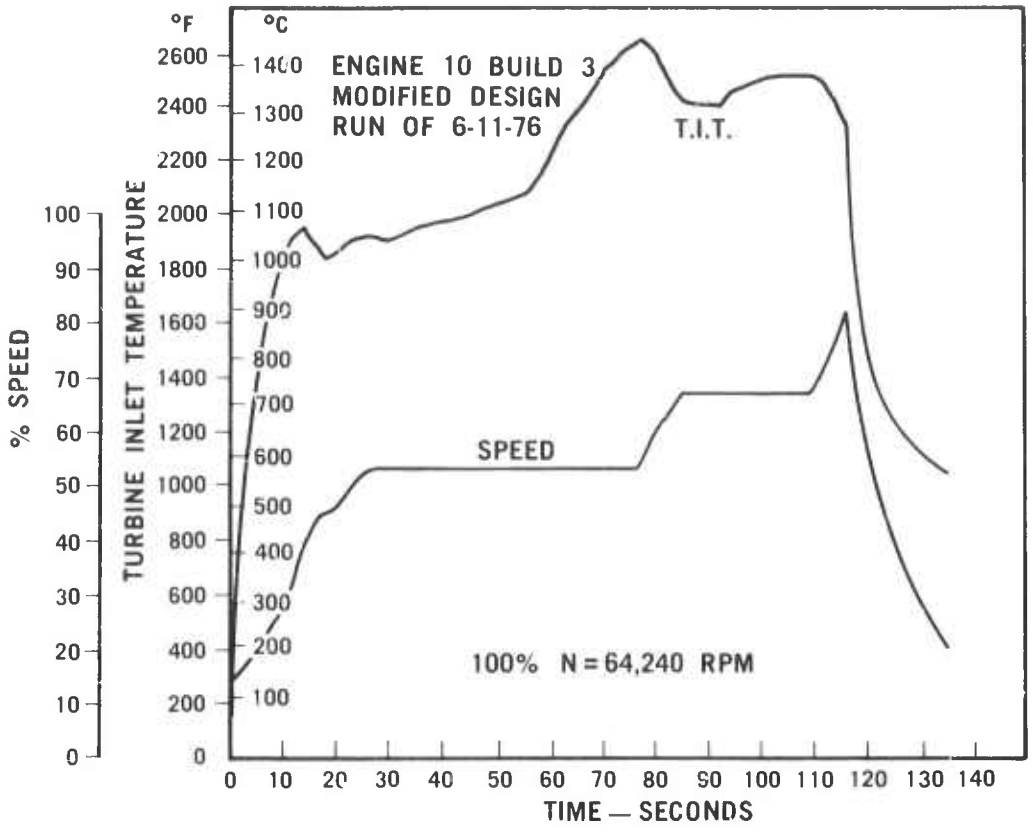

Figure 3.36 First Run of Rotor #709.

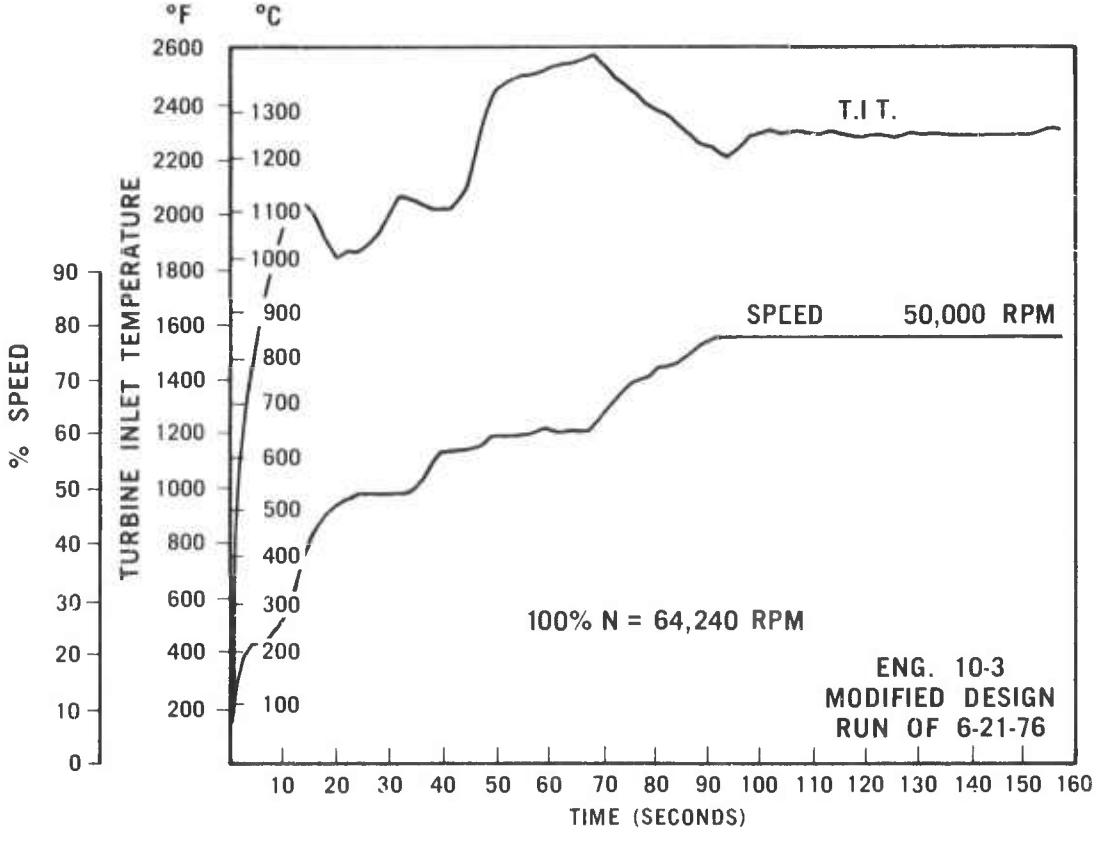

Figure 3.37 Second Run of Rotor #709.

3.2 CERAMIC STATOR, NOSE CONE, ROTOR SHROUD AND COMBUSTOR DEVELOPMENT

SUMMARY

Due to the Turbine Rotor Fabrication Task Force effort during this reporting period, the fabrication of stationary ceramic components was deferred thus limiting the amount of stationary component testing conducted.

One thick-walled silicon carbide "Refel" combustor successfully completed the 200 hour engine duty cycle in the Combustor Test Rig including a total of 26 hours and 40 minutes at 2500°F turbine inlet temperature. Three combustors of a new thin-wall design have been successfully qualified for further engine or rig testing.

Seven new stators of 2.55 gm/cm^3 density and one rotor tip shroud successfully passed an improved qualification light-off test. A reaction bonded silicon carbide stator successfully accumulated 147 hours of testing at 1930°F and remains crack free. The 2500°F flow path test rig was rebuilt and operating controls improved. Work continues on improving temperature measurement techniques.

A nose cone, stator and tip shroud were successfully tested in the modified engine configuration, for over 9 hours, to a maximum turbine inlet temperature of 2500°F.

3.2.1 TESTING

Introduction

The stationary hot flow path components include the combustor, turbine inlet nose cone, common first and second stage stators, and first and second stage rotor tip shrouds. As discussed previously, fabrication of these stationary flow path components was deferred during this reporting period in order to concentrate on injection molding rotor blade rings as part of the Turbine Rotor Fabrication Task Force. As a result, only limited testing of stationary ceramic components made prior to October, 1975 was carried out during this reporting period. This included three types of testing: combustor testing to 2500°F, engine rig testing for light-off qualification and durability evaluation, and stationary ceramic flow path testing to 2500°F.

With the wind-down of the Turbine Rotor Fabrication Task Force, the fabrication of stationary ceramic components has been resumed. When processing of these parts is complete, testing and evaluation of stationary ceramic components will be continued.

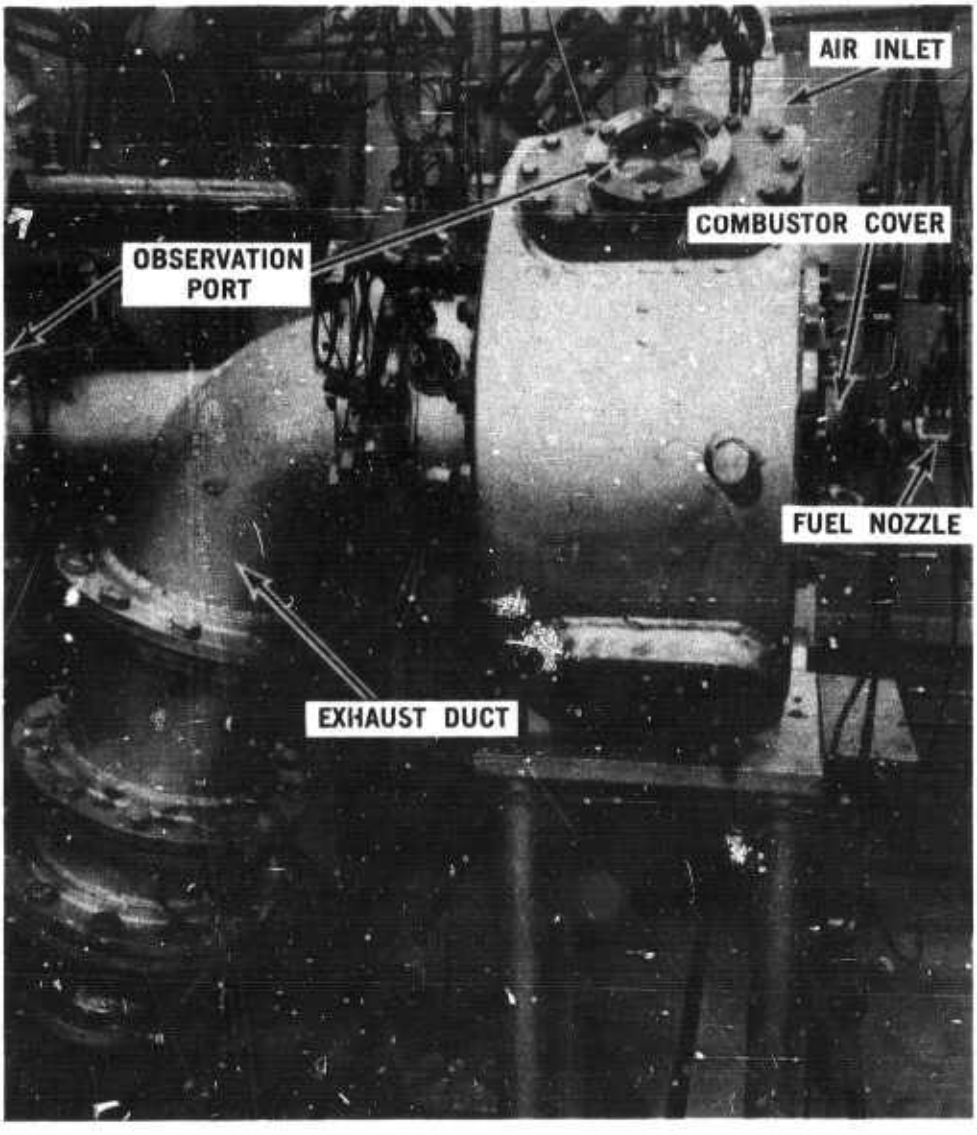

Figure 3.38 Combustor Test Rig

Combustor Testing

Evaluation of reaction bonded silicon carbide (REFEL) combustors[9] was conducted in the steady-state Combustor Test Rig shown in Figure 3.38 and described in some detail in a previous report[6].

One thick-walled "Refel" combustor tube has now accumulated 201 hours: 5 minutes in the steady-state test rig, equivalent to the prescribed 200 hour engine duty cycle. At the 100% speed, 2500°F simulated engine operating condition, 26 hours: 40 minutes have been successfully completed. No cracks or other visual defects are present in the combustor tube. However, during this reporting period, three additional thick-walled combustor tubes failed to pass the 10 hour qualification test described in Table 3.6[9].

Because of these inconsistent results, a new thin-walled design configuration with expected reduced thermal stresses was subjected to test. The first two such combustors passed the 10 hour qualification test as reported previously[9] and during this reporting period, a third thin-wall combustor tube has been qualified with no resulting cracks. A photograph of the new design "Refel" combustor tube is shown in Figure 3.39. A summary of "Refel" silicon carbide combustor tube testing to date is shown in Table 3.7.

TABLE 3.6

ARPA DURABILITY TEST CYCLE

FOR CERAMIC COMBUSTORS

Equivalent Engine Speed %	T_6 °F	P_6 psia	W_a PPS	T_7 °F	Time Hours-Minutes
55	1628	24.7	0.63	1930	4 - 30
59	1590	26.9	0.71	1930	2 - 30
69	1495	33.3	0.93	1930	- 40
77.5	1413	40.8	1.15	1930	- 30
86.5	1321	50.1	1.41	1930	- 30
100	1680	70.9	1.95	2500	1 - 20
					10 hours

T_6 — inlet air temperature to the combustor

P_6 — inlet air pressure to the combustor

W_a — combustor airflow (pounds per second)

T_7 — exit gas temperature from the combustor

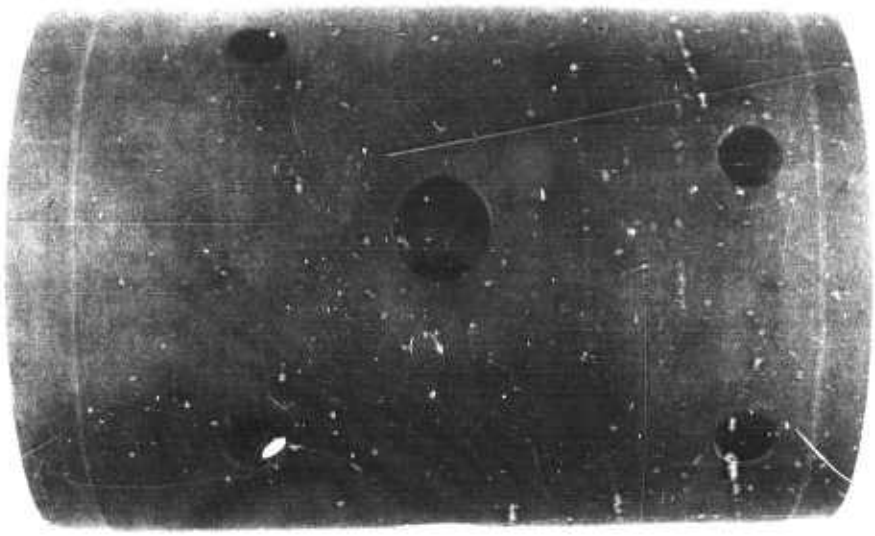

Figure 3.39 Thin-Wall Silicon Carbide "Refel" Combustor.

TABLE 3.7

SUMMARY OF REACTION BONDED SILICON CARBIDE (REFEL)

COMBUSTOR TESTING

Design Number	Serial Number	1930°F Static Testing Hours: Minutes	2500°F Static Testing Hours: Minutes	Component Status	Total Part Time Hours: Minutes
1	1	174:25	26:40	S, N	201:05
1	2	0:00	0:30	F, C	00:30
2	1	9:05	2:20	S, N	11:25
2	2	5:55	1:20	F, C	7:15
2	3	8:40	1:20	F, C	10:00
2	4	0:00	1:20	F, C	1:20
3	1	8:40	1:30	S, N	10:10
3	2	9:00	2:20	S, N	11:20
3	3	8:55	1:20	S, N	10:15

Key to Component Status

C = Cracks F = Failed N = No Cracks S = Serviceable

Engine Rig Testing

Limited testing of turbine inlet nose cones, first and second stage stators, and first and second stage rotor tip shrouds was conducted in engine test rigs. Tables 3.8 to 3.10 show the results to date of engine testing on silicon nitride and silicon carbide stationary components.

Component Qualification

In order to eliminate components with large fabrication and/or processing defects, components are first subjected to a qualification test. This qualification test was modified during this reporting period in order to subject the components to a broader range of thermal environments as shown in Table 3.11. Seven stators of 2.55 g/cc density and one first stage rotor tip shroud successfully passed this test during this reporting period, all being in excellent condition after the test.

1930°F Durability

After completion of qualification testing, some components were subjected to static durability testing in engine test rigs at 1930°F.

Nose cone S/N 872, which had previously developed a crack in the inner bell, was run again after being reworked. The region containing the crack was ground off and the nose cone ran for 146 hours at 1930°F. The test was terminated due to a crack in the nose cone outer shroud.

A reaction bonded silicon carbide stator was evaluated and demonstrated very encouraging results. This stator was run for 147 hours at 1930°F and is free of cracks, as shown in Figure 3.40.

TABLE 3.8

SUMMARY OF NOSE CONE TESTING

Material and Design Identification Number	Serial Number	Static Engine Testing				Cyclic Testing (ARPA)					2500°F Static Testing		Miscellaneous Tests		Component Status	Total Part Time Hours**	Total Part Lights
		Light (C. Id)	Shutdowns Cold	Shutdowns Hot	Hours**	Lights Cold	Lights Hot	Shutdowns Cold	Shutdowns Hot	Hours**	Lights	Hours	Lights	Hours**			
Target		10	9	1	0.2	11	26	-	40	200	4	25					
S	73												142	16.75	F	16.75	142
1	102	25	18	7	24.5	11	96	21	59	221.5					F,B	216.09	105
1	103	19	17	2	6.10	1	2	0	3	50.5					F,O	50.90	22
1	130					5	-	2	6	24.5					F,H	24.50	8
S	202	10	9	1	0.20	9		9	2	6.5	1	5.0	1	18.30	F,C,O,X	30.00	28
2	207	60	51	9	37.9	6	10		16	42.8			1	9.8	F,B	90.50	80
1	301	16	12	1	2.00								15	50.3	F,C,O,X	52.30	61
2	320												10	1.15	F,X	1.15	10
2	321	30	27	3	0.50								29	27.50	F,X	28.00	59
3	806	27	20	7	18.5	1			1	13.25			6	2.50	F,B	34.25	34
3	807	64	58	6	1.23										F,C,X	1.23	64
3	814	19	13	6	33.91										F,C	33.91	19
1	871	14	9	5	62.25										F,B	62.25	14
4	872*	85	51	34	117.15										F,C	117.15	85
1	875	10	9	1	0.25						3	1.2	2	1.85	F,B	6.3	15
1	876	16	9	7	55.50										F,B	55.50	16
4	889	40	36	4	1.00										F,C	1.00	40
5	890	19	14	5	32.1										F,H	32.1	19
1	903	10	9	1	0.25										F,C,X	0.25	10
5	904*												7	.5	F,X	.5	7
4	910	12	11	1	0.25										F,B	0.25	10
4	916	26	18	8	30.90										F,C	30.90	26
4	917	16	9	1	0.25										F,C,X	0.25	10
1	920	10	9	1	0.25										F,B,X	0.25	10

* New entry this reporting period ** Up to at least 1930°F

Serial Numbers 73-321 are 2.2 g/cc density; remaining are 2.55 g/cc density.

Key to Component Status

F Failed
O Failure occurred in other than ARPA duty cycle
H Part failed during handling
C Cracked shroud
B Inner body crack
X Internal material flaw involved in failure

TABLE 3.9

SUMMARY OF STATOR TESTING

Material and Design Identification Number	Serial Number	Static Engine Testing: Light (Cold)	Shutdowns: Cold	Shutdowns: Hot	Hours**	Cyclic Testing (ARPA): Lights: Cold	Lights: Hot	Shutdowns: Cold	Shutdowns: Hot	Hours**	2500°F Static Testing: Lights	Hours	Miscellaneous Tests: Lights	Hours**	Component Status	Total Part Time Hours**	Total Part Lights
Target		10	9	1	0.2	14	26	-	40	200	4	25					
2	372	10	9	1	0.20	1	2	0	3	50.5			2	7.9	F,V,I,O	58.60	15
2	421	10	9	1	0.20								3	2.80	C,X	3.00	13
2	424	10	9	1	0.25								9	2.75	C,X	3.00	19
2	428	10	9	1	0.20	17	14	6	25	103					F,C	103.20	41
2	430	10	9	1	0.20	14	13	6	21	61.5					F,C	61.70	37
5	525*+	39	13	26	146.75										S	146.75	39
1	715	10	9	1	0.20								6	0.10	F,V,O	0.30	16
1	751	11	10	1	0.20								2		C,V,O,X	0.20	13
2	817	34	31	3	0.75										S	0.75	34
1	820	14	13	1	0.30										C,X	0.30	14
1	841	12	11	1	0.20	6	10		16	42.8					F,C	43.00	28
1	848	11	10	1	0.20										F,H	0.20	11
1	852	23	20	3	1.70										F,O	1.70	23
1	858	12	11	1	0.20	6	10		16	42.8					F,C	43.00	28
1	865	12	11	1	0.25								2	9.50	F,V,I,O	10.15	14
1	868	12	11	1	0.25								2	9.50	F,V,I,O	10.15	14
6	879*	10	9	1	.25						2	1.0			S	1.25	12
2	880*	2	9	3	2.8								1	5.00	S	7.8	13
6	884*	10	9	1	.25										S	.25	10
3	889*	54	49	5	17.6								4	6.8	S	24.4	58
3	898	10	9	1	0.25										S	0.25	10
1	916*										1	1.0	4	18.5	F,V,I	19.5	5
1	911	15	9	6	54.25										F,V	54.25	15
2	911A	11	10	1	0.25						1	.25	11	21.75	F,V,I,O	22.25	23
6	921*	10	9	1	.25										S	.25	10
4	924	10	9	1	0.25								1	0.50	F,V,X	0.75	11
4	927*	10	9	1	.25								.	.5	F	.75	17
4	936*	10	9	1	.25										S	.25	10
4	940	29	15	11	32.75										F,C	32.75	29
4	943	10	9	1	0.25						3	4.2	1	1.45	F,C	5.9	14
4	945*	11	9	2	.50								1	.03	F,O	.53	12
1	948*	10	9	1	.25										S	.25	10
1	954	19	9	10	175.00										S	175.00	19
3	955	12	9	3	23.00										F,C	23.00	12

* New entry this reporting period ** Up to at least 1930°F
+ Silicon Carbide part
Serial number 372 is 2.2 g/cc density; remaining are 2.55 g/cc except for 525 which was SiC

Key to Component Status
- S Serviceable
- F Failed
- O Failure occurred in other than ARPA duty cycle
- H Part failed during handling
- C Cracked shroud
- V Vane(s) failed
- X Internal material flaw involved in failure
- I Impact failure from combustor carbon

TABLE 3.10

SUMMARY OF SHROUD TESTING

Material and Design Identification Number	Serial Number	Static Engine Testing: Light (Cold)	Shutdowns: Cold	Shutdowns: Hot	Hours**	Cyclic Testing (ARPA): Lights: Cold	Lights: Hot	Shutdowns: Cold	Shutdowns: Hot	Hours**	2500°F Static Testing: Lights	Hours	Miscellaneous Tests: Lights	Hours**	Component Status	Total Part Time Hours**	Total Part Lights
Target		10	9	1	0.2	14	26	-	40	200	4	25					
First Shrouds																	
5	17	17	9	8	9.83								5	.33	F	9.83	24
1	21	19	17	2	0.40	4	7	0	4	50.50					S	50.90	22
1	111	14	12	1	0.20	61	11	14	68	214.00					S	214.20	115
2	119	15	14	2	0.25										F,C	0.25	15
2	120	12	11	1	0.25										S	0.25	12
	121	10	9	1	0.25										S	0.25	10
Second Shrouds																	
3	2	10	9	1	0.25										F,C	0.25	10
3	3	12	11	1	0.25						3	2.0	3	21.3	S	26.55	22
3	1	10	9	1	0.25										F,C	0.25	10
3	6												3	1.75	F	1.75	3
1	18	19	17	2	0.40	4	7	0	4	50.5					S	50.90	22
1	100					5	9	6	10	6.1			30	1.60	S	8.0	40
1	102					1	9	0	10	6.1					S	6.1	19
1	104												3	5.00	S	5.10	75
3	106	19	9	1	0.20	4	11	51	68	214.00					S	214.20	112

* New entry this reporting period ** Up to at least 1930°F Density 2.6 - 2.7 g/cc

Key to Component Status
- S Serviceable
- F Failed
- C Cracked Shroud

TABLE 3.11

FLOWPATH QUALIFICATION TEST SCHEDULE

Number of Light	Light-Off Temperatures*, °F	Hold Time at 1930°F Seconds
1	70	30
2-5	150	30
6-9	150	60
10	150	300
10 Total Lights		420 Sec. at 1930°F

*Forced cooling used between lights to achieve these temperatures

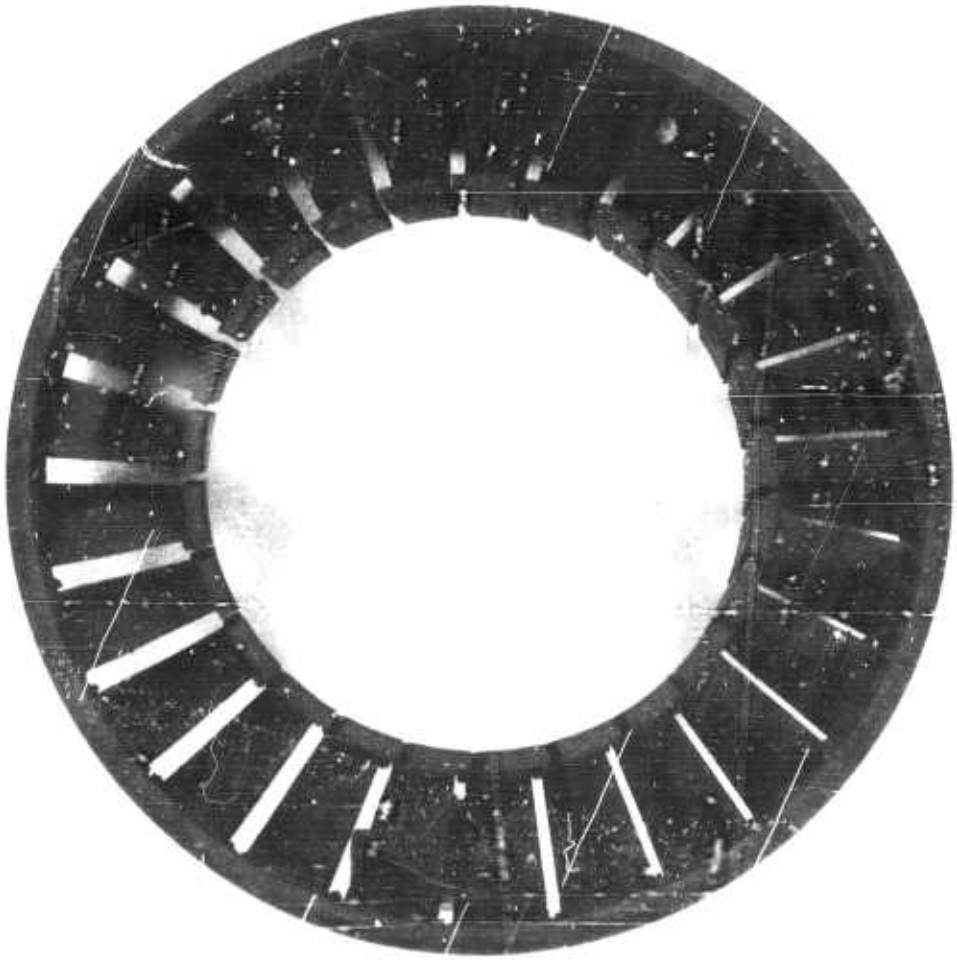

Figure 3.40 Silicon Carbide Stator #525 After 117 Hours at 1930°F in an Engine Test Rig

Stationary Ceramie Flowpath Testing to 2500°F

After eompletion of qualification testing, some eomponents were subjected to statie durability testing at 250C°F. Prior to this reporting period, this effort could only be eonducted in the 2500°F Flow Path Test Rig.[9] With the design build, and cheek-out of a modified engine (see Seetion 3.1) the capability of 2500°F testing h:s been demonstrated in a seeond typ: of test rig. Results from both types of rigs a:e presented.

As planned for in the last report[9], a complete disassembly and rebuild of the 2500°F Flow Path Test Rig w: s performed which involved:

a. Replacement of the entire ceramic ducting system, to replace cracked parts.
b. Installation of a modified ceramic adaptor which functions as a container for the components under test,
c. Installation of an improved exhaust cooling control system, and
d. Incorporation of a newly designed air-pressurized double face metal seal to minimize internal air leaks.

While awaiting post-Turbine Rotor Fabrication Task Foree stationary eomponents, temperature measuring techniques are being updated for overall improvement of the 2500°F Flow Path Test Rig Operation.

Testing of stationary components in the modified engine configuration during this report period is summarized as follows:

- Components tested (1) nose cone
  (1) 1st stage stator
  (1) 1st stage stator insulator ring
  (2) Rotor tip shrouds
- Test Temperature Range — 1750°F to 2500°F
- Total Test Time — 9 hours and 4 minutes

No failures were noted in the hardware upon completion of th:se tests. Subsequent testing of this hardware with a eeramie turbine rotor was covered earlier in Seetion 3.1.3.

4. PROGRESS ON MATERIALS TECHNOLOGY

SUMMARY

Materials technology is a very important portion of the systems approach employed in this project for the development of high temperature gas turbine engines. The generation of ceramic material property data, in progress since the beginning of the project, has been instrumental in component design modifications and failure analysis. As testing and fabrication experience was gained, improvements in materials have also been made. The properties of these improved materials are determined and fed back into design modifications and failure analysis, thus closing the loop. The work on determining material properties and on generating material improvements is reported in this section.

Modulus of Rupture tests were conducted on 274 specimens of hot pressed silicon nitride to investigate the effects of surface finish, post machining heat treatment and process variations. No statistical difference in MOR was found between bars finished by grinding to 10 microinches and bars finished by lapping to 1 microinch. Six post machining heat treatments on Norton NC-132 bars all resulted in a decrease in the room temperature MOR due to oxidation effects. No statistical difference in MOR was found for bars machined from one hot pressed rotor hub nor was any found for bars machined from different hubs fabricated from the same batch of powder. However, hubs made from different batches of milled powder did show a variation in MOR.

MOR tests on 155 bars of 2.7 g/cc density injection molded reaction sintered silicon nitride were conducted on specimens processed the same as engine hardware. The room temperature characteristic bending strengths were lower than previous experimental batches, 36.3 ksi versus 44.3 ksi; however, the Weibull modulus values increased from 6.78 to 11.1 indicating less scatter. MOR tests were also carried out at elevated temperatures, 1700°F, 2100°F, 2300°F and 2500°F. Bending stress rupture tests on 15 specimens resulted in no time dependent failures for this material up to 2200°F. Twelve of the tests were suspended, without failure, after 200+ hours at stresses of 20-30 ksi and temperatures of 1900-2200°F.

The nitridation of silicon compacts of various densities was investigated for the effects of temperature schedule, atmosphere and furnace load. The "constant rate of temperature increase" cycle combined with an atmosphere of 96% N_2/4% H_2 produced strengths on the optimum strength density line (for densities in the 2.55-2.7 g/cc range) for moderate furnace loads. Other temperature schedules, atmospheres and larger furnace loads produced poorer strengths due to localized silicon "melt out" and resulting large porosity. The key to uniform microstructure, fine porosity and associated high strengths appears to be the controlling of the nitriding exotherm so that the silicon compact does not reach 1420°C.

Thermal shock test results on a limited sample of sialon materials indicated an oxygen-related melting phenomenon is associated with Y_2O_3 which was used as a sintering aid. Two samples with 1/2% Y_2O_3 did sustain 1312 cycles of 45 seconds each to 2100°F while others, with 6% Y_2O_3, melted after less than 100 cycles to 2200°F. Current work aimed at producing sialon according to the vacancy-free model is yielding promising results.

The preparation of silicon powder by attritor milling versus the conventional ball milling technique was investigated. However, the flow characteristics, as measured by a standard spiral flow test, indicated the material was inferior to the conventionally processed powder even though similar particle size distributions can be achieved.

4.1 PROPERTIES OF HOT-PRESSED SILICON NITRIDE

Introduction

Room temperature Modulus of Rupture (MOR) tests were conducted on 274 hot pressed silicon nitride specimens. Fifty-six bars were cut from two rotor hubs to investigate the effect of surface finish on MOR. Seventy-eight bars from a billet of Norton NC-132 were used to determine the effect of several post machining heat treatments on MOR. An additional 140 test bars were cut from a total of five rotor hubs to determine the variation in MOR from hub-to-hub, within one hub and as a function of initial material batch.

The statistical analysis of strength data was performed by a "Most Likelihood Estimator"[13] (MLE), computer program. Point estimates (i.e. 50% confidence) as well as estimates of the 90% confidence interval of characteristic MOR and Weibull slope were determined for reasonable sample sizes.

Effect of Surface Preparation

Test specimens were cut from rotor hubs 779 and 781 which were 2% MgO hot pressed silicon nitride material. Fifty-six test bars were prepared according to the procedure in Table 4.1 and twenty-four of these were further hand lapped on progressively finer diamond papers with Al_2O_3 as the final polish. Figures 4.1 and 4.2 show comparisons of the two types of surfaces by Scanning Electron Microscopy (SEM) and by profilometer tracings. The SEM pictures show that the lapped surfaces have no machining grooves and have finer pits. Further lapping, i.e. removing additional 1, 2 and 5 mils of material, did not result in any visible decrease of this pitting. Profilometer traces showed that the ground surfaces were about 10 microinches arithmetic average and the lapped surfaces were about 1 microinch arithmetic average.

Four point bend strength testing was performed according to the Proposed Military Standards for Testing of Ceramic Materials[14] on 1/4 x 1/8 x 1 inch specimens. Tables 4.2 and 4.3 show the resulting MOR data. Based on 90% confidence, the differences in MOR and Weibull slope m between the two types of surface preparation are not statistically significant. This indicates that, relative to the inherent flaws in this material, the surface damage from the three-step grinding process shown in Table 4.1 is not severe enough, relative to other material defects, to control the strength. Therefore, it is not necessary to use more elaborate finishing than the three-step grinding, although, it should be recognized that this conclusion may not be generally applicable to all hot pressed silicon nitride materials.

Post Machining Heat Treatment

An investigation of possible heat treatment benefits was made on Norton's NC-132 hot pressed silicon nitride. While this is a different material from the 2% MgO hot pressed silicon nitride discussed earlier, it is being considered for possible rotor hub application.

Pratt and Whitney[15] have reported significant improvements in strength of NC-132 material by post machining heat treatments in air though their machining proeedures differ from those shown in Table 4.1. The mechanism was suggested to be due to crack healing, although conceivably, stress relieving and/or crack tip blunting by oxidation could have occurred.

To evaluate the possible benefits of heat treatment, seventy-eight test bars were machined from Norton billet G42858-9 according to the previously mentioned

three-step grinding procedure. Thirty bars were used as control samples. The remaining bars, in groups of eight, were heat treated in air at various time-temperature conditions including some approximating the 2200°F — three hours, 2500°F — three hours, and 2500°F — 23 hours used by Pratt and Whitney.

The room temperature MOR results are shown in Tables 4.4 and 4.5. Considering first the 2500°F — 20 hours heat treatment, which gave the best strength improvements in the Pratt and Whitney work, a 43% degradation in characteristic MOR resulted. Continued oxidation to 100 hours resulted in further loss of strength. Even a one-hour treatment at 2500°F resulted in 21% loss of strength. These, together with weight gain data, are plotted in Figure 4.3 showing typical parabolic curves of oxidation with a protective film of oxidation product[9]. The strength curve corresponds to a mirror image of the weight gain curve; thus, the faster the oxidation, the faster the strength degradation.

TABLE 4.1

STANDARD TEST BAR PREPARATION PROCEDURE

Slicing

Wheel Specification	Resin 120 diamond grit
Wheel Speed	5000 — 6000 SFPM*
Downfeed	0.0005" — 0.001" inches/pass
Table Speed	100 — 140 inches/minute

Rough Grind (when needed)

Wheel Specification	Resin 100 diamond grit
Wheel Speed	5000 — 6000 SFPM
Downfeed	0.0015" — 0.002" inches/pass
Crossfeed	1/8 — 1/4 inches/pass
Table Feed	300 — 400 inches/minute

Intermediate Grind

Wheel Specification	Resin 150 diamond grit
Wheel Speed	5000 — 6000 SFPM
Downfeed	0.000" — 0.0015" inches/pass
Crossfeed	1/8 — 1/4 inches/pass
Table Speed	200 inches/minute

Finish Grind

Wheel Specification	Resin 280 diamond grit
Wheel Speed	5000 — 6000 SFPM
Downfeed	0.0003" — 0.0005" inches/pass
Table Speed	100 — 140 inches/minute

All final grinding done parallel to the long axis of the specimen.

All edges beveled approximately 0.005" — 0.010" by lapping in longitudinal direction.

* Surface Feet Per Minute

HPSN Surfaces as Ground

S.E.M. Photographs of Surfaces

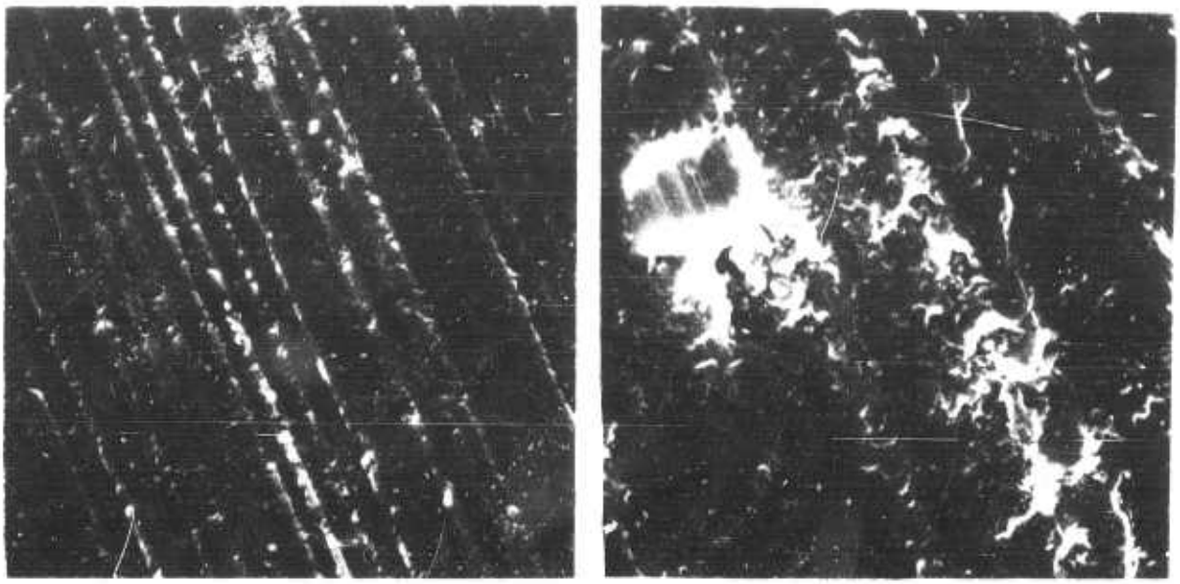

600X 1800X

Profilometer Trace Across Bar Width (1/4")

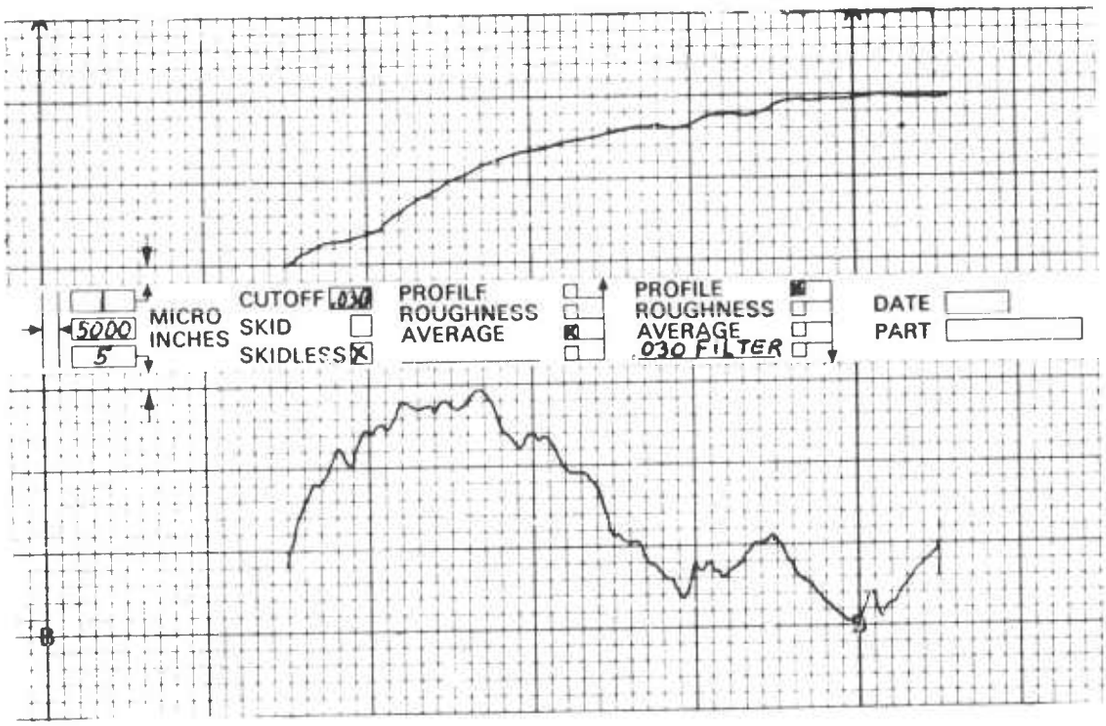

Figure 4.1 HPSN Surfaces as Ground.

S.E.M. Photographs of Surfaces

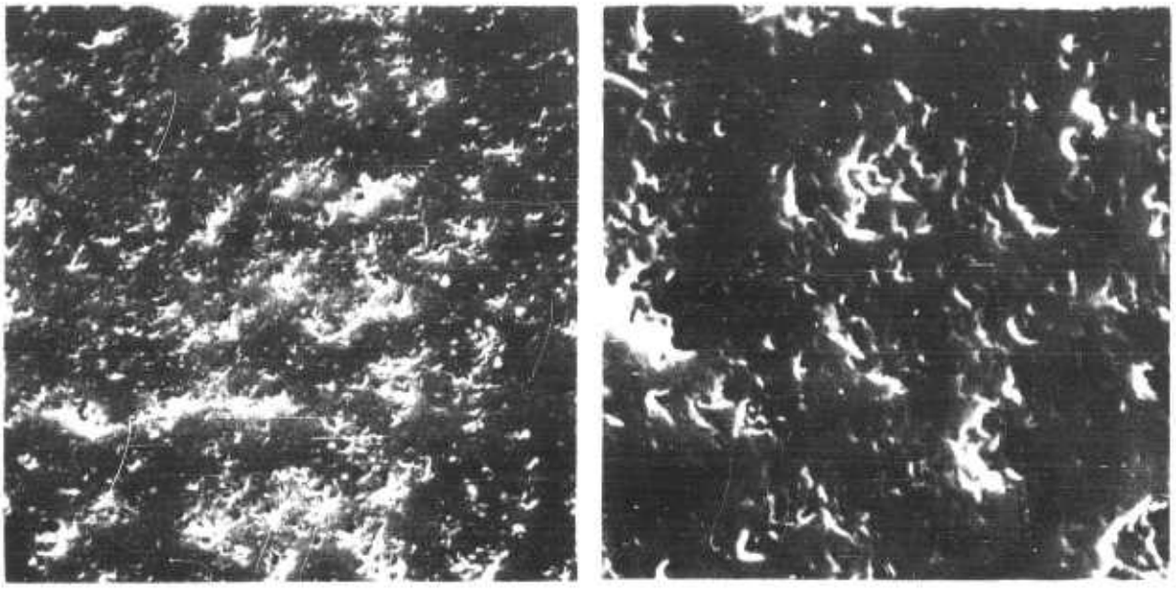

600X 1800X

Profilometer Trace Across Bar Width (1/4")

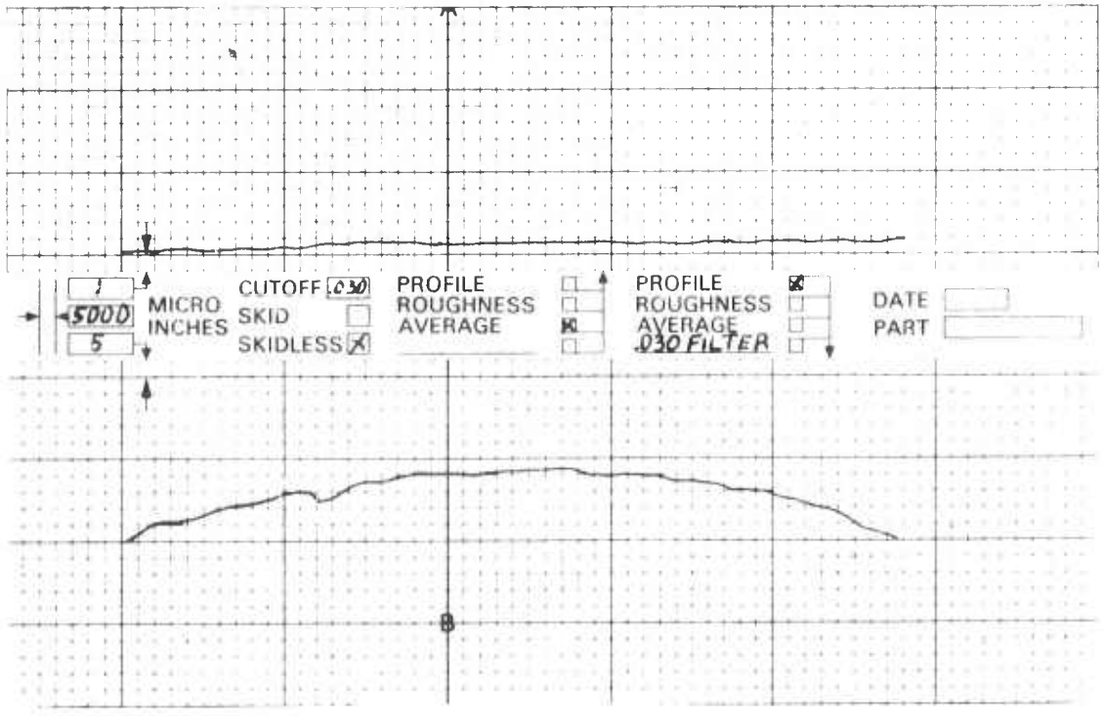

Figure 1.2 HPSN Surfaces after Lapping.

TABLE 4.2

ROOM TEMPERATURE MOR (KSI) OF HPSN

Position in Hub		Hub No. 779		Hub No. 781	
		As Ground	After Lapping	As Ground	After Lapping and 500°F Aging
Hub A	A	103.0	80.9	72.0	72.3
		92.0	78.9	92.4	83.8
Hub B	B	109.0	109.0	105.0	103.0
		91.4	99.9	90.4	87.8
Hub C	C	96.5	65.7	102.0	89.3
		85.7	88.4	102.0	93.3
Hub D	D	90.0	81.4	94.3	93.6
		90.0	94.3	107.0	90.1
Within Hub		77.5	62.2	92.4	75.3
		85.7	87.8	82.1	73.4
		86.4	77.8	87.1	82.7
		72.0	89.3	72.0	90.7
		76.6		104.0	
		85.7		79.5	
		87.8		70.6	
		67.0		77.0	
Characteristic MOR of All Bars					
Point Estimate		91.9	90.0	94.7	90.2
90% Interval Estimate		86.7-97.5	82.4-98.7	89.1-101	85.0-95.9
Weibull Modulus of All Bars					
Point Estimate		8.2	6.5	7.8	9.6
90% Interval Estimate		5.3-10.6	3.8- 8.6	5.1-10.1	5.7-12.8
Number of Bars		16	12	16	12
Characteristic MOR of Web Bars					
Point Estimate		98.3	92.8	99.9	92.8
90% Interval Estimate		91.4-106	82.2-105	93.0-108	86.2-100
Weibull Modulus of Web Bars					
Point Estimate		10.4	6.2	10.5	10.2
90% Interval Estimate		5.1-14.4	3.1- 8.6	5.2-14.6	5.1-14.2
Number of Bars		8	8	8	8
Characteristic MOR of Hub Bars					
Point Estimate		83.0	*	87.9	*
90% Interval Estimate		77.9-88.8		78.3-99.1	
Weibull Modulus of Hub Bars					
Point Estimate		11.7	*	6.5	*
90% Interval Estimate		5.8-16.2		3.2- 9.0	
Number of Bars		8		8	

* Insufficient Data

Test Bar Geometry: 0.125 x 0.25 x 1.25 inches

Test Spans: 0.375 inch top span, 0.750 inch bottom span

Crosshead Speed: 0.02 inches per minute

In every case of heat treatment, there was a decrease in characteristic MOR, which agreed well with oxidation test results reported by Westinghouse[8,9]. However, in some cases in this experiment, the Weibull modulus appeared to be improved by the heat treatment. The net result of whether or not heat treatment is detrimental can not be determined with high (90%) confidence due to an overlap in the Weibull modulus confidence bands; a greater number of oxidized samples would have to be tested to reach this determination. In addition, such results should be applied to the particular ceramic structure in question to evaluate the effect of oxidation on component reliability.

TABLE 4.3

ROOM TEMPERATURE MOR KSI OF HPSN

Combined Data; Hubs 779 and 781

	As Ground	After Lapping
Characteristic MOR of All Bars		
Point Estimate	93.3	90.2
90% Interval Estimate	89.8-97.1	86.1-94.6
Weibull Modulus of All Bars		
Point Estimate	8.3	8.1
90% Interval Estimate	6.3-10.1	5.8-10.0
Number of Bars	32	24
Characteristic MOR of Web Bars		
Point Estimate	99.1	92.9
90% Interval Estimate	95.1-103	87.7-98.6
Weibull Modulus of Web Bars		
Point Estimate	11.6	8.3
90% Interval Estimate	7.5-14.9	5.4-10.7
Number of Bars	16	16
Characteristic MOR of Hub Bars		
Point Estimate	85.7	83.8
90% Interval Estimate	80.7-91.1	77.2-91.3
Weibull Modulus of Hub Bars		
Point Estimate	8.0	9.1
90% Interval Estimate	5.2-10.3	4.5-12.7
Number of Bars	16	8

TABLE 4.4

EFFECT OF OXIDATION ON ROOM TEMPERATURE STRENGTH

Oxidation Temperature, °F	Individual MOR Values (psi)			
	Oxidation Time (Hours)			
	0	1	20	100
1900	101,000	88,300		
	101,000	104,000		
	102,000	108,000		
	104,000	111,000		
	108,000	113,000		
	111,000	122,000		
	112,000	127,000		
	113,000	135,000		
	115,000			
	116,000			
2250	117,000	105,000		69,400
	118,000	109,000		73,700
	119,000	114,000		73,700
	119,000	118,000		78,000
	121,000	119,000		78,000
	122,000	122,000		81,100
	122,000	123,000		81,800
	122,000	124,000		85,200
	127,000			
	129,000			
2500	130,000	90,700	63,600	61,900
	130,000	95,300	67,000	64,800
	131,000	96,200	69,400	66,200
	131,000	97,900	70,600	66,500
	131,000	99,100	71,700	66,800
	134,000	99,400	74,300	67,000
	134,000	101,000	74,600	68,000
	137,000	103,000		74,900
	139,000			
	144,000			

Test bar geometry: 0.125 x 0.250 x 1.25 inch.

Test Spans: 0.375 inch top span, 0.750 inch bottom span.

Crosshead Speed: 0.02 inches per minute.

TABLE 4.5

EFFECT OF OXIDATION ON NORTON NC-132

ROOM TEMPERATURE WEIBULL MOR (KSI)

Oxidation Temperature °F		Time at Temperature (Hours) 1	20	100
1900	Characteristic MOR			
	Point Estimate	120		
	90% Interval Estimate	109-132		
	Weibull Modulus			
	Point Estimate	7.86		
	90% Interval Estimate	3.9-10.9		
	Weight Change			
	%	0.001 loss		
	mg/cm^2	0.02 loss		
	Number of Bars	8		
2250	Characteristic MOR			
	Point Estimate	120		79.6
	90% Interval Estimate	115-124		75.3-84.4
	Weibull Modulus			
	Point Estimate	19.7		13.4
	90% Interval Estimate	9.8-27.4		6.7-18.7
	Weight Change			
	%	0.001 gain		0.091 gain
	mg/cm^2	0.02 gain		0.29 gain
	Number of Bars	8		8
2500	Characteristic MOR			
	Point Estimate	99.4	71.8	68.8
	90% Interval Estimate	96.8-102	68.7-75.2	65.2-72.7
	Weibull Modulus			
	Point Estimate	27.5	18.9	14.1
	90% Interval Estimate	13.6-38.1	8.6-26.6	7.0-19.6
	Weight Change			
	%	0.086 gain	0.242 gain	0.448 gain
	mg/cm^2	0.27 gain	0.78 gain	1.43 gain
	Number of Bars	8	7	8

BASELINE MOR DATA ON UNOXIDIZED BARS

Characteristic MOR	
Point Estimate	127
90% Interval Estimate	123-130
Weibull Modulus	
Point Estimate	11.4
90% Interval Estimate	8.5-13.9
Number of Bars	36

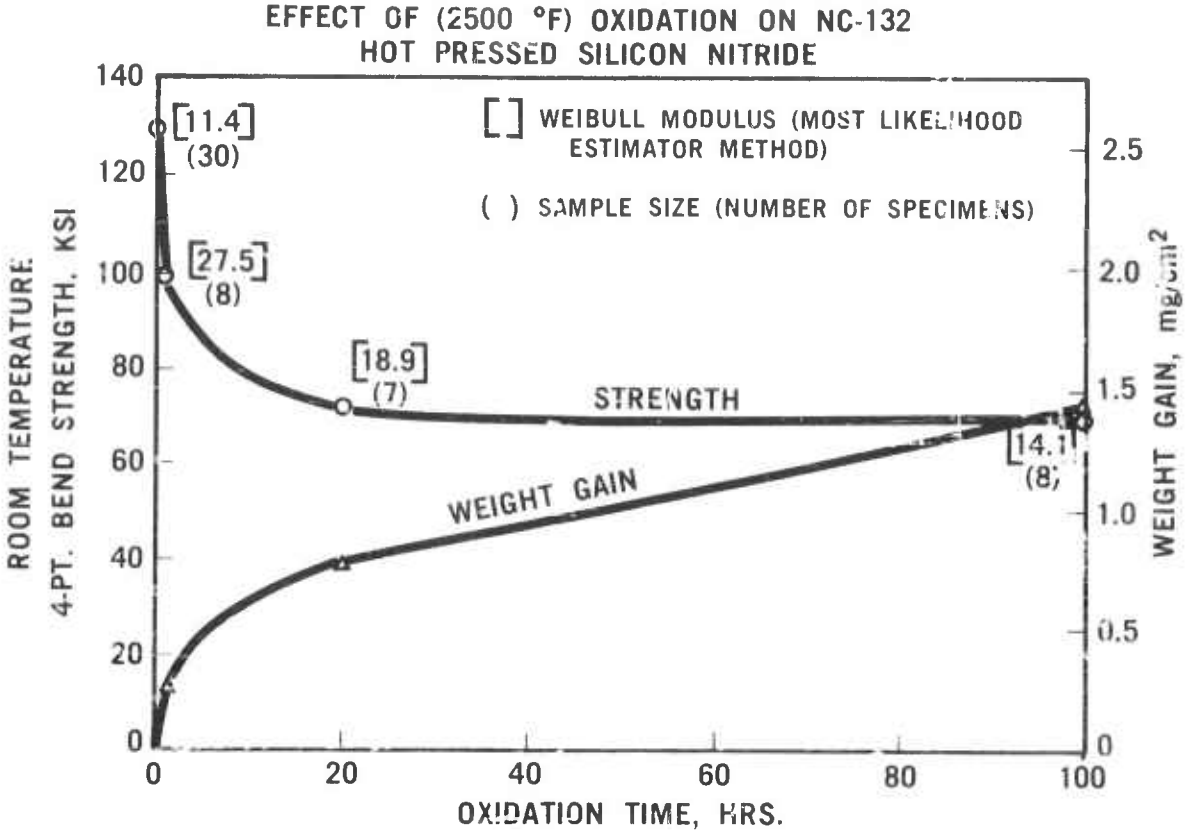

Figure 4.3 Effect of 1371°C (2500°F) Oxidation on NC-132 HPSN.

Effect of Batch and Location Variables

The purpose of this task was to determine the consistency of strength parameters from rotor hub to hub, and from area to area within hubs. The latter was particularly important in deciding whether separate strength parameters had to be employed for different finite elements in reliability analysis for correlation of MOR with spin failure rpm.

For this purpose, 140 test bars were cut from five rotor hubs (#814, 823, 824, 825 and 834) which had been hot pressed from 2% MgO silicon nitride powder. Hubs #814, 823, 824 and 825 were pressed from the same milling batch whereas hub #834 was pressed from another milling batch. Figure 4.4 shows the test bar locations. As before, the sample geometry and test conditions were based on the Proposed Military Standards[14]. The raw data are presented in Table 4.6 and the statistical evaluation results are shown in Table 4.7. A fair consistency of strength parameters from hub to hub (made from the same milling batch) is evident.

The variability of strength with milling batch can be seen by comparing the strength parameters of hub #834 with those of the other four hubs. Hub #834 is inferior in both the web and curvic areas. Since no difference in the milling conditions was known, the source of the variation was not clear. However, particle size analysis showed that the lower strength batch had a coarser average particle size of 1.84 microns versus 1.44 for the other batch.

The consistency of strength from area to area within the hubs is discernible from the lack of a statistically significant difference between the web and curvic areas within each hub and in the combined data for all hubs, and between the outer surface layers and the interiors. A meaningful comparison of surface layers of each hub with the interior can not be made because of small sample sizes available for statistical analysis.

Therefore, it has been concluded that, for the chemistry and processing conditions used to make such rotor hubs, a single set of strength parameters can be used for all the finite elements of the rotor in reliability calculations. However, the data would be applicable only to the same milling batch. In order for the data to reflect the variability from batch to batch of powder milling, MOR data for different batches should be combined. The application of the above information is presented in section 3.1.3 on correlation of MOR data with spin failure rpm.

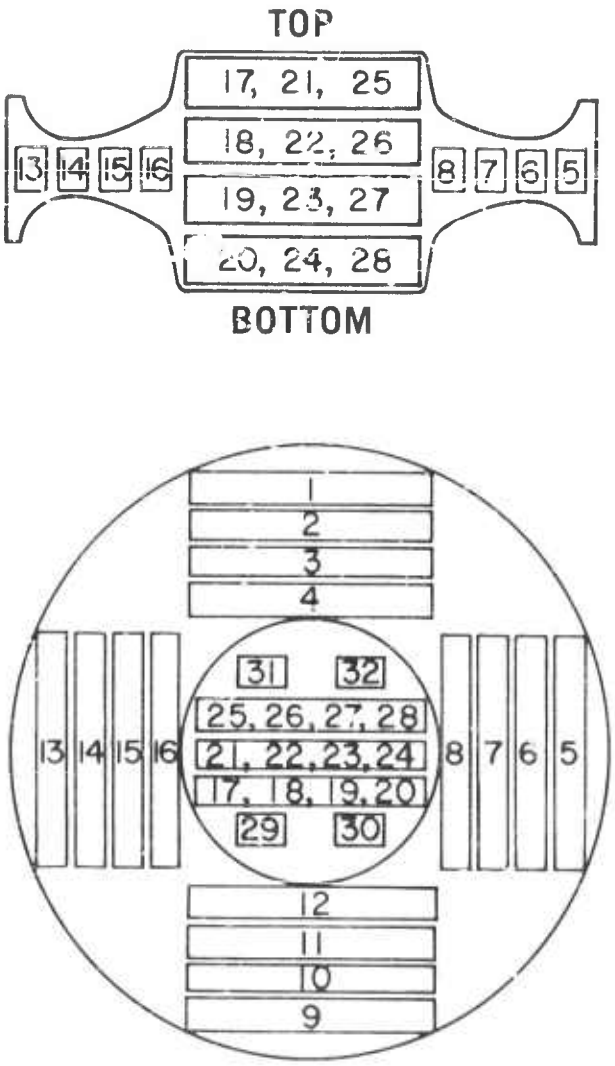

Figure 4.4 Location of Test Bars Cut From Rotor Hubs.

TABLE 4.6

ROOM TEMPERATURE MOR DATA (KSI)

Bar Number		Hub Number 814	823	824	825	834
Web Area						
1		85.5	68.0	98.1	-	91.0
5	Nearest	98.8	84.7	89.6	79.2	73.4
9	Rim	80.9	99.2	90.7	93.6	92.2
13		100.0	89.7	93.9	83.8	85.7
2		98.8	105.0	101.0	117.0	76.3
6		82.1	96.8	93.3	103.0	79.2
10		87.1	111.0	97.2	77.8	90.7
14		69.1	87.6	102.0	102.0	75.2
3		82.7	101.0	77.5	60.2	87.6
7		95.0	92.2	97.2	77.9	77.8
11		76.9	111.0	96.8	92.7	90.0
15		77.8	-	103.0	85.2	86.4
4		95.0	91.0	107.0	91.0	79.5
8	Nearest	79.8	88.0	101.0	90.6	-
12	Curvic	76.3	109.0	94.3	60.8	77.5
16		94.3	112.0	88.1	84.5	73.7
Curvic Area						
17		113.0	101.0	108.0	104.0	92.2
21		110.0	103.0	66.8	92.4	98.6
25	Outer	96.5	69.4	95.0	96.8	98.2
20	Areas	90.9	106.0	103.0	104.0	78.5
24		87.6	99.6	99.6	108.0	101.0
28		89.6	107.0	90.4	89.9	94.2
18		93.3	80.6	101.0	81.4	90.1
22		96.8	113.0	84.1	97.9	80.6
26	Central	89.9	102.0	104.0	86.4	75.2
19	Areas	94.2	93.3	71.3	85.0	84.7
23		96.8	99.4	99.4	94.2	95.0
27		106.0	90.6	83.8	66.2	90.4

- Indicates bar with obvious defect.

TABLE 4.7

ROOM TEMPERATURE MOR OF HPSN (KSI)

	Hub Number	Web Area	Curvic Area	All Bars
Characteristic MOR	814			
Point Estimate		90.4	101	95.5
90% Interval Estimate		86.1-95.2	95.5-107	91.9-99.2
Weibull Modulus				
Point Estimate		9.6	10.5	9.1
90% Interval Estimate		6.3-12.4	6.2-13.9	6.7-11.1
Number of Bars		16	12	28
Characteristic MOR	823			
Point Estimate		101	102	102
90% Interval Estimate		96.0-107	96.2-108	98.1-105
Weibull Modulus				
Point Estimate		9.0	10.1	10.0
90% Interval Estimate		5.8-11.7	6.0-13.4	7.3-12.2
Number of Bars		15	12	27
Characteristic MOR	824			
Point Estimate		98.3	97.4	98.2
90% Interval Estimate		95.7-102	91.1-104	95.5-101
Weibull Modulus				
Point Estimate		15.8	8.6	12.4
90% Interval Estimate		10.3-20.4	5.1-11.4	9.2-15.2
Number of Bars		16	12	28
Characteristic MOR	825			
Point Estimate		92.7	96.9	94.7
90% Interval Estimate		85.2-101	91.0-103	90.2-99.5
Weibull Modulus				
Point Estimate		5.9	9.2	7.3
90% Interval Estimate		3.8-7.7	5.5-12.3	5.3-8.9
Number of Bars		15	12	27
Characteristic MOR	834			
Point Estimate		85.5	93.5	89.5
90% Interval Estimate		82.2-89.0	89.2-98.0	86.7-92.5
Weibull Modulus				
Point Estimate		12.7	12.3	11.0
90% Interval Estimate		8.1-16.5	7.3-16.3	8.1-13.6
Number of Bars		15	12	27
Characteristic MOR	All			
Point Estimate	Hubs	94.6	98.3	96.3
90% Interval Estimate		92.3-96.9	96.1-101	94.4-98.2
Weibull Modulus				
Point Estimate		8.4	10.3	9.1
90% Interval Estimate		7.1-9.5	8.5-11.9	8.0-10.2
Number of Bars		77	60	137
Characteristic MOR	Outer			
Point Estimate	Surfaces		100	
90% Interval Estimate			97.6-103	
Weibull Modulus				
Point Estimate			12.3	
90% Interval Estimate			9.2-15.0	
Number of Bars			30	
Characteristic MOR	Interior			
Point Estimate			96.0	
90% Interval Estimate			92.4-99.7	
Weibull Modulus				
Point Estimate			8.9	
90% Interval Estimate			6.6-10.8	
Number of Bars			30	

4.2 PROPERTIES OF INJECTION MOLDED REACTION SINTERED SILICON NITRIDE

Introduction

In previous reports[8,9], various physical properties of 2.7 gm/cm^3 injection molded silicon nitride have been reported. These values were for material at various stages of development and the data was used for process evaluation and estimates of material capability. The data reported in this section is from test bars processed the same as engine hardware.

Material Properties

MOR data at various temperatures, including Weibull modulus values, for 140 test bars is presented in Table 4.8. The characteristic MOR values are lower than previously reported values for experimental batches due to problems encountered in scaling up the nitriding process. These problems are disucssed in Section 4.3 of this report. It should be pointed out, however, that although the room temperature characteristic strength is lower, 36.3 ksi versus 44.3 ksi[9], the Weibull modulus has increased, 11.1 versus 6.78[9].

TABLE 4.8

WEIBULL DATA VERSUS TEMPERATURE OF

2.7 gm/cm^3 INJECTION MOLDED SILICON NITRIDE

	Temperature $^oF/^oC$				
	78/25	1700/927	2100/1149	2300/1260	2500/1370
Characteristic MOR *(ksi)					
Point Estimate	36.3	33.0	32.5	33.2	31.7
90% Interval Estimate	35.2-37.4	32.2-33.9	31.6-33.5	32.1-34.4	30.5-32.9
Weibull Modulus *					
Point Estimate	11.1	14.3	12.1	9.7	9.4
90% Interval Estimate	8.2-13.5	10.5-17.6	8.9-14.8	7.2-11.8	6.9-11.6
Number of Bars	29	27	28	29	27

3/8" x 3/4" Test Fixture; 4 Point Bending

1/8" x 1/4" Sample Size; As Nitrided Surfaces

0.020 inches/minute crosshead rate

* Maximum Likelihood Estimator Program [13]

The results of fifteen bending stress rupture tests on this material are presented in Table 4.9. As indicated, the samples either failed immediately or were suspended after 200 or more hours without failure. Some immediate failures at 30 ksi were to be expected based on the Weibull statistics presented in Table 4.8 at elevated temperatures. No time dependent failures have been noted for this material up to 2200°F (1204°C) which again is to be expected since no evidence of slow crack growth was found in this material[9], even at temperatures up to 2550°F (1400°C).

TABLE 4.9

BENDING STRESS RUPTURE RESULTS OF 2.7 GM/CM^3

INJECTION MOLDED SILICON NITRIDE

Temperature (°F/°C)	Stress (ksi)	Time (Hours)	Comments
1900/1038	20	210	No Failure
	20	208	No Failure
	20	212	No Failure
	25	279	No Failure
	30	211	No Failure
	30	0	Failed on Load
	30	0	Failed on Load
2100/1149	20	215	No Failure
	20	215	No Failure
	20	240	No Failure
	25	211	No Failure
	30	243	No Failure
	30	0	Failed on Load
2200/1204	20	200	No Failure
	25	200	No Failure

4.3 NITRIDING DEVELOPMENTS

Introduction

Previous interim reports[7,8,9] described the development of nitriding cycles for the production of reaction sintered silicon nitride hardware. This section summarizes the previous work and includes several new micrographs. In addition, data is presented which will form the basis for scaling up the nitriding process for large furnace loads and still produce good strength material.

Nitriding Developments

Figure 4.5 shows the three basic temperature schedules investigated. Table 4.10 shows the degree of nitriding achieved for each cycle and atmosphere for densities from 2.3 to 2.8 g/cc. As shown, all cycles and atmospheres nitride equally well for densities up to 2.7 g/cc. However, the 2.8 g/cc material can only be nitrided to 96% with the cycles investigated. This material has large areas of unreacted silicon in the structure which is not desirable for a turbine material.

The strength-density relationship for the various nitriding cycles and atmospheres are given in Figure 4.6. The data shows that the 3 step cycle results in the strength reaching a maximum of around 30 ksi at a density of 2.7 g/cc. However, the strength starts to level out at the 2.55 g/cc density level. The multi-step cycle yields a maximum strength level (35 ksi) at the 2.55 g/cc level and then decreases to the 25-30 ksi level for higher densities. The constant rate cycle is best up to the 2.7 g/cc density level where it reaches a maximum strength of 44 ksi. The effect of H_2/N_2 nitriding atmospheres is most evident at the low densities where the 3-step cycle was used and at the higher densities with the constant rate cycle.

Figure 4.7 shows the microstructure of materials of different densities and nitriding cycles but all having strengths between 25 and 30 ksi. It is obvious that the

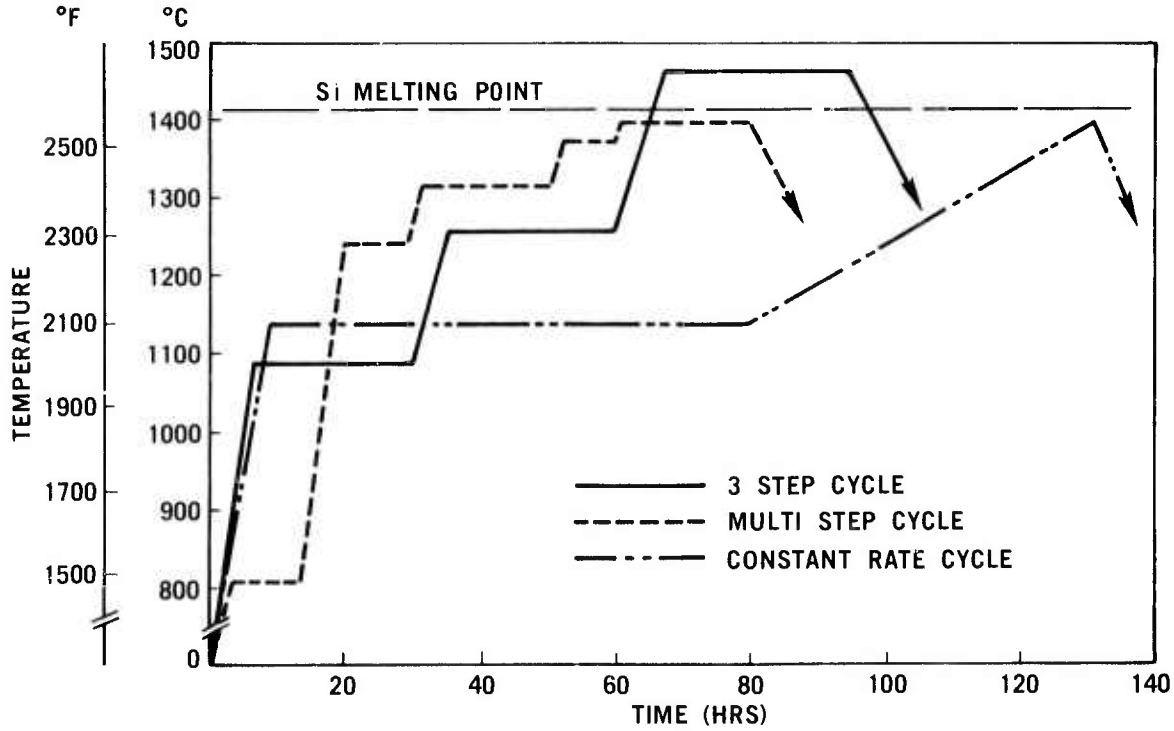

Figure 4.5 Nitriding Temperature Schedules.

pore distributions are different for each density level, however, the largest individual pores are in the 25 to 30 μ m range. These large pores show evidence of having been formed by silicon "melt out" and are mainly responsible for limiting the strength of the material.

TABLE 4.10

PERCENT OF SILICON CONVERTED TO SILICON NITRIDE FOR VARIOUS NITRIDING CYCLES AND DENSITY LEVELS

Nitriding Cycle	Atmosphere	2.3 g/cc	2.55 g/cc*	2.7 g/cc*	2.8 g/cc*
3 Step	100% N_2	97.5	97.0	98.5	94.7
	1% — 4% H_2/N_2	97.1	-	96.7	-
Multi-Step	100% N_2	97.0	99 0	98.1	95.9
	1% — 4% H_2/N_2	-	98.3	98.4	95.9
Constant Rate	100% N_2	-	98.3	98.0	-
	1% — 4% H_2/N_2	-	98.3	98.0	94.7

* 2 1/2% Fe_2O_3 added as a nitriding aid. This has been compensated for in the conversion data

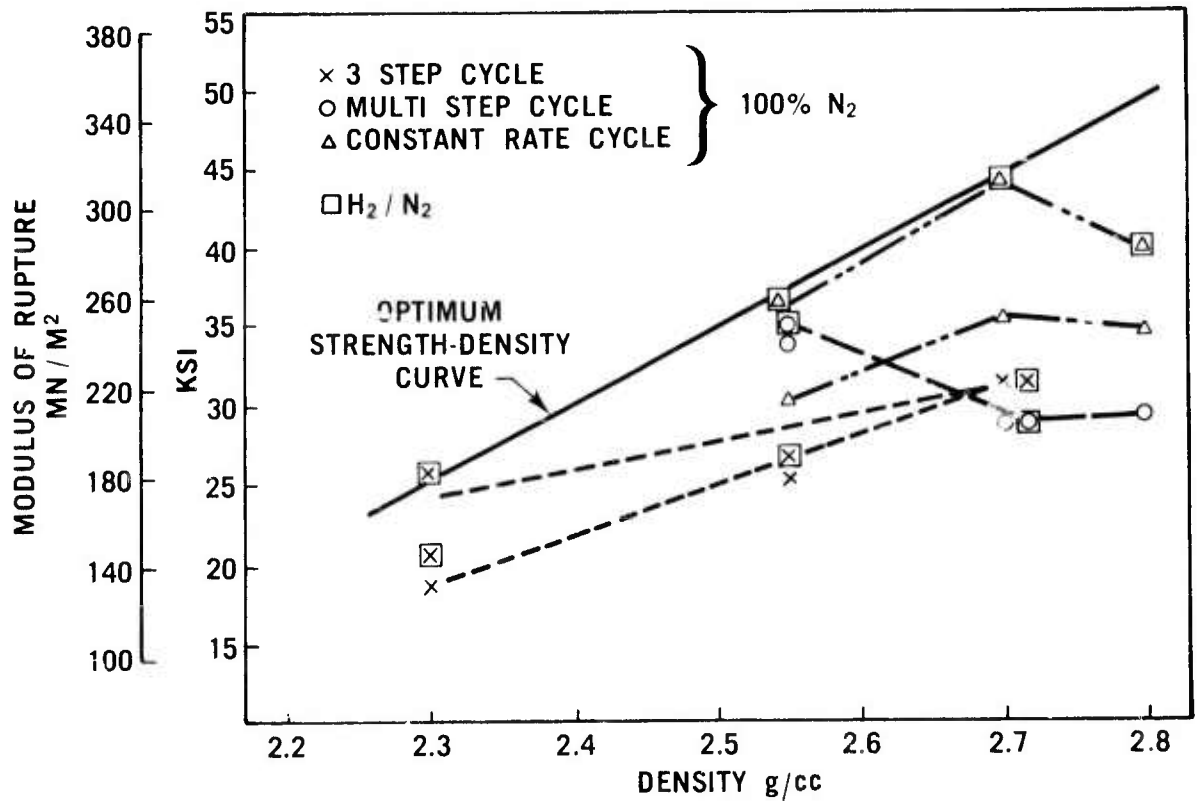

Figure 4.6 Strength Versus Density - Silicon Nitride.

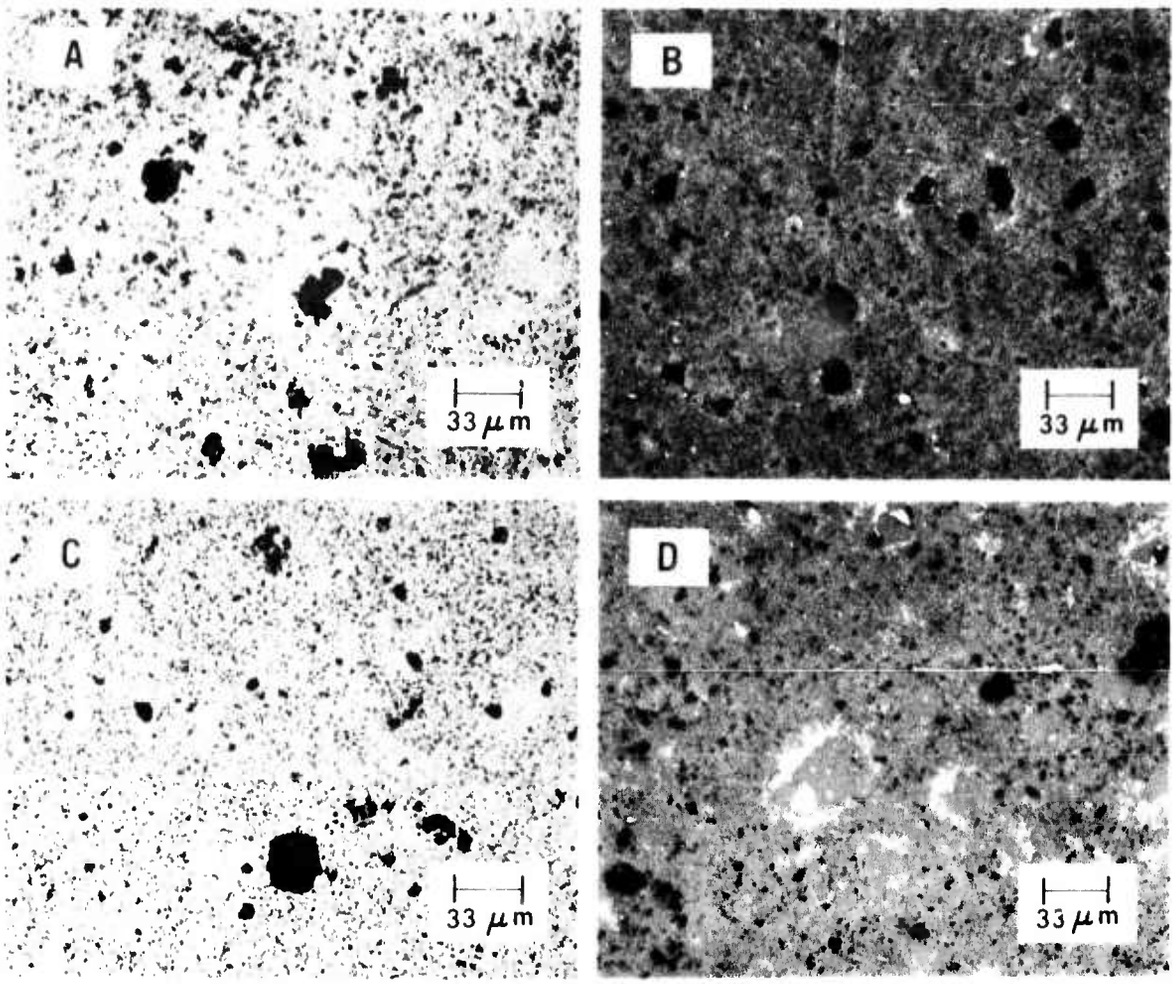

Figure 4.7 Micrographs of Different Density Silicon Nitrides.
(A) 2.3 g/ee (B) 2.55 g/ec (C) 2.7 g/ce (D) 2.8 g/ce

Table 4.11 shows in detail the properties of the 2.7 g/ec material nitrided under the various eonditions listed. The only eyele that yielded material on the optimum strength density line was the constant rate eyele with a 96% N_2/4% H_2 atmosphere. Figure 4.8 shows the microstrueture of 2.7 g/ec materials nitrided with these various cyeles. The microstructure of the three step nitriding cycle, Figure 4.8(A), (with a maximum nitriding temperature of 1450°C(2642°F) shows much evidenee of silicon "melt out" and the resulting large porosity deseribed by Evans and Davidge[16]. The arrow points to a large dense region of silicon nitride (gray) with areas of silieon metal interspersed (white). This region probably was formed when a silieon partiele melted and was dispersed into the surrounding strueture. Adjoining this dense region is a large pore, probably formed when the silieon melted. Examination of the structure of the multistep cycle (Figure 4.8B) shows many similar regions indieating that molten silicon was present at some stage of the nitriding proeess even though the furnace temperature of this eycle was only 1400°C (2552°F), below the melting point of silieon. From these mierographs, it is eoneluded that the dense regions with adjoining large porosity aet as flaws and cause the low material strength. The structure of the multistep eycle leads to the eonclusion that the exotherm accompanying the nitriding reaction caused the temperature of the test sample to exeeed 1420°C (2588°F).

TABLE 4.11

CHARACTERIZATION OF 2.7 G/CC NITRIDED TEST SPECIMENS

Nitriding Cycle	Nitriding Atmosphere	Average MOR (ksi)	M	# of Samples	Phase Composition % α	% β	% Si
3 Step	100% N_2	33	15	5	70	27	-
	96% N_2/4% H_2	28	-	8	-	-	-
Multi-Step	100% N_2	26	8	12	63	34	-
	96% N_2/4% H_2	31	-	5	-	-	-
Constant Rate	100% N_2	35	13	11	72	24	1
	99% N_2/1% H_2	38	9.5	12	73	25	-
	99% N_2/4% H_2	43	8	31	70	27	-

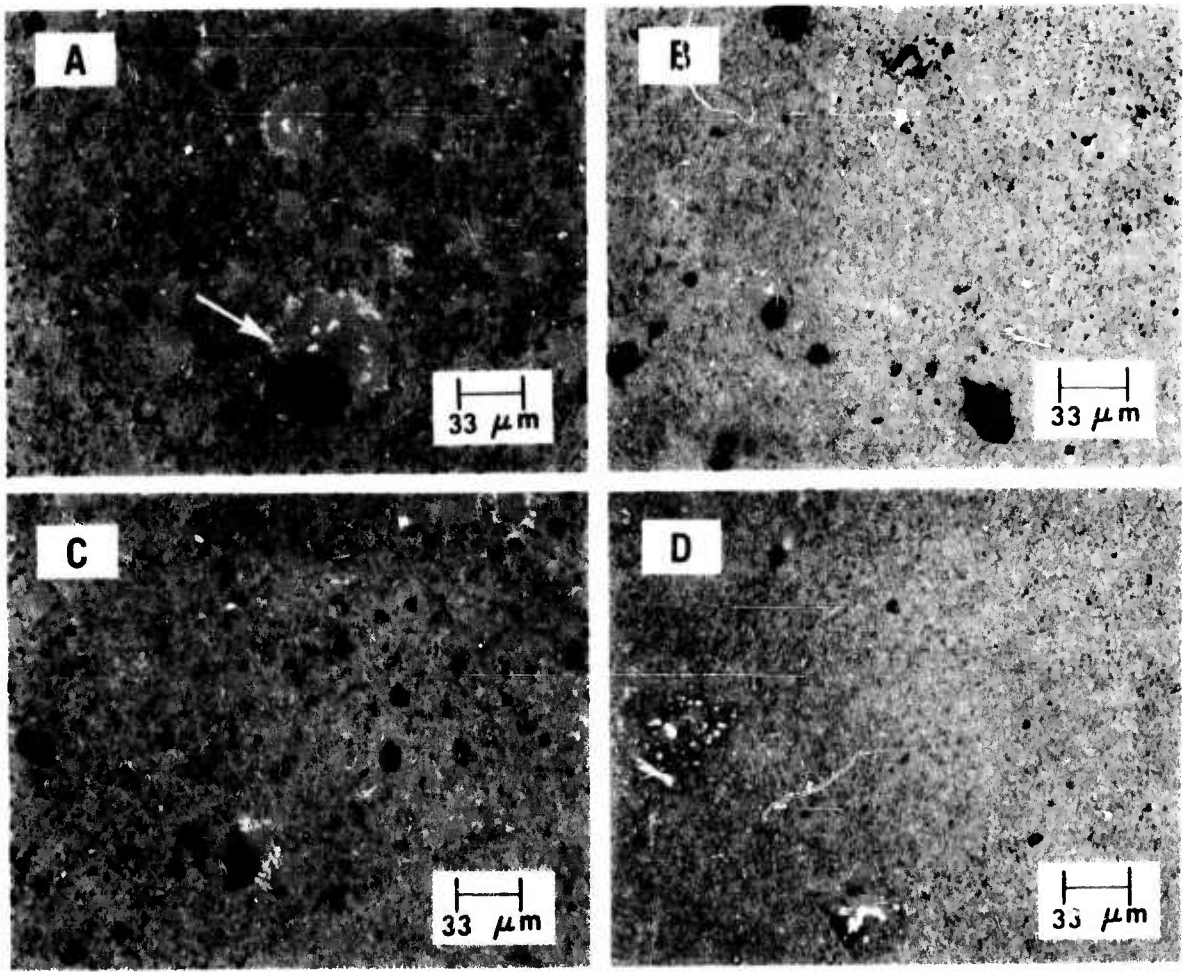

Figure 4.8 Micrographs of 2.7 g/cc Silicon Nitride.
(A) 3-step cycle - 100% N_2 (B) Multi-Step Cycle - 100% N_2
(C) Constant Rate Cycle - 100% N_2
(D) Constant Rate Cycle - 96% N_2/4% H_2

The strength (Table 4.11) and microstructure of the 100% N_2 atmosphere run (Figure 4.8C) shows the same phenomena as with the previous cycles; that is low strength and evidence of localized temperatures in excess of 1420°C (2588°F). These results also show that the H_2/N_2 atmosphere yielded higher strengths (43 ksi average with individual test specimens having strengths as high as 58 ksi). The microstructure of the 4% H_2 run (Figure 4.8D) shows the structure contains much less porosity, is more uniform and, most important, contains no evidence that the melting point of silicon was exceeded.

The constant rate cycle was investigated further to determine the effect of the hold time at 1177°C (2150°F) and to see if this hold time could be reduced. Table 4.12 shows the results of partial nitridings performed at 1177°C (2150°F) for times up to 72 hours. The data shows that while no additional nitriding was observed using weight gain measurements, the phase composition of the 72 hour treatment contains a higher percentage of Si_3N_4 at the expense of the silicon. It appears that no more α Si_3N_4 is formed at temperatures above 1177°C (2150°F) since the total α Si_3N_4 present in completely nitrided specimens is from 70-73%.

TABLE 4.12

RESULTS OF PARTIAL NITRIDING AT 1177°C (2150°F),

4% H_2/96% N_2 ATMOSPHERE

Time at 1177°C (2150°F)	% Nitrided	Phase Composition % α	% β	% Si	α Si_3N_4 Ratio β Si_3N_4
0 Hours	19.2	1	1	98	1.0
24 Hours	60.8	62	15	23	4.13
72 Hours	59.2	73	15	11	4.86

Figure 4.9 shows the micrographs obtained from samples nitrided using various 1177°C (2150°F) hold times in the constant rate cycle with a 4% H_2/96% N_2 atmosphere. Figure 4.9A shows a poor structure with much porosity and evidence of temperature exceeding 1420°C (2588°F) when there was "no hold" at 1177°C (2150°F). By holding for 24 hours at 1177°C (2150°F) the microstructure greatly improves and the 72 hour hold yields the most desirable microstructure (Figure 4.9 (C)).

Practical considerations necessitate that large quantities of silicon be nitrided at one time and this could make the nitriding exotherm more pronounced. Experiments were performed to determine the effect on the Si_3N_4 properties of nitriding large quantities of silicon. Only the rate cycle with 4% H_2/96% N_2 atmosphere was used, with the results being compared to previous small load results.

Test bars were placed in a developmental nitriding furnace along with turbine components of 2.7 g/cc density. The loads were varied between 1200 g and 10,000 g of silicon. The constant rate cycle with a three day 1177°C (2150°F) hold was used in conjunction with the 4% H_2/96% N_2 atmosphere.

The results, Table 4.13, show that, with the 1200 g load, there was no evidence of a temperature overshoot at the hold temperature of 1143°C (2089°F). The percent of silicon nitride and the strength was acceptable.

This run was repeated with a larger load (1600 g) and with the furnace controller being adjusted to yield an actual 1177°C (2150°F) hold temperature. This time a 10°C (18°F) temperature overshoot was noted in the first hour of the hold period. Accompanying this overshoot was a reduction of furnace pressure from 3 psig to 1 1/2 psig, indicating a rapid consumption of nitrogen. The percent of silicon nitrided was good, while the strength of the test bars was low (27.2 ksi).

The microstructure of the 1200 g run, with no temperature overshoot (Figure 4.10 A) shows a fairly uniform structure with only small indications of temperature exceeding 1420°C (2588°F). However, the second run (1600 g, 10°C (18°F) overshoot) (Figure 4.10 B) shows large porosity and many large areas

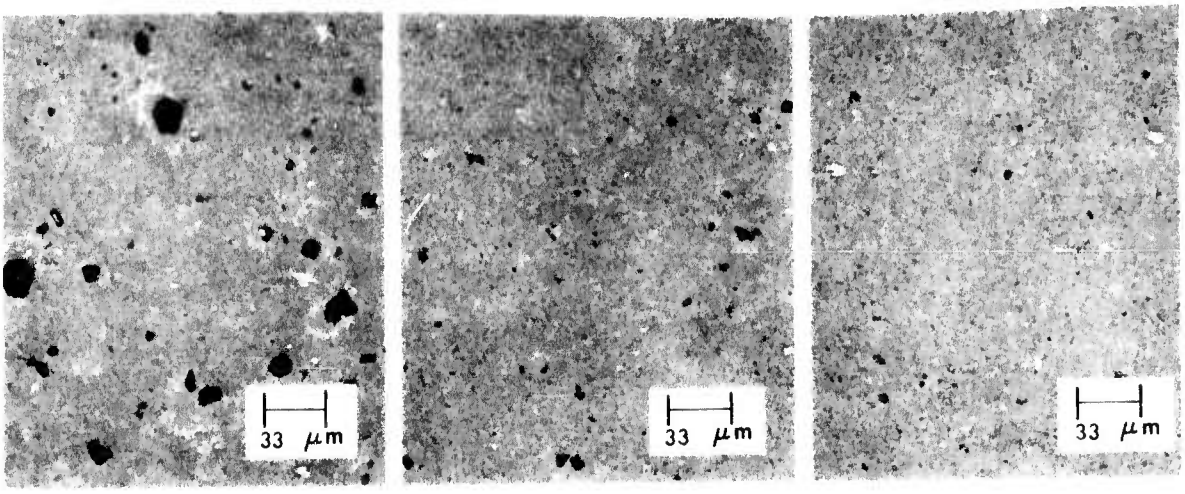

Figure 4.9 Effect of 1177°C (2150°F) Hold on Microstructure of 2.7 g/cc Material
(A) No hold (B) One day hold (C) Three day hold

TABLE 4.13

LARGE FURNACE LOAD RESULTS

Nitriding Cycle	ATM	WT Silicon	Temperature Set Point °C	Temperature Set Point °F	Temperature Overshoot °C	Temperature Overshoot °F	% Nitrided	Characteristic MOR (ksi)	m	# of Samples
Constant Rate	4% H_2/ 96% N_2	1200 g	1143	2089	None		98.1 %	44.2	7.5	25
Constant Rate	4% H_2/ 96% N_2	1600 g	1177	2150	10	18	98.1 %	27.2	8.0	25
Cycle Stopped after 2 hours at 1177°C (2150°F)	4% H_2/ 96% N_2	10,000 g	1177	2150	10	18	Exuded and melted silicon indicating temperatures over 1420°C (2588°F).			

where silicon meltout occurred, indicating that 1420°C (2588°F) was exceeded in this cycle.

The last run consisted of a 10,000 g load with a 1177°C (2150°F) hold. Again there was a 10°C (18°F) overshoot, however, the pressure loss was much larger (+3 psig to -4 psig). The run was aborted two hours into the hold period. Examination of the samples revealed large amounts of exuded silicon was present on the outside surfaces. This indicates that while the furnace temperature did not exceed 1177°C (2150°F), the part temperature exceeded 1420°C (2588°F), clearly showing the severity of the exothermic nitriding reaction.

It has been clearly shown that to obtain the high strength possible from reaction sintered Si_3N_4, one must develop a uniform microstructure of fine porosity. Large dense regions of Si_3N_4 and large pores, both typical of nitriding above the melting point of silicon, have been shown to lower the strength of the material, and consequently must be climinated. In order to accomplish this, the effect of the nitriding exotherm must be controlled, so that at no time do excessive localized areas of the silicon compact exceed 1420°C.

The constant rate cycle was designed to control the nitriding exotherm. However, when compared to other cycles, all using 100% N_2 nitriding atmospheres, no significant improvement was noted in either microstructure or strength. Significant improvements in both these properties were noted when a 4% H_2/96% N_2 nitriding atmosphere was employed. For small nitriding loads, this cycle and atmosphere exhibited no evidence of 1420°C (2588°F) being exceeded.

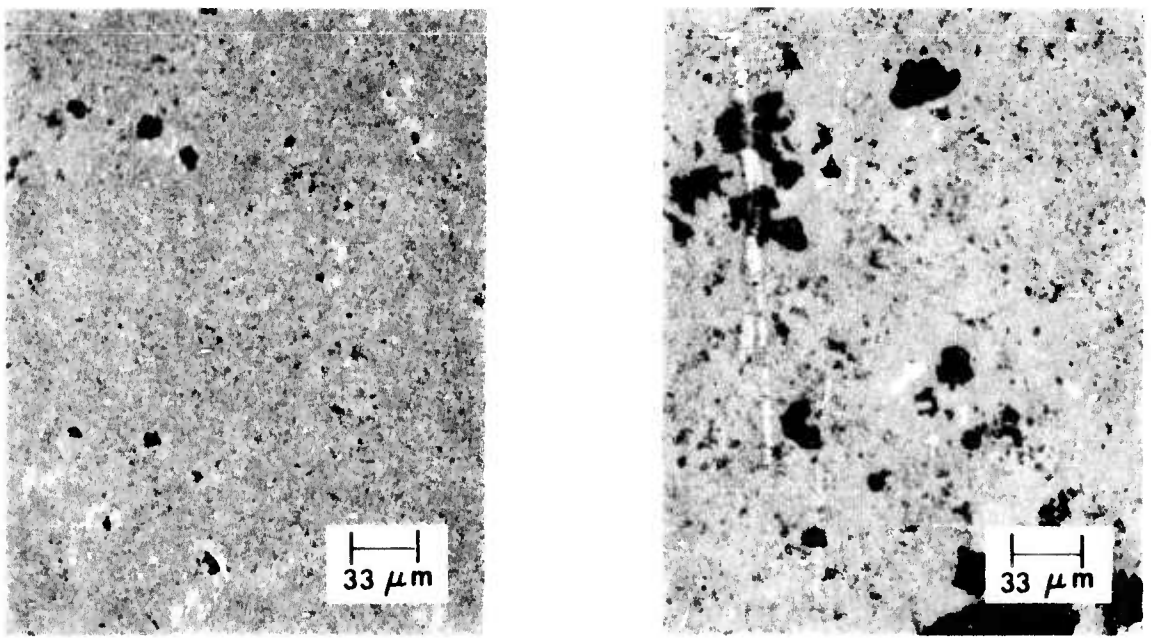

Figure 4.10 Effect of Large Furnace Loads on Microstructure of 2.7 g/cc Material
(A) 1200 grams - No Temperature Overshoot - 44.2 ksi
(B) 1600 grams - 10°C (18°F) Temperature Overshoot - 27.2 ksi

4.4 SIALON MATERIALS

Introduction

Studies of sialons in the Si_3N_4-Al_2O_3 system have shown that, with addition of Y_2O_3 as a sintering aid, materials with room temperature strengths in the 80-90,000 psi range were obtained by pressureless sintering [9]. Even without a sintering aid, strengths of 60,000 psi were attained. However, these strengths were not retained at elevated temperature because of the presence of a glassy phase. In addition, those sialons prepared with more than a very small amount of Y_2O_3 tended to melt at about 1200°C (2192°F) in the presence of oxygen. The extent of melting increased with increasing Y_2O_3 content in the sialon and with increasing oxygen content in the atmosphere when these sialons were tested.

Sialon Developments

Figure 4.11 shows the effect on eight specimens of a sialon, prepared with 6% Y_2O_3, of fewer than 100 thermal shock cycles, using the thermal shock test rig, of 45 seconds each at 1204°C(2200°F). Figure 4.12 shows the effect on four different

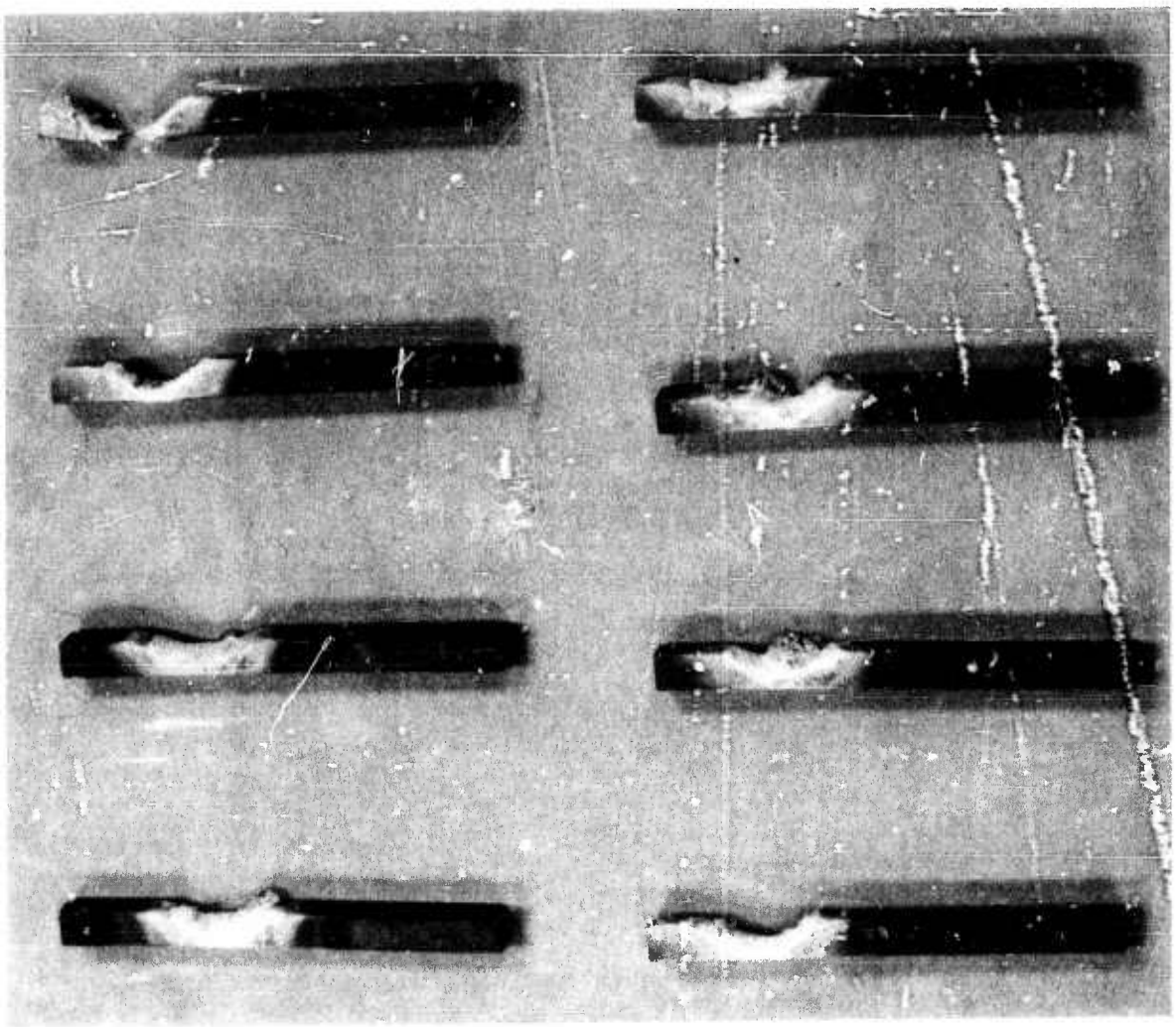

Figure 4.11 Eight Sialon Samples (84% AME Si_3N_4, 16% Al_2O_3, with 6% Y_2O_3 Sintering Aid) After Less Than 100 Thermal Shock Cycles to 2200°F for 45 seconds.

sialons prepared with 1% or less Y_2O_3 of 1312 cycles of 45 seconds each at 1149°C (2100°F). This oxygen-related melting phenomenon seems to rule out Y_2O_3 as a sintering aid for Si_3N_4-Al_2O_3 sialons.

Attempts to deal with the glassy phase are proceeding along two paths. One path involves crystallization of the glass by means of suitable heat treatment, while the other involved consideration of methods of preparing sialon without glass from the outset. Crystallization studies of sialons prepared with Y_2O_3 additive were mentioned in the previous report [9]. Testing of additive-free Si_3N_4-Al_2O_3 sialons have shown a decrease in room temperature strength after crystallization, and at times, no further decrease at elevated temperature. Clearly, optimum crystallization conditions have not yet been found.

If the assumption that sialon is simply a solution of Al_2O_3 in Si_3N_4 is incorrect, then the glassy phase might be the by-product of incorrect stoichiometry. It might also result from impurities in the starting materials — SiO_2 contaminants in the

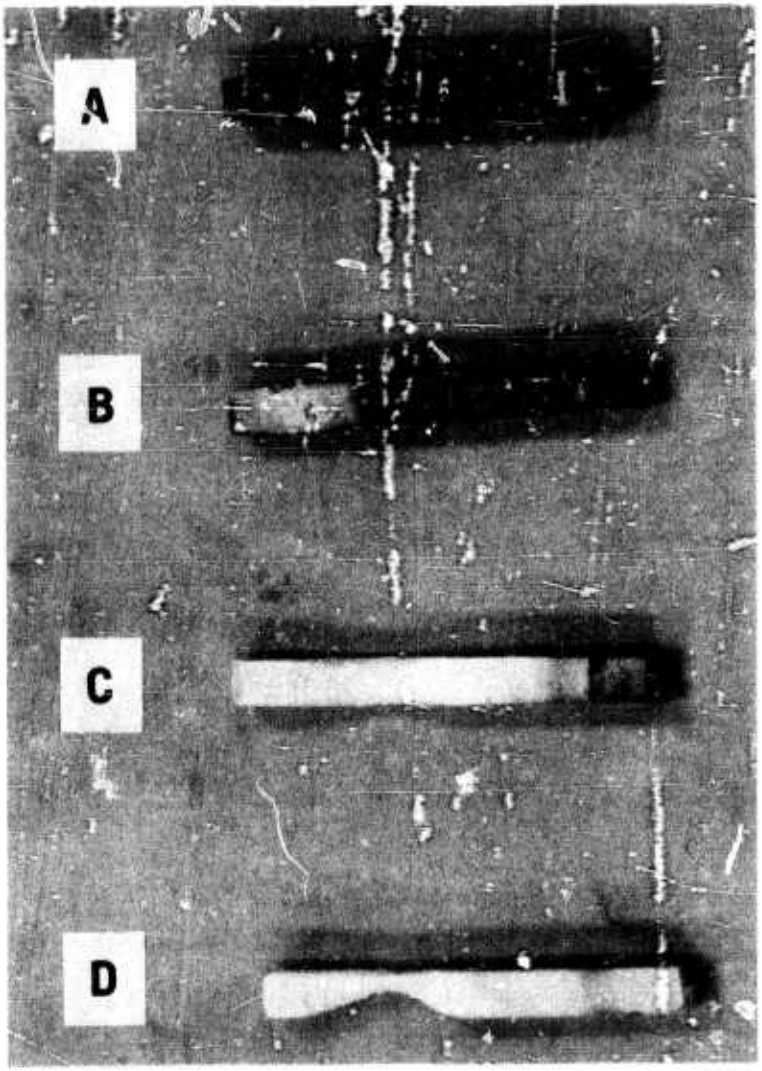

Figure 4.12 Four Sialon Samples After 1312 Thermal Shock Cycles to 2100°F for 45 Seconds.
(A) 84% A.M.E. Si_3N_4, 16% Al_2O_3, 1/2% Y_2O_3
(B) 84% A.M.E. Si_3N_4, 16% Al_2O_3, 1% Y_2O_3
(C) 84% Plessey Si_3N_4, 16% Al_2O_3, 1/2% Y_2O_3
(D) 84% Plessey Si_3N_4, 16% Al_2O_3, 1% Y_2O_3

Si_3N_4, for example. Possibilities such as these are currently being considered in the context of the vacancy-free model of sialon, $Si_{6-x}Al_xO_xN_{8-x}$.

If the sialon is indeed $Si_{6-x}Al_xO_xN_{8-x}$ rather than $Si_{6-3/4x}Al_{2/3x}O_xN_{8-x}$, then attempts to prepare it from only Si_3N_4 and Al_2O_3 will lead to by-products as well. These may be volatile-leaving only sialon in the sample-or nonvolatile, leaving other phases, (possibly glassy) along with the sialon. On the other hand, preparation from Si_3N_4 along with an equimolar mixture of Al_2O_3 and AlN should lead to single phase sialon. Since Si_3N_4 usually contains some SiO_2 contaminant, and AlN frequently contains Al_2O_3, reactions are actually carried out in the system Si_3N_4-Al_2O_3-AlN-SiO_2, and should follow the stoichiometry of a reaction such as

$$(2-\frac{5x}{12})\ Si_3N_4 + (\frac{2x}{3})\ AlN + (\frac{x}{6})\ Al_2O_3 + (\frac{x}{4})\ SiO_2 \longrightarrow Si_{6-x}Al_xO_xN_{8-x}.$$

Current work aimed at producing sialons according to the vacancy-free model by pressureless sintering has yielded promising preliminary results. Although room temperature strengths as high as those of the Si_3N_4-Al_2O_3-Y_2O_3 materials have not yet been obtained, materials of moderate strength, which retain that strength at 1200°C (2192°F) have been prepared. Work is proceeding on increasing overall strength levels.

4.5 SILICON MILLING STUDIES

Introduction

The previous report [9] presented interim results on the use of the attritor mill as a replacement for 140 hour ball milling of silicon feed material. This effort dealt primarily with the measurement of silicon particle size, and it was shown that the attritor mill was capable of producing a silicon particle distribution very similar to the 140 hour ball milling technique. During this reporting period, the work was expanded to include spiral flow measurements on molded compositions made from attritor-milled silicon.

Procedure and Results

ASTM D-3123-72 test procedure was used to measure spiral flow of the various silicon molding compositions. Test conditions were material temperature 200°F., and die temperature 80°F. Spiral flow was measured for injection pressures of 1500 and 2000 psi. Spiral flow results are shown in Table 4.14.

TABLE 4.14

EFFECT OF ATTRITOR MILLING ON SPIRAL FLOW CHARACTERISTICS OF SILICON POWDER

Batch Number	Speed (rpm)		Time (Minutes)		Spiral Flow (Inches)	
	Grind	Unload	Grind	Unload	1500 psi	2000 psi
32-36	550	550	30	10	1-4	2-3
37	550	550	60	12	0	0
38	550	550	90	15	5	6
39	550	250	30	30	2	2
40	550	250	60	25	1	3
41	200	200[a]	45	20	0	1
42	200	200[b]	45	30	7	5
43[c]	550	550	45	15	3	3
44[d]	550	550	45	20	0	0
Std.[e]	-	-	-	-	10	10

a. Discharge port opened at start of grind.

b. Discharge port opened and closed for 10 minute intervals until mill was empty.

c. Milled with 0.5 percent ethyl acetate.

d. Milled with 1.0 percent oleic acid.

e. Standard 140 hour ball milled silicon.

Batches 32 through 36 were formulated with silicon milled in the attritor under the same conditions that produced particle size distributions very similar to standard 140 hour ball milled silicon. The spiral flow results did not show the same correlation between 140 hour grind and attritor milled material as preliminary results indicated in the previous report [9]. In all cases, spiral flow was much below 10 inches measured on the standard material.

Batches 37 through 42 represent silicon obtained from the attritor under various conditions of grinding and discharge speed, retention and grinding time. Batches 43 and 44 were studied to show the effect of ethyl acetate and oleic acid additives on milling. It is obvious from the results, shown in Table 4.14, that changes in these parameters did not produce silicon with spiral flows equivalent to the 140 hour ball milled silicon.

No investigation was made into why the attritor-milled material behaved as it did as it was judged that such an investigation was not warranted at this time since ball milling, while time consuming, provided consistent results.

5. REFERENCES

1. McLean, A. F., Fisher, E. A., Harrison, D. E., "Brittle Materials Design, High Temperature Gas Turbine". AMMRC-CTR-72-3, Interim Report, March, 1972.

2. McLean, A. F., Fisher, E. A., Bratton, R. J., "Brittle Materials Design, High Temperature Gas Turbine". AMMRC-CTR-72-19, Interim Report, September, 1972.

3. McLean, A. F., Fisher, E. A., Bratton, R. J., "Brittle Materials Design, High Temperature Gas Turbine". AMMRC-CTR-73-9, Interim Report, March, 1973.

4. McLean, A. F., Fisher, E. A., Bratton, R. J., "Brittle Materials Design, High Temperature Gas Turbine". AMMRC-CTR-73-32, Interim Report, September, 1973.

5. McLean, A. F., Fisher, E. A., Bratton, R. J., "Brittle Materials Design, High Temperature Gas Turbine". AMMRC-CTR-74-26, Interim Report, April, 1974.

6. McLean, A. F., Fisher, E. A., Bratton, R. J., "Brittle Materials Design, High Temperature Gas Turbine". AMMRC-CTR-74-59, Interim Report, September, 1974.

7. McLean, A. F., Fisher, E. A., Bratton, R. J., Miller, D. G., "Brittle Materials Design, High Temperature Gas Turbine". AMMRC-CTR-75-8, Interim Report, April, 1975.

8. McLean, A. F., Fisher, E. A., Bratton, R. J., Miller, D. G., "Brittle Materials Design, High Temperature Gas Turbine". AMMRC-CTR-75-28, Interim Report, September, 1975.

9. McLean, A. F., Baker, R. R., Bratton, R. J., Miller, D. G., "Brittle Materials Design, High Temperature Gas Turbine". AMMRC-CTR-76-12, Interim Report, April, 1976.

10. McLean, A. F., Baker, R. R., "Brittle Materials Design, High Temperature Gas Turbine". AMMRC-CTR-76-31, Interim Report, October, 1976.

11. Katsanis, Theodore, "Fortran Program for Calculating Transonic Velocities on a Blade-to-Blade Stream Surface of a Turbomachine". NASA TN D-5427, 1969.

12. Glassman, A. J., "Turbine Design and Application", Volume 2, NASA SP-290, 1973.

13. Thoman, D. R., Bain, L. J., and Antle, C. E., 1969 "Inferences on the Parameters of the Weibull Distribution", Technometrics, 11, 445-460.

14. Proposed Military Standard, "Test Methods for Structural Ceramics", Army Materials and Mechanics Research Center, October 15, 1973.

15. Carruthers, W. D., and Walker, B. H., "Design, Fabrication and Evaluation of Gatorized Ceramic-Wrought Alloy Attachment Concepts", Status Report No. 4, Navy Contract N00019-74-C-0484, by Pratt and Whitney Aircraft Florida Research and Development Center.

16. Evans, A. G., and Davidge, R. W., "The Strength and Oxidation of Reaction Sintered Silicon Nitride", Journal of Material Science, 5, 1970, p. 314.

17. Miller, D. G., Bratton, R. J., Lange, F. F., Singhal, S. C., Booker Jr., C. R., "Brittle Materials Design, High Temperature Gas Turbine." AMMRC-CTR-76-32, Westinghouse Final Report, December, 1976.

ARMY MATERIALS AND MECHANICS RESEARCH CENTER
WATERTOWN, MASSACHUSETTS 02172

TECHNICAL REPORT DISTRIBUTION

No. of Copies	To
1	Advanced Research Projects Agency, 1400 Wilson Boulevard, Arlington, Virginia 22209
2	ATTN: Director
1	Deputy Director
1	Director of Materials Sciences - Dr. A. L. Bement
1	Deputy Director Materials Sciences - Dr. E. C. van Reuth
1	Technical Information Office - Mr. F. A. Koether
1	Air Force Aeroprpulsion Laboratory Wright-Patterson Air Force Base, Dayton, Ohio 45433
	Aerospace Research Laboratory, ATTN: ARL-LL, Wright-Patterson Air Force Base, Dayton, Ohio 45433
1	ATTN: Dr. Henry Graham
1	Mr. Larry Hjelm
1	Major L. Jacobson
1	Dr. James Wimmer
	Air Force Materials Laboratory
1	Major Roger Austin, Wright-Patterson Air Force Base, Dayton, Ohio 45433
1	Dr. Mike Buckley, LLP, Wright-Patterson Air Force Base, Dayton, Ohio 45433
1	Mr. Gail Eichelman, Manufacturing Processes Division, Wright-Patterson Air Force Base, Dayton, Ohio 45433
1	Mr. S. Lyons, Wright Patterson Air Force Base, Dayton, Ohio 45433
1	Dr. R. Ruh, LLS, Wright-Patterson Air Force Base, Dayton, Ohio 45433

ARMY MATERIALS AND MECHANICS RESEARCH CENTER
WATERTOWN, MASSACHUSETTS 02172

TECHNICAL REPORT DISTRIBUTION

No. of Copies	To
1	Capt. Smyth, Wright-Patterson Air Force Base, Dayton, Ohio 45433
	Air Force Research and Development Dr. A. Lovelace, Deputy Assistant Secretary (R&D) Office of Assistant Secretary of the Air Force (Research and Development), Room 4E973, Pentagon, Washington D.C. 20330
1	Air Force Systems Command Major Jose Baca, Headquarters, DLFP, Propulsion and Power Branch, Andrews Air Force Base, Washington D. C. 20034
	Argonne National Laboratory
1	Dr. Paul G. Shewmon, D212, 9700 South Cass Avenue, Argonne, Illinois 60439
	Argonne National Laboratory
1	Mr. R. N. Singh, Materials Science Division, 9700 South Cass Avenue, Argonne, Illinois 60439
	U. S. Army Air Mobility Research and Development Laboratory
2	J. Accurio, Director, Lewis Directorate, NASA, Lewis Research Center, 21000 Brookpark Road, Cleveland, Ohio 44135
1	R. Berrisford, Chief, Structures Division, Eustis Directorate, Ft. Eustis, Virginia 23604
1	T. Coleman, Director, Langley Directorate, Langley Research Center, Langley Field, Virginia 23365
2	F. Immen, J. Wheatly, Advanced Systems Research Office, Ames Research Center, Moffett field, California 94035
1	J. White, Assistant Technical Director, Eustis Directorate, Fort Eustis, Virginia 23604
	U. S. Army Aviation Material Laboratories
1	Commanding Officer, Fort Eustis, Virginia 23604
	U. S. Army Aviation School Library
1	Librarian, Fort Rucker, Alabama 36360 Bldg. 5907

ARMY MATERIALS AND MECHANICS RESEARCH CENTER
WATERTOWN, MASSACHUSETTS 02172

TECHNICAL REPORT DISTRIBUTION

No. of Copies	To
	U. S. Army Aviation Systems Command
1	Commanding General, ATTN: R. Long, Deputy Director RD&E, P. O. Box 209, St. Louis, Missouri 63166
	U. S. Army Engineers
1	Commanding Officer, Waterways Experiment Station, Vicksburg, Mississippi 39180 ATTN: Research Center Library
	U. S. Army Material Command
2	Commanding General, Washington D. C. 20315 AMCRD-TC (Dr. E1-Bisi) ANCDL (Dr. Dillaway)
	Army Materials Command Headquarters
1	Dr. Donald Weidhuner, Chief, Power Division, Research Development and Engineering Directorate, 5001 Eisenhower Avenue, Alexandria, Virginia 22304
	Army Materials and Mechanics Research Center
	Director, Watertown, Massachusetts 02172
2	ATTN: AMXMR-PL
1	AMXMR-PR
1	AMXMR-CT
1	AMXMR-AP
1	AMXMR-X (Dr. Wright)
1	AMXMR-EO (Dr. Katz)
2	AMXMR-TM (Dr. Lenoe)
2	AMXMR-D (Dr. Priest)
1	AMXMR-EO (Dr. Messier)
2	AMXMR-P (Dr. Burke)
1	AMXMR-MS (Mr. MacDonald)
1	AMXMR-E (Dr. Larson)
	Lt. Col. E. E. Chick
4	U.S. Army MERDEC
	Command Officer, Fort Belvoir. Virginia 22060
	ATTN: STSFB-EP (Mr. Frank Jordan)
	STSFB-EP (Mr. W. McGovern)
	AMCPM-FM (Mr. Allen Elkins)
	AMXFB-EM (Mr. George F. Sams)

ARMY MATERIALS AND MECHANICS RESEARCH CENTER
WATERTOWN, MASSACHUSETTS 02172

TECHNICAL REPORT DISTRIBUTION

No. of Copies	To
	Army Missile Command
1	Commanding General, ATTN: AMCRD-F, J. Beebe, Washington D.C. 20315
1	Commanding General, Redstone Arsenal, Alabama 35809 ATTN: Technical Library
1	Commanding General, ATTN: AMCDL, Webb Taylor, 5001 Eisenhower Avenue, Alexandria, Virginia 22304
	USACDC Ordnance Agency, Aberdeen Proving Ground
1	Commanding Officer, Maryland 21005, ATTN: Technical Library Building 313
1	Commanding Officer, Maryland 21005, ATTN: Library, Building 350
	Army Research and Development
1	Office, Chief Research and Development, Department of the Army, ATTN: R. Ballard, Physical and Engineering Sciences Division, Washington, D.C. 20315
1	Office Chief Research and Development, Department of Army, ATTN: Col. J. Barnett, Physical and Engineering Sciences Division, Washington, D.C. 20315
1	Commanding Officer, Army Research Office (Durham), Bx CM, Duke Station Durham, North Carolina 27006 ATTN: Dr. H. M. Davis
8	Lt. Col. James Kennedy, Chief, Materials Branch, European Research Office U.S. Army R & D Group, (EUR), Box 15, FPO New York 09510
1	Mr. H. Morrow, Eustis Directorate, AMRDL, Fort Eustis, Virginia 23604
	U.S. Army Tank-Automotive Command
5	Commanding General, Warren, Michigan 48090, ATTN: AMSTA-BSL, Research Library Br, ATTN: AMSTA-RKM (Mr. C. Green), ATTN: AMSTA-RGR (Mr. Engel), ATTN: AMSTA (Dr. Banks), ATTN: AMSTA (Mr. L. Barnett)
	U.S. Army Weapons Command
1	Commanding General, Research and Development Directorate, Rock Island, Illinois 61201, ATTN: AMSWE-RDR

ARMY MATERIALS AND MECHANICS RESEARCH CENTER
WATERTOWN, MASSACHUSETTS 02172

TECHNICAL REPORT DISTRIBUTION

No. of Copies	To
	U.S. Atomic Energy Commission
1	Dr. Joseph Griffo, Space Nuclear Systems Division, Century XXI Building, Mail Station F-309, Washington D.C. 20545
1	Dr. Alan Womack, Assistant Director, Gas Cooled Reactors, Washington D.C. 20545
	British Embassy
1	Dr. R. Warren, Contract Officer, Defence Research and Development Staff, 3100 Massachusetts Avenue N.W., Washington D. C. 20008
	Bureau of Mines
1	Dr. E. P. Flint, Room 4513, Interior Building, Washington D. C. 20240
1	Mr. Ron Lowrey, P. O. Box 70, Albany, Oregon 97321
1	Mr. M. A. Schwartz, Tuscaloosa Metallurgy Research Laboratory, P. O. Box 1, University, Alabama 35486
12	Defense Documentation Center Commander, Cameron Station, Building 5, 5010 Duke Street, Alexandria, Virginia 22314
1	Department of Transportation Mr. Michael Lauriente, 400 Seventh Street, S. W., Washington, D. C. 20590
1	Directorate for Energy W. C. Christensen, Assistant for Resources, OASD (I & L), Room 2B341 Pentagon, Washington, D. C. 20301
1	Office of the Director of Defense Mr. R. M. Standahar, Research and Engineering, Room 3D1085, Pentagon, Washington, D. C. 20301
	Energy Research and Development Administration
5	Division of Transportation, 20 Massachusetts Avenue, N.W. Washington D. C. 20545 ATTN: Mr. George Thur (TEC) Mr. Frank Moore (CLNRT) Mr. Robert Schulz (TEC) Mr. John Neal (CLNRT) Mr. Thomas Sebestyen (TEC)

ARMY MATERIALS AND MECHANICS RESEARCH CENTER
WATERTOWN, MASSACHUSETTS 02172

TECHNICAL REPORT DISTRIBUTION

No. of Copies	To
1	Mr. E. N. C. Dalder, Materials and Radiation Effects Branch, Division of Magnetic Fusion Energy, MSG-234, Washington D.C. 20545
1	Dr. C. Martin Stickley, Division of Laser Fusion, Mail Station A-364, Washington, D.C. 20545
1	Mrs. Patricia Mooney, Office of Management and Budget, Coordination Branch, Room 8001, New Executive Office Bldg., Washington, D. C. 20503
1	Mr. Steve Wander, Division of Fossile Fuels, Washington, D. C. 20545
1	Dr. S. M. Wolf, Division of Physical Research, Mail Station J-309, Washington, D. C. 20545
1	Federal Energy Office Mr. Thomas Gross, Staff Member, Office of Energy Conservation, Room 4234, Columbia Plaza Bldg., Washington, D. C. 20461
1	Federal Power Commission Dr. Charles Berg, Chief Engineer, Room 2100 825 North Capital Street, N. E., Washington, D. C. 20426
1	USA Foreign Science and Technology Center Commander, ATTN: AMXST-SD3, Mr. C. Petschke, 220 7th Street NE, Charlottesville, Virginia 22901
	National Academy of Sciences
1	Mr. Donald G. Groves, Staff Engineer, National Materials Advisory Board, 2101 Constitution Avenue, N. W., Washington, D.C. 20418
	National Aeronautics and Space Administration
2	Ms. Bolick, Goddard Space Flight Center, Greenbelt, Maryland 20771
1	Dr. G. C. Deutsch, Assistant Director of Research (Materials), Code RR-1, NASA, Washington, D.C. 20546
1	Mr. James J. Gangler, Advanced Research and Technology Division, Code RRM, Room B556, Headquarters, Washington, D.C. 20546
1	Mr. P. R. Miller, NASA Headquarters, Code RPD, 600 Independence Avenue, S.W., Washington, D.C. 20546
1	Mr. Neil T. Saunders, Ch. Materials Application Branch, Lewis Research Center, Cleveland, Ohio 44135

ARMY MATERIALS AND MECHANICS RESEARCH CENTER
WATERTOWN, MASSACHUSETTS 02172

TECHNICAL REPORT DISTRIBUTION

No. of Copies	To
7	NASA Lewis Research Center, 21000 Brookpark Road, Cleveland, Ohio 44135 ATTN: Mr. W. Saunders; Dr. S. K. Dutta; Dr. Hubert Probst; Mr. C. Blankenship; Dr. Robert C. Bill; Mr. M. Krasner; Mr. Donald Guentert
	National Bureau of Standards
1	Dr. Robb Thomson, Senior Research Scientist, Room B109, Bldg. 225, Washington, D. C. 20234
1	Dr. Donald Vieth, Administration Bldg., Room A1002, Washington, D. C. 20234
1	Dr. John B. Wachtman, Jr., Division Chief, Inorganic Materials Division, Room A359, Materials Building, Washington, D. C. 20234
1	Dr. S. Wiederhorn, Physical Properties Section, Institute for Materials Research, Washington, D. C. 20234
	National Science Foundation
1	Dr. Raymond Bisplinghoff, Deputy Administrator, 1800 G. Street, N. W., Washington, D. C. 20550
1	Mr. R. Reynik, Director, Division of Materials Research, 1800 G. Street, N. W., Washington, D. C. 20550
1	Dr. Leonard Topper, Office of Energy R & D Policy, Room 537, 1800 G. Street, N. W., Washington, D. C. 20550
	U. S. Naval Air Propulsion Test Center
1	Mr. Robert Benham, AEP-22, (AE), Philadelphia, Pennsylvania 19112
1	Mr. Joe Glotz, Department of the Navy, Trenton, New Jersey 08628
	Naval Air Systems Command
1	Mr. Irving Machlin, High Temperature Materials Divsion, Materials and Processes Branch, (NAIR-52031D), Department of the Navy, Washington, D. C. 20360
1	Mr. Charles F. Bersch, Department of the Navy, Washington, D. C. 20360
	Office of Naval Research
1	Dr. A. M. Diness, Metallurgy Branch, Code 471, 800 N. Quincy Street, Arlington, Virginia 22217

ARMY MATERIALS AND MECHANICS RESEARCH CENTER
WATERTOWN, MASSACHUSETTS 02172

TECHNICAL REPORT DISTRIBUTION

No. of Copies	To
1	Mr. Keith Ellingsworth, Power Program, Arlington, Virginia 22217
1	Mr. R. Rice, Washington, D.C. 20390
	Naval Ships Engineering
1	Mr. John Fairbanks, Prince George Center, Hyattsville, Maryland 20782
	Naval Ships Research and Development Center
1	Mr. George A. Wacker, Head Metal Physics Branch, Annapolis, Maryland 21402, ATTN: Code 2812
1	Mr. W. Wheatfall, Code 2812, Annapolis, Maryland 21402
	Naval Ship Systems Command Headquarters
1	Mr. Roy Peterson, Chief, Pollution Abatement and Gas Turbine Research, Ship Research and Technology Division, 2531 Jefferson Davis Highway, Arlington, Virginia 20362
	Naval Underwater System Center
1	Mr. John Miguel, Newport, Rhode Island
	Naval Weapons Center
1	Dr. W. Thielbaln, Code 4061, China Lake, California 93555
2	Dr. James I. Bryant, Office of the Chief of Research, Development and Acquisition, ATTN: DAMA-CSS, the Pentagon, Washington, D.C. 20310
1	Mr. Tyler Port, Special Assistant, OASA, (I&L), Room 3E620, Pentagon, Washington, D.C. 20301

ARMY MATERIALS AND MECHANICS RESEARCH CENTER
WATERTOWN, MASSACHUSETTS 02172

TECHNICAL REPORT DISTRIBUTION

No. of Copies	To
1	Aerojet Liquid Rocket Company Mr. O. I. Ford, Technical Manager, Combustor Systems, P. O. Box 18222, Sacramento, California 95813
1	The Aerospace Corporation Mr. Donald Lapades, P. O. Box 92957, Los Angeles, California 90009
	AiResearch Manufacturing Company
1	Dr. Robert F. Kirby, Materials Engineering Dept. 93-393M, Sky Harbor Airport, 402 South 36th Street, Phoenix, Arizona 85034
1	Mr. McCoy, Materials Engineering, Dept. 93-393M, 402 South 36th Street, Phoenix, Arizona 85034
1	Supervisor, Propulsion Engine Advanced Technology Dept., 93-12M Sky Harbor Airport, 402 South 36th Street, Phoenix, Arizona 85034
1	Mr. Dennis W. Swain, Department 93-19M, P. O. Box 5217, Phoenix, Arizona 85010
1	American Lava Corporation Dr. J. T. Bailey, Chattanoga, Tennessee 37405
1	Arthur D. Little, Incorporated Mr. D. William Lee, Acorn Park, Cambridge, Massachusetts 02140
	Avco Corporation
1	Mr. Louis J. Fiedler, Materials and Process Technology Lab., 550 S. Main Street, Stratford, Connecticut 06497
1	Dr. T. Vasilos, Applied Technology Division, Lowell Industrial Park, Lowell, Massachusetts 01851
1	Babcock and Wilcox Dr. A. W. Illyn, Technical Director, Refractories Division, Old Savannah Road, Augusta, Georgia 30903
	Battelle Columbus Laboratories
1	Mr. Winston Duckworth and Mr. Lewis E. Hulbert, 505 King Avenue, Columbus, Ohio 43201
1	Mr. James Lynch, Metals and Ceramics Information Center, 505 King Avenue, Columbus, Ohio 43201

ARMY MATERIALS AND MECHANICS RESEARCH CENTER
WATERTOWN, MASSACHUSETTS 02172

TECHNICAL REPORT DISTRIBUTION

No. of Copies	To
	Battelle Memorial Institute
1	Mr. William Combs, 2030 M Street N.W. Washington, D.C. 20036
1	Metals and Ceramics Information Center, 505 King Avenue, Columbus, Ohio 43201
	Bell Aerospace Company
1	Dr. Wilfred H. Dukes, Assistant Director Engineering for Development, P.O. Box 29307, New Orleans, Louisiana 70189
	Bell Aerospace Company
1	Mr. A. E. Leach, Manager, Process Development Engineering, Mail Zone C-33, P. O. Box 1, Buffalo, New York 14240
1	Mr. Nelson R. Roth, P.O. Box #1, Department V70, Buffalo, New York 14240
1	Cabot Corporation Mr. S. T. Wlodek, Stellite Division, 1020 West Park Avenue, Kokomo, Indiana 46901
	The Carborundum Company
1	Dr. John A. Coppola, Project Manager, Research and Development Division, Niagara Falls, New York 14302
1	Mr. C. H. McMurty, Project Manager, Research and Development Division, Niagara Falls, New York 14302
1	Caterpillar Tractor Company Mr. A. R. Canady, Technical Center, Building F, Peoria, Illinois 61602
1	Ceradyne Incorporated Mr. J. A. Rubin, President, P.O. Box 11030, 3030 South Red Hill Avenue, Santa Ana, California 92705
1	Ceramic Finishing Company Dr. H. P. Kirchner, P. O. Box 498, State College, Pennsylvania 16801
1	Ceramic Systems Incorporated Mr. Eldor R. Herrmann, 11402 Schaefer Highway, Detroit, Michigan 48227

ARMY MATERIALS AND MECHANICS RESEARCH CENTER
WATERTOWN, MASSACHUSETTS 02172

TECHNICAL REPORT DISTRIBUTION

No. of Copies	To
	Chrysler Corporation
1	Mr. C. E. Wagner, Senior Research Staff Engineer, CIMS: 418-37-18, P. O. Box 1118, Detroit, Michigan 48231
1	Mr. Philip J. Willson, Chemical Research, Box 1118, CIMS: 418-19-18, Detroit, Michigan 48231
1	Colt Industries Mr. E. J. Dulis, President, Materials Research Center, Box 88, Pittsburgh, Pennsylvania 15230
1	Coors Porcelain Company Research Department, 17750 West 32nd Avenue, Golden, Colorado 80401
1	Corning Glass Works Mr. John C. Lanning, Manager, Erwin Plant, Advanced Engine Components Department, Corning, New York 14830
1	Creare Incorporated Ms. Sharon Wright, Technical Library, Hanover, New Hampshire 03755
1	Curtis-Wright Corporation Mr. S. Walosin, One Passaic Street, Woodridge, New Jersey 07075
2	Cummins Engine Company, Incorporated Mr. R. Kano, Mr. K. J. Mather, Columbus, Indiana 47201
1	Deposits and Composites, Incorporated Mr. Richard E. Engdahl, 1821 Michael Faraday Drive, Reston, Virginia 22090
	Dow Corning Corporation
1	Mr. G. Kookootsedes, Market Development, Resins and Chemicals, Midland, Michigan 48640
1	Mr. Donald E. Weyer, Midland, Michigan 48640
1	Eagle-Picher Industries Mr. J. J. Stiglich, 200 9th Avenue N.E. Miami, Oklahoma 74354

ARMY MATERIALS AND MECHANICS RESEARCH CENTER
WATERTOWN, MASSACHUSETTS 02172

TECHNICAL REPORT DISTRIBUTION

No. of Copies	To
1	Eaton Corporation Mr. William E. Gurwell, Research Center 26201 Northwestern Highway, Southfield, Michigan 48076
1	EF Industries, Incorporated Mr. J. D. Mote, 1301 Courtesy Road Louisville, Colorado 80027
1	Electric Power Research Institute Dr. Richard E. Balzhiser, P. O. Box 10412, 3412 Hillview Avenue Palo Alto, California 94304
1	Dr. Arthur Cohn, P.O. Box 10412, 3412 Hillview Avenue, Palo Alto, California 94304
1	Energy Research Corporation Bethel, Connecticut 06801
1	Esso Research and Engineering Company Dr. John V. Milewski, Government Research Laboratory, P. O. Box 8, Linden, New Jersey 07036
1	Ferro Corporation Mr. Y. Baskin, Manager Inorganic Chemical Research, Technical Center, 7500 East Pleasant Valley Road, Independence, Ohio 44131
1	Fiber Materials Mr. Paul F. Jahn, Vice President, Broadway and Main Street, Graniteville, Massachusetts 01829
1	Garrett Corporation Mr. H. R. Schelp, 9851 Sepulveda Boulevard, Los Angeles, California 90009
1	Gas Turbine International Mr. Jack W. Sawyer, 4519 Eighteen Street North Arlington, Virginia 22207
1	Gas Turbine World Mr. Victor de Biasi, Editor, P. O. Box 494, Southport, Connecticut 06490

ARMY MATERIALS AND MECHANICS RESEARCH CENTER
WATERTOWN, MASSACHUSETTS 02172

TECHNICAL REPORT DISTRIBUTION

No. of Copies	To
	General Atomics Corporation
1	Mr. N. B. Elsner, Box 81608, San Diego, California 92138
1	Mr. Karl Koyama, Box 81608, San Diego, California 92138
1	Dr. Robert K. Thomas, FA4-4, Reactor Engineering, P. O. Box 81608, San Diego, California 92138
	General Electric
1	Dr. C. A. Bruch, Manager, Advanced Studies, Aircraft Engine Group, Cincinnati, Ohio 45215
1	Dr. J. E. Burke, Corporate Research and Development, P. O. Box 8, Schenectady, New York 12301
1	Dr. H. von E. Doering, Manager, Fuels/Corrosion Unit, Gas Turbine Products Division, Building 53-311, Schenectady, New York 12345
1	Dr. Soloman Musikant, Manager, Metallurgy and Ceramics Lab General Electric Valley Forge, Valley Forge, Pennsylvania
1	Dr. Michael J. Noone, Space Sciences Laboratory, Box 8555, Philadelphia, Pennsylvania 19101
1	Mr. Arthur L. Ross, Valley Forge Space Center, P. O. Box 8555, Philadelphia, Pennsylvania 19101
1	Mr. Chester T. Sims, Manager, Advanced Materials, Gas Turbine Products Division., Schenectady, New York 12301
	General Motors Corporation
1	Dr. Morris Berg, AC Spark Plug Division, Flint, Michigan 48556
1	Dr. John S. Collman, Head, Power Systems Development, Research Laboratories, Warren, Michigan 48090
1	Dr. Robert W. Gibson, Jr., Head, Library Department GM Technical Center, Warren, Michigan 48090
1	Mr. M. Herman, Detroit Diesel Allison Division, Indianapolis Operations, P. O. Box 894, Indianapolis, Indiana 46206

ARMY MATERIALS AND MECHANICS RESEARCH CENTER
WATERTOWN, MASSACHUSETTS 02172

TECHNICAL REPORT DISTRIBUTION

No. of Copies	To
1	Mr. Michael E. Naylor, General Motors Technical Divsion, Passenger Car Turbine Division, Warren, Michigan 48090
1	Mr. O. Prachar, Passenger Car Turbine Department, Engineering Staff, General Motors Technical Center, Warren, Michigan 48090
1	Dr. Edward Reynolds, General Motors Technical Center, Passenger Car Turbine Division, Warren, Michigan 48090
	GTE Sylvania
1	Dr. Richard Kliener, Tonawanda, Pennsylvania 18848
1	Dr. William H. Rhodes, GTE Laboratories, Waltham Research Center, 40 Sylvan Road, Waltham, Massachusetts 02154
1	Howmet Corporation Mr. Wm. R. Freeman, Jr., Vice President and Technical Director, Superalloy Group, One Misco Drive, Whitehall, Michigan 47461
1	Industrial Materials Technology Dr. Robert Widmer, President, 19 Wheeling Avenue, Woburn, Massachusetts
1	Institut fur Werkstoff-Forshung Dr. W. Bunk, DFVLR, 505 Porz-Wahn, Linder Hohe, Germany
	International Harvester Company
1	Mr. A. R. Stetson, Chief, Process Research Laboratories, Mail Zone R-1, Solar Division of Int. Harvester Company, 2200 Pacific Highway, San Diego, California 92112
1	Mr. M. J. Klein, Research Staff Specialist, Mail Zone R-1, Solar Division of International Harvester, 2200 Pacific Highway, P. O. Box 80966, San Diego, California 92138
1	The International Nickel Company, Incorporated Mr. Gaylor D. Smith, 1 New York Plaza, New York, New York 10004
2	Kawecki-Berylco Industries, Incorporated Mr. E. Laich, Mr. R. J. Longenecker, P. O. Box 1462, Reading, Pennsylvania 19603
1	Kaman Sciences Corporation Mr. William D. Long, Manager, Product Development, K-Ramics, Garden of the Gods Road, Colorado Springs, Colorado 80907

ARMY MATERIALS AND MECHANICS RESEARCH CENTER
WATERTOWN, MASSACHUSETTS 02172

TECHNICAL REPORT DISTRIBUTION

No. of Copies	To
	Lawrence Livermore Laboratory
1	Mr. C. F. Cline, L-503, Box 808, Livermore, California 94550
1	Dr. Michael Guinan, B. Div./L-24, P.O. Box 808, Livermore, California 94550
1	Dr. Mark Wilkins, B Div./L-24, P. O. Box 808, Livermore, California 94500
1	Lawrence Radiation Laboratory Mr. R. L. Lormand, P. O. Box 808, Livermore, California 94550
1	Manlabs, Incorporated Dr. L. Kaufman, Project Director, 21 Erie Street, Cambridge, Massachusetts 02139
1	Materials Consultants, Incorporated Dr. Jerry Plunkett, President, 2150 South Josephine Street Denver, Colorado 80210
1	Materials Research and Computer Simulation Mr. William Oldfield, 634 Berkeley Place, Westerville, Ohio 43081
1	Materials Science Corporation Technical Library, Blue Bell Office Campus, Merion Towle Building, Blue Bell, Pennsylvania 19422
1	Mechanical Technology, Incorporated Mr. D. W. McLaughlin, Research and Development Division, 968 Albany-Shaker Road, Latham, New York 12110
1	National Beryllia Corporation Dr. Peter L. Fleischner, Haskell, New Jersey 07420
1	Northern Research and Engineering Corporation Ms. Rayna Lee Caplan, Librarian, 219 Vassar Street, Cambridge, Massachusetts 02139
	Norton Company
1	Mr. M. Blake, One New Bond Street, Worcester, Massachusetts 01606
1	Mr. E. W. Hauck, Market Manager, Engine Components, One New Bond Street, Worcester, Massachusetts 01606

ARMY MATERIALS AND MECHANICS RESEARCH CENTER
WATERTOWN, MASSACHUSETTS 02172

TECHNICAL REPORT DISTRIBUTION

No. of Copies	To
1	Mr. M. L. Torti, One New Bond Street, Worcester, Massachusetts 01606
1	Owens-Corning Fiberglass Corporation Mr. P. E. McConnell, Technical Center, Granville, Ohio 43023
	Owens Illinois Glass
1	Mr. L. M. Donley, 1900 North Westwood Avenue, Toledo, Ohio 43601
1	Mr. Y. K. Pei, 1020 North Westwood Avenue, Toledo, Ohio 43607
	PPG Industries, Incorporated
1	Mrs. Jane Bookmyer, Information Services Division, P. O. Box 11472 Pittsburgh, Pennsylvania 15238
1	Mr. F. G. Stroke, Asst. Manager Market Development, 1 Gateway Center, Pittsburgh, Pennsylvania 15222
	Pratt and Whitney Corporation
1	Mr. James F. Holloway, Materials Project Engineer, 400 Main Street, E. Hartford, Connecticut 06108
1	Mr. M. Allen Magid, Materials Marketing Engineer, Florida R & D Center P. O. Box 2691, West Palm Beach, Florida 33402
1	Mr. Francis L. VerSnyder, Manager, Materials Engineering and Research Lab, 400 Main Street, E. Hartford, Connecticut 06108
1	Program Development Consultant Dr. Robert A. Harmon, 25 Schalren Drive, Latham, New York 12110
1	The Rand Corporation Dr. Eugene C. Gritton, Physical Sciences Department, 1700 Main Street, Santa Monica, California 90406
	Raytheon Company
1	Ms. Madaleine Bennett, Librarian, Research Division Library, Foundry Avenue, Waltham, Massachusetts 02154
	Raytheon Company
1	Dr. Stanley Waugh, Research Division, 28 Seyon Street, Waltham, Massachusetts 02154
1	R. I. A. S. Mrs. R. J. Benacquista, 3808 Acosta Road, Fairfax, Virginia 22030

ARMY MATERIALS AND MECHANICS RESEARCH CENTER
WATERTOWN, MASSACHUSETTS 02172

TECHNICAL REPORT DISTRIBUTION

No. of Copies	To
	Rockwell International Corporation
1	Mr. F. E. Krainess, D/391-204 AB70, 12214 Lakewood Boulevard, Downey, California 90241
1	Dr. Don Thompson, Science Center, 1049 Camino Dos Rios, Thousand Oaks, California 91360
1	Rohr Industries, Incorporated Mr. Joseph Simpson, Technical Library, P. O. Box 1516, Chula Vista, California 92012
1	SKF Industries, Incorporated Warren Jameson and Harish Dalal, Engineering and Research Center, 1100 1st Avenue, King of Prussia, Pennsylvania 19406
1	Southern Research Institute Mr. H. Stuart Starrett, Head, Mechanics Section, 2000 Ninth Avenue South, Birmingham, Alabama 35205
1	Special Metals Corporation Mr. Willard H. Sutton, Manager, Ceramics Projects, New Hartford, New York 13413
1	Stackpole Carbon Company Mr. P. W. Parsons, Manager, Commercial Research Department, St. Marys, Pennsylvania 15857
1	Stone and Webster Engineering Corporation Mr. David Cormier, Nuclear Planning Division, 87 Nash Memorial, Road, Abington, Maryland 02351
	Teledyne
1	Mr. Robert Beck, Department Head, Development Materials 1330 Laskey Road, Toledo, Ohio 43601
1	Dr. Eli Benstien, Director of Engineering, 1330 Laskey Road, Toledo, Ohio 43601
1	Mrs. Marlene S. Dowdell, Librarian, 1330 Laskey Road, Toledo, Ohio 43601
	TRW Incorporated
1	Mr. J. A. Alexander, Manager, Materials Research Department, 23555 Euclid Avenue, Cleveland, Ohio 44117

ARMY MATERIALS AND MECHANICS RESEARCH CENTER
WATERTOWN, MASSACHUSETTS 02172

TECHNICAL REPORT DISTRIBUTION

No. of Copies	To
1	Dr. John S. Foster, Jr., Vice President for Energy Research and Development, One Space Park, Redondo Beach, California 90278
1	Technical Library, TRW Equipment, 23555 Euclid Avenue, Cleveland, Ohio 44117
1	Dr. Neal Richardson, One Space Park, Redondo Beach, California 90278
	Turbodyne Corporation
1	Ms. Diane Konsor, 711 Anderson Avenue North, St. Cloud, Minnesota 56301
1	Mr. Donald J. Legacy, Wellsville, New York 14895
1	Mr. John Polyansky, Gas Turbine Design Engineering, 626 Lincoln Avenue S.E., St. Cloud, Minnesota 56301
	Turbo Power and Marine Systems, Incorporated
1	Mr. Carl Merz, Farmington, Connecticut 06032
1	Mr. C. A. Vassilakis, New Britain Avenue, Farmington, Connecticut 06032
1	Union Carbide Corporation Dr. O. Conrad Trulson, Carbide Products Division, 270 Park Avenue, New York, New York 10017
1	United Aircraft Research Laboratories Dr. Frank Galasso, East Hartford, Connecticut 06108
1	United Technologies Research Center Dr. J. J. Brennan, East Hartford, Connecticut 06108
1	Whittaker Corporation Mr. V. A. Chase, Chief of Development Laboratory, Research and Development Division, 3540 Aero Court, San Diego, California 92123
1	Williams Research Corporation Mr. R. Barry Strachan, Walled Lake, Michigan 48088
1	Wyman-Gordon Company Mr. Wayne Everett, Research and Development, North Grafton, Maine 01536

ARMY MATERIALS AND MECHANICS RESEARCH CENTER
WATERTOWN, MASSACHUSETTS 02172

TECHNICAL REPORT DISTRIBUTION

No. of Copies	To
1	Brown University Professor Marc Richman, Engineering Division, Providence, Rhode Island 02912
	California Institute of Technology
1	Mr. Thomas J. Ahrens, Assoc. Prof. of Geophysics, Seismological Laboratory, 295 San Rafel Avenue, P. O. Bin 2, Arroyo Annex, Pasadena, California 91109
1	Dr. William A. Edminston, Jet Propulsion Laboratory - Bldg 157, 4800 Oak Grove Drive, Pasadena, California 91103
1	Carnegie-Mellon University Professor M. C. Shaw, Head, Department of Mechanical Engineering, Pittsburgh, Pennsylvania 15213
1	Georgia Tech. Mr. J. D. Walton, Jr., EES, Atlanta, Georgia 30332
1	Harvard University Professor Michael F. Ashby, Gordon McKay Professor of Metallurgy, Pierce Hall, Cambridge, Massachusetts 02138
	Illinois Institute of Technology
1	Mr. Seymour Bortz, IIT Research Institute, 10 West 35th Street, Chicago, Illinois 43601
1	Dr. Keith E. McKee, Director of Research Engineering Mechanics Div., IIT Research Institute, 10 West 35th Street, Chicago, Illinois 60616
1	Iowa State University Dr. Thomas D. McGee, Professor of Ceramic Engineering, Ames, Iowa 50010
1	Lehigh University Dr. R. M. Spriggs, Assistant to the President, Bethlehem, Pennsylvania 18015
	Massachusetts Institute of Technology
1	Professor Merton Flemings, Cambridge, Massachusetts 02139
1	Professor D. W. Kingery, Room 13-4090, Cambridge, Massachusetts 02139
1	Professor Frank S. McClintock, Department of Mechanical Engineering, Cambridge, Massachusetts 02139

ARMY MATERIALS AND MECHANICS RESEARCH CENTER
WATERTOWN, MASSACHUSETTS 02172

TECHNICAL REPORT DISTRIBUTION

No. of Copies	To
1	Dr. Donald R. Uhlmann, Associate Professor of Ceramics, Department of Metallurgy and Materials Science, Cambridge, Massachusetts 02139
1	North Carolina State University Professor Robert F. Davis, Department of Materials Science, Box 5427, Raleigh, North Carolina 27607
1	Northwestern University Professor Morris E. Fine, The Technological Institute, Dept. of Materials Science, Evanston, Illinois
	Stanford University
1	Dr. Paul Jorgensen, Associate Director, Materials Laboratory, Menlo Park, California 94025
1	Ms. Lucille Steelman, Order Librarian, ATTN: G-037 Library, Menlo Park, California 94025
1	Southern Methodist University Professor T. L. Chu, Institute of Technology, Electronic Sciences Center, Dallas, Texas 75222
1	University of Bridgeport Dr. Joseph E. Motherway, Bridgeport, Connecticut 06602
1	University of California Professor Earl R. Parker, Department of Materials Science and Engineering, 286 Hearst Mining Building Berkeley, California 94720
1	University of Illinois Dean Daniel C. Drucker, Engineering College, Urbana, Illinois 61801
	University of Michigan
1	Professor Edward E. Hucke, Materials and Metallurgical Engineering, Ann Arbor, Michigan 48104
1	Dr. Maurice J. Sinnott, Department of Chemical and Metallurgical Engineering, Ann Arbor, Michigan 48104
	University of Pennsylvania
1	Professor R. P. Kroon, Philadelphia, Pennsylvania 19104

ARMY MATERIALS AND MECHANICS RESEARCH CENTER
WATERTOWN, MASSACHUSETTS 02172

TECHNICAL REPORT DISTRIBUTION

No. of Copies	To
1	Dr. Charles J. McMahon, Jr., Assoc. Prof. Materials Science, School of Metallurgy and Materials Science, Philadelphia, Pennsylvania 19104
1	Professor Burton Paul, Department of Mechanical Engineering, Philadelphia, Pennsylvania 19104
1	University of Utah Professor I. B. Cutler, College of Engineering, Division of Materials Science and Engineering, Salt Lake City, Utah 84112

4 Authors

312 Total Copies Distributed

Army Materials and Mechanics Research Center
Watertown, Massachusetts 02172

AD _____

BRITTLE MATERIALS DESIGN
HIGH TEMPERATURE GAS TURBINE

Arthur F. McLean, Robert R. Baker, Ford
Motor Company, Dearborn, Michigan 48121

Technical Report AMMRC CTR 76-31, October, 1976
104 pages, 54 illus., 25 tables, 17 references.
Contract DAAG 46-71-C-0162, ARPA Order Number
1849 Tenth Interim Report, January 1, 1976 to
June 30, 1976

Key Words

Gas Turbine Engine
Brittle Design
Ceramics
High Temperature Materials
Silicon Nitride
Silicon Carbide
Non-Destructive Tests
Mechanical Properties

ABSTRACT

The demonstration of uncooled brittle materials in structural applications at 2500°F is the objective of the "Brittle Materials Design, High Temperature Gas Turbine" program. Ford Motor Company, the contractor, will utilize a small vehicular gas turbine comprising an entire ceramic hot flow path including the highly stressed turbine rotors. Westinghouse, the subcontractor, originally planned to evaluate ceramic first stage stator vanes in an actual 30 MW test turbine engine, however, this objective was revised to demonstrate ceramic stator vanes in a static test rig. Both companies had in-house research programs in this area prior to this contract.

In the stationary gas turbine project, the test of ceramic stator vanes in a static rig for 100 cycles up to temperatures of 2500°F has been completed. This accomplishment meets the revised objectives for the stationary turbine project and therefore, this project is completed as of the end of this reporting period. The report of the last six months progress will be included in the final report for the project and published separately.

A significant achievement, in the vehicular turbine project, was the test of a partially bladed duo-density silicon nitride turbine rotor in an experimental high temperature gas turbine engine up to a speed of 52,400 rpm and turbine inlet temperature of 2650°F before failure on a subsequent run. A modification of the ceramic hot gas flow path of the 320 turbine engine to accomplish this test is described in detail. Two rotors, with blades of 10% length, were successfully tested for 45 minutes at 32,000 rpm and 2000°F turbine inlet temperature. Rotor testing capability at elevated temperatures was initiated in two hot spin rigs which were checked out with six available ceramic rotors. Cold spin test results of nine hot pressed silicon nitride rotor hubs correlated well with analytical predictions based on Weibull MOR data from 140 test bars cut from five additional hubs. Testing of the stationary components continued with a "Refel" silicon carbide combustor tube successfully accumulating over 200 hours in the steady-state test rig, equivalent to the prescribed 200 hour engine duty cycle goal. Twenty-six hours and 40 minutes of this testing was at a turbine inlet temperature of 2500°F. Three additional thin wall combustor tubes have been successfully qualified for further engine or rig testing. Seven monolithic silicon nitride stators of 2.55 g cc density and a rotor tip shroud successfully passed an improved qualification light-off test. A reaction bonded silicon carbide stator accumulated 147 hours of operation at 1930°F and remains crack free. Testing of stationary components at turbine inlet temperatures up to 2500°F continued with over nine hours of test time accumulated without failures.

An important fabrication development to make duo-density turbine rotors in three pieces was conceived and demonstrated a significant reduction of applied loads during hot press bonding generally eliminating blade and rim cracking. Alignment of the hot press rams and furnace was completed in addition to eliminating base plate creep by utilizing hot pressed silicon carbide base plates. During the course of process development approximately 500 design D' blade rings of 2.7 g cc density were injection molded, twelve were flaw free after nitriding. A number of additional desired mechanical and process changes were identified to improve the yield of flaw free blade rings. The development of the blade fill operation was completed with the optimization of the slip casting fixtures and processes coupled with a laser removal technique.

Modulus of Rupture tests were conducted on 274 specimens of hot pressed silicon nitride to investigate the effects of surface finish, post machining heat treatments and process variations. MOR tests on 155 bars of 2.7 g cc density injection molded reaction sintered silicon nitride were completed to determine room and elevated temperature strengths. Bending stress rupture tests on 15 specimens resulted in no time dependent failures for this material up to 2200°F. Twelve of the tests were suspended, without failure, after 200 plus hours at stresses of 20-30 ksi and temperatures of 1900-2200°F. The nitridation of silicon compacts of various densities was investigated for the effects of temperature schedule, atmosphere and furnace load. The key to uniform microstructure, fine porosity and associated high strengths is the control of localized nitriding exotherms so that no silicon melt out occurs.

Army Materials and Mechanics Research Center
Watertown, Massachusetts 02172

AD _____

BRITTLE MATERIALS DESIGN
HIGH TEMPERATURE GAS TURBINE

Arthur F. McLean, Robert R. Baker, Ford
Motor Company, Dearborn, Michigan 48121

Technical Report AMMRC CTR 76-31, October, 1976
104 pages, 54 illus., 25 tables, 17 references.
Contract DAAG 46-71-C-0162, ARPA Order Number
1849 Tenth Interim Report, January 1, 1976 to
June 30, 1976

Key Words

Gas Turbine Engine
Brittle Design
Ceramics
High Temperature Materials
Silicon Nitride
Silicon Carbide
Non-Destructive Tests
Mechanical Properties

ABSTRACT

The demonstration of uncooled brittle materials in structural applications at 2500°F is the objective of the "Brittle Materials Design, High Temperature Gas Turbine" program. Ford Motor Company, the contractor, will utilize a small vehicular gas turbine comprising an entire ceramic hot flow path including the highly stressed turbine rotors. Westinghouse, the subcontractor, originally planned to evaluate ceramic first stage stator vanes in an actual 30 MW test turbine engine, however, this objective was revised to demonstrate ceramic stator vanes in a static test rig. Both companies had in-house research programs in this area prior to this contract.

In the stationary gas turbine project, the test of ceramic stator vanes in a static rig for 100 cycles up to temperatures of 2500°F has been completed. This accomplishment meets the revised objectives for the stationary turbine project and therefore, this project is completed as of the end of this reporting period. The report of the last six months progress will be included in the final report for the project and published separately.

A significant achievement, in the vehicular turbine project, was the test of a partially bladed duo-density silicon nitride turbine rotor in an experimental high temperature gas turbine engine up to a speed of 52,400 rpm and turbine inlet temperature of 2650°F before failure on a subsequent run. A modification of the ceramic hot gas flow path of the 320 turbine engine to accomplish this test is described in detail. Two rotors, with blades of 10% length, were successfully tested for 45 minutes at 32,000 rpm and 2000°F turbine inlet temperature. Rotor testing capability at elevated temperatures was initiated in two hot spin rigs which were checked out with six available ceramic rotors. Cold spin test results of nine hot pressed silicon nitride rotor hubs correlated well with analytical predictions based on Weibull MOR data from 140 test bars cut from five additional hubs. Testing of the stationary components continued with a "Refel" silicon carbide combustor tube successfully accumulating over 200 hours in the steady-state test rig, equivalent to the prescribed 200 hour engine duty cycle goal. Twenty-six hours and 40 minutes of this testing was at a turbine inlet temperature of 2500°F. Three additional thin wall combustor tubes have been successfully qualified for further engine or rig testing. Seven monolithic silicon nitride stators of 2.55 g cc density and a rotor tip shroud successfully passed an improved qualification light-off test. A reaction bonded silicon carbide stator accumulated 147 hours of operation at 1930°F and remains crack free. Testing of stationary components at turbine inlet temperatures up to 2500°F continued with over nine hours of test time accumulated without failures.

An important fabrication development to make duo-density turbine rotors in three pieces was conceived and demonstrated a significant reduction of applied loads during hot press bonding generally eliminating blade and rim cracking. Alignment of the hot press rams and furnace was completed in addition to eliminating base plate creep by utilizing hot pressed silicon carbide base plates. During the course of process development approximately 500 design D' blade rings of 2.7 g cc density were injection molded, twelve were flaw free after nitriding. A number of additional desired mechanical and process changes were identified to improve the yield of flaw free blade rings. The development of the blade fill operation was completed with the optimization of the slip casting fixtures and processes coupled with a laser removal technique.

Modulus of Rupture tests were conducted on 274 specimens of hot pressed silicon nitride to investigate the effects of surface finish, post machining heat treatments and process variations. MOR tests on 155 bars of 2.7 g cc density injection molded reaction sintered silicon nitride were completed to determine room and elevated temperature strengths. Bending stress rupture tests on 15 specimens resulted in no time dependent failures for this material up to 2200°F. Twelve of the tests were suspended, without failure, after 200 plus hours at stresses of 20-30 ksi and temperatures of 1900-2200°F. The nitridation of silicon compacts of various densities was investigated for the effects of temperature schedule, atmosphere and furnace load. The key to uniform microstructure, fine porosity and associated high strengths is the control of localized nitriding exotherms so that no silicon melt out occurs.

Army Materials and Mechanics Research Center
Watertown, Massachusetts 02172

AD _____

BRITTLE MATERIALS DESIGN
HIGH TEMPERATURE GAS TURBINE

Arthur F. McLean, Robert R. Baker, Ford
Motor Company, Dearborn, Michigan 48121

Technical Report AMMRC CTR 76-41, October, 1976
104 pages, 84 illus., 25 tables, 17 references.
Contract DAAG 46-71-C-0162, ARPA Order Number
1849 Tenth Interim Report, January 1, 1976 to
June 30, 1976

Key Words

Gas Turbine Engine
Brittle Design
Ceramics
High Temperature Materials
Silicon Nitride
Silicon Carbide
Non-Destructive Tests
Mechanical Properties

ABSTRACT

The demonstration of uncooled brittle materials in structural applications at 2500°F is the objective of the Brittle Materials Design, High Temperature Gas Turbine program. Ford Motor Company, the contractor, will utilize a small vehicular gas turbine comprising an entire ceramic hot flow path including the highly stressed turbine rotors. Westinghouse, the subcontractor, originally planned to evaluate ceramic first stage stator vanes in an actual 40 MW test turbine engine, however, this objective was revised to demonstrate ceramic stator vanes in a static test rig. Both companies had in-house research programs in this area prior to this contract.

In the stationary gas turbine project, the test of ceramic stator vanes in a static rig for 100 cycles up to temperatures of 2500°F has been completed. This accomplishment meets the revised objectives for the stationary turbine project and therefore, this project is completed as of the end of this reporting period. The report of the last six months progress will be included in the final report for the project and published separately.

A significant achievement, in the vehicular turbine project, was the test of a partially bladed duo-density silicon nitride turbine rotor in an experimental high temperature gas turbine engine up to a speed of 52,500 rpm and turbine inlet temperature of 2650°F before failure on a subsequent run. A modification of the ceramic hot gas flow path of the 350 turbine engine to accomplish this test is described in detail. Two rotors, with blades of 10" length, were successfully tested for 45 minutes at 32,000 rpm and 2000°F turbine inlet temperature. Rotor testing capability at elevated temperatures was initiated in two hot spin rigs which were checked out with six available ceramic rotors. Cold spin test results of nine hot pressed silicon nitride rotor hubs correlated well with analytical predictions based on Weibull MOR data from 140 test bars cut from five additional hubs. Testing of the stationary components continued with a Refel silicon carbide combustor tube successfully accumulating over 200 hours in the steady-state test rig, equivalent to the prescribed 200 hour engine duty cycle goal. Twenty-six hours and 40 minutes of this testing was at a turbine inlet temperature of 2500°F. Three additional thin wall combustor tubes have been successfully qualified for further engine or rig testing. Seven monolithic silicon nitride stators of 2.55 g cc density and a rotor tip shroud successfully passed an improved qualification light-off test. A reaction bonded silicon carbide stator accumulated 147 hours of operation at 1930°F and remains crack free. Testing of stationary components at turbine inlet temperatures up to 2500°F continued with over nine hours of test time accumulated without failures.

An important fabrication development to make duo-density turbine rotors in three pieces was conceived and demonstrated a significant reduction of applied loads during hot press bonding generally eliminating blade and rim cracking. Alignment of the hot press rams and furnace was completed in addition to eliminating base plate creep by utilizing hot pressed silicon carbide base plates. During the course of process development approximately 500 design D' blade rings of 2.7 g cc density were injection molded, twelve were flaw free after nitriding. A number of additional desired mechanical and process changes were identified to improve the yield of flaw free blade rings. The development of the blade fill operation was completed with the optimization of the slip casting fixtures and processes coupled with a laser removal technique.

Modulus of Rupture tests were conducted on 274 specimens of hot pressed silicon nitride to investigate the effects of surface finish, post machining heat treatments and process variations. MOR tests on 155 bars of 2.7 g cc density injection molded reaction sintered silicon nitride were completed to determine room and elevated temperature strengths. Bending stress rupture tests on 15 specimens resulted in no time dependent failures for this material up to 2200°F. Twelve of the tests were suspended, without failure, after 200 plus hours at stresses of 20-30 ksi and temperatures of 1900-2200°F. The nitridation of silicon compacts of various densities was investigated for the effects of temperature schedule, atmosphere and furnace load. The key to uniform microstructure, fine porosity and associated high strengths is the control of localized nitriding exotherms so that no silicon melt out occurs.

Army Materials and Mechanics Research Center
Watertown, Massachusetts 02172

AD _____

BRITTLE MATERIALS DESIGN
HIGH TEMPERATURE GAS TURBINE

Arthur F. McLean, Robert R. Baker, Ford
Motor Company, Dearborn, Michigan 48121

Technical Report AMMRC CTR 76-41, October, 1976
104 pages, 84 illus., 25 tables, 17 references.
Contract DAAG 46-71-C-0162, ARPA Order Number
1849 Tenth Interim Report, January 1, 1976 to
June 30, 1976

Key Words

Gas Turbine Engine
Brittle Design
Ceramics
High Temperature Materials
Silicon Nitride
Silicon Carbide
Non-Destructive Tests
Mechanical Properties

ABSTRACT

The demonstration of uncooled brittle materials in structural applications at 2500°F is the objective of the Brittle Materials Design, High Temperature Gas Turbine program. Ford Motor Company, the contractor, will utilize a small vehicular gas turbine comprising an entire ceramic hot flow path including the highly stressed turbine rotors. Westinghouse, the subcontractor, originally planned to evaluate ceramic first stage stator vanes in an actual 40 MW test turbine engine, however, this objective was revised to demonstrate ceramic stator vanes in a static test rig. Both companies had in-house research programs in this area prior to this contract.

In the stationary gas turbine project, the test of ceramic stator vanes in a static rig for 100 cycles up to temperatures of 2500°F has been completed. This accomplishment meets the revised objectives for the stationary turbine project and therefore, this project is completed as of the end of this reporting period. The report of the last six months progress will be included in the final report for the project and published separately.

A significant achievement, in the vehicular turbine project, was the test of a partially bladed duo-density silicon nitride turbine rotor in an experimental high temperature gas turbine engine up to a speed of 52,500 rpm and turbine inlet temperature of 2650°F before failure on a subsequent run. A modification of the ceramic hot gas flow path of the 350 turbine engine to accomplish this test is described in detail. Two rotors, with blades of 10" length, were successfully tested for 45 minutes at 32,000 rpm and 2000°F turbine inlet temperature. Rotor testing capability at elevated temperatures was initiated in two hot spin rigs which were checked out with six available ceramic rotors. Cold spin test results of nine hot pressed silicon nitride rotor hubs correlated well with analytical predictions based on Weibull MOR data from 140 test bars cut from five additional hubs. Testing of the stationary components continued with a Refel silicon carbide combustor tube successfully accumulating over 200 hours in the steady-state test rig, equivalent to the prescribed 200 hour engine duty cycle goal. Twenty-six hours and 40 minutes of this testing was at a turbine inlet temperature of 2500°F. Three additional thin wall combustor tubes have been successfully qualified for further engine or rig testing. Seven monolithic silicon nitride stators of 2.55 g cc density and a rotor tip shroud successfully passed an improved qualification light-off test. A reaction bonded silicon carbide stator accumulated 147 hours of operation at 1930°F and remains crack free. Testing of stationary components at turbine inlet temperatures up to 2500°F continued with over nine hours of test time accumulated without failures.

An important fabrication development to make duo-density turbine rotors in three pieces was conceived and demonstrated a significant reduction of applied loads during hot press bonding generally eliminating blade and rim cracking. Alignment of the hot press rams and furnace was completed in addition to eliminating base plate creep by utilizing hot pressed silicon carbide base plates. During the course of process development approximately 500 design D' blade rings of 2.7 g cc density were injection molded, twelve were flaw free after nitriding. A number of additional desired mechanical and process changes were identified to improve the yield of flaw free blade rings. The development of the blade fill operation was completed with the optimization of the slip casting fixtures and processes coupled with a laser removal technique.

Modulus of Rupture tests were conducted on 274 specimens of hot pressed silicon nitride to investigate the effects of surface finish, post machining heat treatments and process variations. MOR tests on 155 bars of 2.7 g cc density injection molded reaction sintered silicon nitride were completed to determine room and elevated temperature strengths. Bending stress rupture tests on 15 specimens resulted in no time dependent failures for this material up to 2200°F. Twelve of the tests were suspended, without failure, after 200 plus hours at stresses of 20-30 ksi and temperatures of 1900-2200°F. The nitridation of silicon compacts of various densities was investigated for the effects of temperature schedule, atmosphere and furnace load. The key to uniform microstructure, fine porosity and associated high strengths is the control of localized nitriding exotherms so that no silicon melt out occurs.

UNCLASSIFIED

SECURITY CLASSIFICATION OF THIS PAGE *(When Data Entered)*

REPORT DOCUMENTATION PAGE	READ INSTRUCTIONS BEFORE COMPLETING FORM
1. REPORT NUMBER: AMMRC CTR-76-31	2. GOVT ACCESSION NO.
3. RECIPIENT'S CATALOG NUMBER	
4. TITLE *(and Subtitle)*: Brittle Materials Design, High Temperature Gas Turbine	5. TYPE OF REPORT & PERIOD COVERED: Interim Report Number 10, 1/1/76 to 6/30/76
6. PERFORMING ORG. REPORT NUMBER	
7. AUTHOR(s): A. F. McLean, Ford Motor Company; R. R. Baker, Ford Motor Company	8. CONTRACT OR GRANT NUMBER(s): DAAG 46-71-C-0162, ARPA Order 1849
9. PERFORMING ORGANIZATION NAME AND ADDRESS: Ford Motor Company, Dearborn, Mi 48121	10. PROGRAM ELEMENT, PROJECT, TASK AREA & WORK UNIT NUMBERS: D/A Project: ARPA Order 1849; AMCMS Code: ; Agency Accession: DA OD 4733
11. CONTROLLING OFFICE NAME AND ADDRESS: Army Materials and Mechanics Research Center, Watertown, Massachusetts 02172	12. REPORT DATE: October, 1976
	13. NUMBER OF PAGES: 104
14. MONITORING AGENCY NAME & ADDRESS *(if different from Controlling Office)*	15. SECURITY CLASS. *(of this report)*: Unclassified
	15a. DECLASSIFICATION/DOWNGRADING SCHEDULE

16. DISTRIBUTION STATEMENT *(of this Report)*

Distribution limited to U.S. Government agencies only: Test and Evaluation data; Oct. 76. Other requests for this document must be referred to the Director, Army, Materials and Mechanics Research Center, ATTN: AMXMR-PL, Watertown, Massachusetts 02172

17. DISTRIBUTION STATEMENT *(of the abstract entered in Block 20, if different from Report)*

18. SUPPLEMENTARY NOTES

19. KEY WORDS *(Continue on reverse side if necessary and identify by block number)*

Gas Turbine Engine	Silicon Nitride
Brittle Design	Silicon Carbide
Ceramics	Non-Destructive Test
High Temperature Materials	Mechanical Properties

20. ABSTRACT *(Continue on reverse side if necessary and identify by block number)*

(See reverse side)

DD FORM 1 JAN 73 1473 EDITION OF 1 NOV 65 IS OBSOLETE

UNCLASSIFIED

SECURITY CLASSIFICATION OF THIS PAGE *(When Data Entered)*

ABSTRACT

The demonstration of uncooled brittle materials in structural applications at 2500°F is the objective of the "Brittle Materials Design, High Temperature Gas Turbine" program. Ford Motor Company, the contractor, will utilize a small vehicular gas turbine comprising an entire ceramic hot flow path including the highly stressed turbine rotors. Westinghouse, the subcontractor, originally planned to evaluate ceramic first stage stator vanes in an actual 30 MW test turbine engine; however, this objective was revised to demonstrate ceramic stator vanes in a static test rig. Both companies had in-house research programs in this area prior to this contract.

In the stationary gas turbine project, the test of ceramic stator vanes in a static rig for 100 cycles up to temperatures of 2500°F has been completed. This accomplishment meets the revised objectives for the stationary turbine project and therefore, this project is completed as of the end of this reporting period. The report of the last six months progress will be included in the final report for the project and published separately.

A significant achievement, in the vehicular turbine project, was the test of a partially bladed duo-density silicon nitride turbine rotor in an experimental high temperature gas turbine engine up to a speed of 52,800 rpm and turbine inlet temperature of 2650°F before failure on a subsequent run. A modification of the ceramic hot gas flow path of the 820 turbine engine to accomplish this test is described in detail. Two rotors, with blades of 10% length, were successfully tested for 45 minutes at 32,000 rpm and 2000°F turbine inlet temperature. Rotor testing capability at elevated temperatures was initiated in two hot spin rigs which were checked out with six available ceramic rotors. Cold spin test results of nine hot pressed silicon nitride rotor hubs correlated well with analytical predictions based on Weibull MOR data from 140 test bars cut from five additional hubs. Testing of the stationary components continued with a "Refel" silicon carbide combustor tube successfully accumulating over 200 hours in the steady-state test rig, equivalent to the prescribed 200 hour engine duty cycle goal. Twenty-six hours and 40 minutes of this testing was at a turbine inlet temperature of 2500°F. Three additional thin wall combustor tubes have been successfully qualified for further engine or rig testing. Seven monolithic silicon nitride stators of 2.55 g/cc density and a rotor tip shroud successfully passed an improved qualification light-off test. A reaction bonded silicon carbide stator accumulated 147 hours of operation at 1930°F and remains crack free. Testing of stationary components at turbine inlet temperatures up to 2500°F continued with over nine hours of test time accumulated without failures.

An important fabrication development to make duo-density turbine rotors in three pieces was conceived and demonstrated a significant reduction of applied loads during hot press bonding generally eliminating blade and rim cracking. Alignment of the hot press rams and furnace was completed in addition to eliminating base plate creep by utilizing hot pressed silicon carbide base plates. During the course of process development approximately 500 design D' blade rings of 2.7 g/cc density were injection molded, twelve were flaw free after nitriding. A number of additional desired mechanical and process changes were identified to improve the yield of flaw free blade rings. The development of the blade fill operation was completed with the optimization of the slip casting fixtures and processes coupled with a laser removal technique.

Modulus of Rupture tests were conducted on 274 specimens of hot pressed silicon nitride to investigate the effects of surface finish, post machining heat treatments and process variations. MOR tests on 155 bars of 2.7 g/cc density injection molded reaction sintered silicon nitride were completed to determine room and elevated temperature strengths. Bending stress rupture tests on 15 specimens resulted in no time dependent failures for this material up to 2200°F. Twelve of the tests were suspended, without failure, after 200 plus hours at stresses of 20-30 ksi and temperatures of 1900-2200°F. The nitridation of silicon compacts of various densities was investigated for the effects of temperature schedule, atmosphere and furnace load. The key to uniform microstructure, fine porosity and associated high strengths is the control of localized nitriding exotherms so that no silicon melt out occurs.